

**THE IMPACT OF AGRICULTURE ON GLOBAL
AIR QUALITY: A COMPARATIVE ANALYSIS OF
CLIMATE CHANGE MITIGATION SCENARIOS WITH
CO-BENEFIT ON HUMAN HEALTH**

JANSAKOO THANAPAT

Abstract

In the foreseeable future, the global population is anticipated to experience substantial growth. Projections indicate that the world's population will increase by approximately 9.7 billion individuals by the year 2050, with a potential peak at nearly 10.5 billion in the 2080s. This demographic shift underscores the pressing requirement for a significant expansion in food production to adequately satisfy the escalating demand. Presently, approximately 50% of the Earth's land is allocated for various agricultural activities, encompassing cropland, aquaculture, and livestock farming. This extensive use of land for agricultural purposes underscores the critical role agriculture plays in providing food and resources for the world's population. It is worth noting that the precise percentage of land dedicated to agriculture may vary by region, with some areas relying more heavily on agriculture for sustenance and economic activity than others. Nonetheless, these agricultural activities possess the capacity to increase the levels of greenhouse gases (GHGs) and airborne pollutants in the atmosphere, potentially leading to negative repercussions for both human society and ecosystems.

Agriculture plays a significant role in contributing to GHGs, primarily through a variety of practices inherent to food production. These GHGs, including CO₂, CH₄, and N₂O, are released during several agricultural activities. For instance, livestock, particularly ruminants like cattle, emit CH₄ as a byproduct of their digestion process. Furthermore, the mismanagement of livestock manure can also lead to the release of CH₄ and N₂O into the atmosphere. Apart from GHGs, agriculture also serves as a notable source of air pollutants, such as ammonia, which can contribute to the formation of ground-level ozone and fine particulate matter. These pollutants, in turn, can have adverse effects on human health, exacerbating respiratory issues and other health concerns. To assess the potential concentrations of these air pollutants and their subsequent impact on public health, atmospheric chemical transport models (CTMs) have widely utilized.

Understanding the limitations associated with these CTMs is crucial. These models are essential tools for evaluating the complex dynamics of atmospheric chemistry and pollutant dispersion. However, they come with various challenges and constraints. These limitations can include the simplification of complex atmospheric processes, uncertainties in emission data, and the need for

extensive computational resources. Additionally, CTMs may not always capture localized variations accurately, which can be especially significant in agricultural areas where emissions and pollutant transport can be highly variable.

In this study, we conducted a comparison of CTM outcomes under both low and high spatial resolutions to explore their impacts on the model's accuracy in simulating air quality. The results indicate that investing significant time and resources in using high-spatial resolution in simulations may not necessarily lead to a substantial enhancement in model accuracy. The application of nested-grid simulation in the 2015 under baseline scenario data set resulted in estimated tropospheric O₃ and PM_{2.5} concentrations that exhibited a tendency to be overestimated when compared to observed data. Specifically, the O₃ concentration was overestimated by approximately 3.5 ppbv, which constituted an 11.8% overestimation on a monthly basis. In contrast, the PM_{2.5} concentration was overestimated by around 20.9 µg/m³, marking a substantial overestimation of 122%. This suggests that the benefits of finer-grained spatial data may not always justify the costs associated with obtaining and processing such data. While this finding may lead to slight variations in both health and agricultural outcomes, the impact of this lack of significant improvement in model accuracy is more pronounced in specific regions. This indicates that certain regions exhibit a more pronounced impact on the quality of predictions and outcomes when high-spatial resolution simulations are applied. For instance, the implementation of the nested-grid simulation led to a 7% increase in losses in the Middle East, and a similar trend was observed in Turkey and North Africa, as these regions are in close proximity to one another. Furthermore, in mitigation scenarios, the disparities between nested and non-nested simulations are most significant. Therefore, when assessing the cost-effectiveness of mitigation strategies, it is crucial to consider both nested-grid simulations and model uncertainty.

Additionally, we analyzed the influence of agricultural activity on air quality through a sensitivity analysis of NH₃ and NO_x emissions from the agricultural sector. The results revealed that reducing ammonia emissions can effectively mitigate PM_{2.5} pollution in the EU and Asia while potentially increasing O₃ levels. However, the impact on PM_{2.5} levels in Africa is relatively modest. On the other hand, reducing NO_x emissions doesn't directly control PM_{2.5} levels but can potentially reduce O₃ concentration. In the context of ammonia reduction scenarios, a notable decrease in mortality

rates is expected, and when strategies for reducing both NH₃ and NO_x are combined, the reduction in mortality is significantly enhanced. This discovery highlights the substantial potential of these reduction strategies in mitigating mortality.

In an effort to align with real-world circumstances, we introduced climate change mitigation scenarios with the goal of maintaining CO₂ emissions below 500 Gt after 2020, thus restraining global warming. Additionally, we integrated dietary modifications advocated by the EAT-Lancet Commission as a component of our air quality simulation scenarios. Our primary objective was to evaluate the co-benefits of dietary adjustments on future greenhouse gas emissions, air quality, and human health, and to analyze the impact of dietary transformation policies within the framework of climate change mitigation.

Our research found that integrating dietary changes with climate change mitigation measures offers a more comprehensive approach to improving air quality in specific regions. For instance, there are additional PM_{2.5} reductions from climate change mitigation scenario in EU approximately 3.86%, 2.58%, and 2.68% by 2030, 2050, and 2100, respectively while the relative alterations in global average ozone concentrations between these scenarios were calculated to be approximately -0.50%, -0.80%, and -0.13% for the years 2030, 2050, and 2100, respectively. These results suggest that the incorporation of dietary modifications alongside climate change mitigation measures has a minimal extra influence on ozone concentrations. Therefore, it's essential to exercise caution and consider potential adverse effects on ozone concentrations in certain areas especially in Africa.

Enforcing dietary modifications to enhance future air quality can likewise lead to a reduction in the costs associated with the health burden especially in the high polluted region and developing country. The convergence of climate change mitigation and dietary modification, following the recommendations of the EAT-Lancet commission, offers a promising avenue to attain a sustainable and healthier future for both humanity and the planet.

Table of Contents

Chapter	Page
ABSTRACT.....	i
TABLE OF CONTENTS.....	i
TABLE OF FIGURES.....	v
TABLE OF TABLES.....	vii
CHAPTER 1 GENERAL INTRODUCTION.....	1
1.1 Current situation of climate change and air pollution.....	1
1.2 Effect of climate change on air pollution.....	6
1.3 The influencing of agricultural activity on future climate change and air pollution.....	8
1.4 Global mortality related to ambient air pollution exposure.....	13
1.5 Agricultural implication related to air pollution.....	16
1.6 Co-benefit of climate change mitigation policy on future GHGs and air pollution.....	18
1.7 Research objective.....	21
1.8 Chapter organization.....	21
1.9 Reference.....	23
CHAPTER 2 MODEL DESCRIPTION.....	34
2.1 Overall modeling framework.....	34
2.2 AIM/Hub.....	34
2.2.1 Model Structure.....	37
2.3 AIM/Downscaling.....	40
2.4 GEOS-Chem.....	43
2.4.1 GEOS-Chem chemistry mechanisms.....	44
2.4.2 GEOS-Chem emissions.....	48
2.5 Human health exposure model.....	51
2.5.1 The Integrated Exposure-Response Model (IER).....	52
2.5.2 The Global Exposure Mortality Model (GEMM).....	54
2.5.3 Log-linear function.....	57
2.6 The Lund–Potsdam–Jena managed land 2 crop model.....	58
2.6.1 Crop Growth Simulation.....	59
2.6.2 Land Use Dynamics.....	59

2.6.3	Climate Change Impact Assessment.....	59
2.6.4	Policy Analysis	59
2.6.5	Regional and Global Applications	59
2.7	Reference.....	60
CHAPTER 3 COMPARISON OF GLOBAL AIR POLLUTION IMPACTS ACROSS HORIZONTAL RESOLUTIONS.		62
3.1	Abstract	62
3.2	Introduction	63
3.3	Methodology	65
3.3.1	Target area and spatial resolution.....	65
3.3.2	Emission scenarios.....	67
3.3.3	Comparison of model outputs with monitoring station observations	68
3.3.4	Agricultural impacts.....	69
3.3.5	Mortality due to PM _{2.5} exposure	70
3.4	Results	71
3.4.1	Spatial distribution of tropospheric O ₃ and PM _{2.5} concentrations representation in nested-grid simulations.....	71
3.4.2	Model validation	72
3.4.3	PM _{2.5} exposure and mortality.....	75
3.4.4	Crop production losses due to O ₃ exposure	76
3.5	Discussion	77
3.5.1	Model evaluation	77
3.5.2	Impact assessment.....	78
3.5.3	Limitation.....	79
3.6	Summary and conclusions.....	80
3.7	Reference.....	82
CHAPTER 4 THE INFLUENCE OF AGRICULTURAL AMMONIA EMISSIONS REDUCTION ON AIR POLLUTION AND HUMAN HEALTH		87
4.1	Abstract	87
4.2	Introduction	88
4.3	Methodology	90
4.3.1	Air pollution simulations	90
4.3.2	Sensitivity Analysis of Ammonia Emission Reduction on Air Pollution and Human Health.....	90

4.3.3	Health Implication Analysis.....	92
4.4	Results	93
4.4.1	PM _{2.5} and O ₃ sensitivity to NH ₃ and NO _x emission reduction scenarios	93
4.4.2	Seasonal effects of ammonia emission reductions on PM _{2.5}	98
4.4.3	Health implication assessment of PM _{2.5} concentration change	101
4.5	Discussion	103
4.5.1	Effect of ammonia emission reduction on PM _{2.5} and O ₃ level.....	103
4.5.2	Limitation.....	104
4.6	Summary and conclusions.....	105
4.7	Reference.....	107

CHAPTER 5 CO-BENEFITS OF AIR QUALITY FOR HUMAN HEALTH FROM CLIMATE CHANGE MITIGATION THROUGH DIETARY CHANGE AND FOOD LOSS PREVENTION

POLICY.....109

5.1	Abstract	109
5.2	Introduction	110
5.3	Methodology	112
5.3.1	Overview.....	112
5.3.2	Scenario and experiment design	113
5.3.3	Integrated Assessment Model (AIM/Hub).....	114
5.3.4	GEOS-Chem simulation	116
5.3.5	Premature mortality attributable to long-term exposure to ambient PM _{2.5} and O ₃	117
5.3.6	Economic value of mortality reduction.....	118
5.4	Results	119
5.4.1	Implication of dietary change policy on future food demand and supply	119
5.4.2	Impact of dietary changes on future global GHGs and air pollutants precursor gases.....	122
5.4.3	Effect of dietary change on future air quality	125
	Table 5-2	129
5.4.4	Reductions in premature mortality.....	132
5.4.5	Economic impact	133
5.5	Discussion	136
5.5.1	The Potential for emission reduction through dietary change and food losses prevention policy	136
5.5.2	The impact of agricultural emissions on ambient PM _{2.5} and O ₃ concentration	137

5.5.3	The societal benefits of reducing mortality through improved air quality from dietary change and climate change mitigation policy	138
5.5.4	Policy recommendation	140
5.5.5	Uncertainty and limitation	141
5.6	Summary and conclusions.....	142
5.7	Reference.....	144
CHAPTER 6 SUMMARY AND CONCLUSION		150
6.1	Summary	150
6.2	Limitation and recommendation	152
LIST OF PUBLICATIONS.....		153
ACKNOWLEDGEMENT		154

Table of Figures

Figure	Page
Figure 1-1 Selected significant climate anomalies and events in 2022	2
Figure 1-2 Global average PM _{2.5} concentration	5
Figure 1-3 Ozone and methane formation/depletion cycle.....	11
Figure 1-4 Secondary Inorganic Aerosol Formation	12
Figure 1-5 Locations settlements with data on PM _{2.5} concentrations, 2010–2019.....	14
Figure 1-6 Chapter organization	22
Figure 2-1 SSPs mapped in the challenges to mitigation/adaptation space.....	36
Figure 2-2 The AIM/Hub overview model structure	38
Figure 2-3 GEOS-Chem model framework.....	44
Figure 2-4 The Lund-Potsdam-Jena Managed Land (LPJmL) Crop Model conceptual framework.....	58
Figure 3-1 The framework of GEOS-Chem simulations and the impact assessment	66
Figure 3-2 GEOS-Chem nested-grid domain (0.5°× 0.625°) for the target area.....	67
Figure 3-3 Spatial distributions of the O ₃ and PM _{2.5} concentrations for cases simulated without and with a nested grid.....	73
Figure 3-4 Comparison of the number of worldwide premature deaths attributable to exposure to PM _{2.5} in the simulations with and without nested grids, and changes in the number of deaths by region due to the application of the nested-grid simulation.....	75
Figure 3-5 Comparison of the worldwide crop production loss due to O ₃ exposure in the simulations with and without nested grids, and changes in crop production loss by region due to the application of the nested-grid simulation.....	76
Figure 4-1 Spatial plot of PM _{2.5} concentration relative changing (%) between baseline and scenario 3-8.....	94
Figure 4-2 The relative annual PM _{2.5} concentrations changes between baseline scenario and sensitivity case.....	95
Figure 4-3 The fraction of fine-particle mass sensitive to ammonia (%)	96
Figure 4-4 Spatial plot of O ₃ concentration relative changing (%) between baseline and scenario 3-8	97
Figure 4-5 Daily average PM _{2.5} concentrations comparing between baseline and scenario 1-4 in 2015....	99
Figure 4-6 Seasoning chemical regime from emission reduction	100
Figure 4-7 PM _{2.5} associated premature deaths (GEMM-5COD) change comparing between baseline and scenario 1-8.....	102
Figure 5-1 Research framework visualization	112

Figure 5-2 Total, crop, and livestock food demand for baseline scenario, dietary change and food losses prevention, climate change mitigation, and integrate policy projection for 2005-2100	120
Figure 5-3 Crop production for baseline scenario, dietary change and food losses prevention, climate change mitigation, and integrate policy projection for 2005-2100.....	121
Figure 5-4 Mechanisms of dietary changes on GHG emissions, air pollutant precursors, and human health	122
Figure 5-5 Comparison of global GHGs and air pollutants emission for baseline scenario, dietary change and food losses prevention, climate change mitigation, and integrate policy projection for 2005-2100.....	124
Figure 5-6 the percent relative change (%) of PM _{2.5} and O ₃ concentrations due to dietary change and food loss prevention policy comparing with baseline scenario in 2030, 2050, and 2100	126
Figure 5-7 temporal resolution PM _{2.5} and O ₃ concentrations comparing between baseline and climate change mitigation policy between 2015 to 2100	127
Figure 5-8 Regional comparison relative change (%) of PM _{2.5} and O ₃ due to Integrated Policy (SC2+SC3) comparing with climate change mitigation scenario.....	131
Figure 5-9 Regional comparison mortality change (1000 yr ⁻¹) of PM _{2.5} and O ₃ between dietary change and food loss prevention policy and baseline and and climate change mitigation scenario and integrated policy.....	133
Figure 5-10 VSLY cost changing (%) comparing of dietary and food loss prevention policy, climate change mitigation, and integrated policy with the baseline scenario.....	135

Table of Tables

Table	Page
Table 1-1 Examples of species-specific responses to O ₃	16
Table 2-1 Socioeconomic region codes	35
Table 2-2 Emission sources in AIM/Hub.....	39
Table 2-3 Downscaling algorithm emission source groups and weight used	40
Table 2-4 Information about the available chemistry mechanisms in GEOS-Chem.....	45
Table 2-5 Emission sources for CEDS	48
Table 2-6 Integrated Exposure–Response (IER) parameter estimates by cause of death.....	53
Table 2-7 GEMM parameter estimates by cause of death, with inclusion of Chinese Male Cohort.....	54
Table 2-8 GEMM parameter estimates by cause of death, without inclusion of Chinese Male Cohort.....	56
Table 3-1 Sources of air quality monitoring data and number of observations.....	69
Table 3-2 the impact function coefficients for each crop in the study.....	70
Table 3-3 Changes in the MAE due to the nested-grid simulation of the modeled/observed O ₃ concentrations (ppbv).....	74
Table 3-4 Changes in the MAE due to the nested-grid simulation of the modeled/observed PM _{2.5} concentration (µg/m ³).....	74
Table 4-1 Scenario description	91
Table 4-2 Air pollution monitoring station locations based on agricultural land use.....	92
Table 4-3 PM _{2.5} associated premature deaths change between baseline scenario and sensitivity cases separate by disease (%)	103
Table 5-1 Summarizes the scenario set.....	114
Table 5-2 Regional Ammonia (NH ₃) emissions (Mt/yr) comparing across sector, scenario and simulation year (2015, 2030, 2050, 2100).....	128

Chapter 1

General Introduction

1.1 Current situation of climate change and air pollution.

Climate change undeniably stands as a paramount concern and captivating subject matter that has garnered extensive attention from scientists committed to its comprehensive study and the pursuit of efficacious mitigation strategies. Climate change refer to alterations in temperature regimes and atmospheric conditions. These alterations may arise from natural factors such as fluctuations in solar activity or significant volcanic eruptions. However, since the 19th century, anthropogenic activity has emerged as the predominant catalyst for climate change (IPCC, 2019).

In more recent history, from the Industrial Revolution in the late 18th century onwards, human activities have significantly impacted global temperatures (Mahmoud & Gan, 2018). The burning of fossil fuels, deforestation, and industrial processes have released large quantities of greenhouse gases, such as carbon dioxide (CO₂) and methane (CH₄), into the atmosphere. These gases trap heat from the sun, leading to the greenhouse effect and a steady increase in global temperatures (Jain, 1993; Kweku et al., 2018; Weart, 2008). This phenomenon is commonly referred to as anthropogenic or human-induced global warming. IEA report that Global energy-related CO₂ emissions increased by 0.9% or 321 million metric tons (Mt) in 2022, reaching a new record high of more than 36.8 billion metric tons (Gt). Emissions from emerging market and developing economies in Asia, excluding China, experienced the most significant growth in 2022, rising by 4.2%, equivalent to an increase of 206 Mt of CO₂. More than half of this regional increase in emissions can be attributed to coal-fired power generation.

According to the 2022 Annual Climate Report from the National Oceanic and Atmospheric Administration (NOAA), the combined temperature of land and ocean has exhibited a consistent increase, with an average rate of approximately +0.86 (± 0.15) degrees Celsius since 1880. In terms of global precipitation, the estimated mean for 2022, derived from the GPCP Monthly analyses, is approximately 2.67 mm per day (Adler et al., 2017, 2018). This figure is just slightly below the

40-year climatological mean of 2.69 mm per day, with the ocean and land components having mean values of 2.85 and 2.30 mm per day, respectively.

Climate change can cause direct and indirect threats to human societies, affecting various aspects of our lives. One of the most immediate and concerning consequences is the increased frequency and severity of extreme weather events (Huber & Gullede, 2011; Konisky et al., 2016; McBean, 2004). Heatwaves, hurricanes, droughts, and flooding have become more common, causing loss of life, property damage, and displacement of communities. These events disrupt infrastructure, disrupt food and water supplies, and strain healthcare systems, particularly in vulnerable regions (Figure 1-1).

In parallel, the Intergovernmental Panel on Climate Change (IPCC) in 2018 released a pivotal special report that underscored the paramount importance of limiting global warming to a maximum of 1.5°C above pre-industrial levels, as opposed to allowing it to escalate to 2°C, as delineated in the Paris Agreement. This distinction arises from the acknowledgment that adhering to a 2-degree Celsius limit may prove insufficient in implementing the necessary mitigation measures to effectively shield our planet from the adverse consequences of climate change.

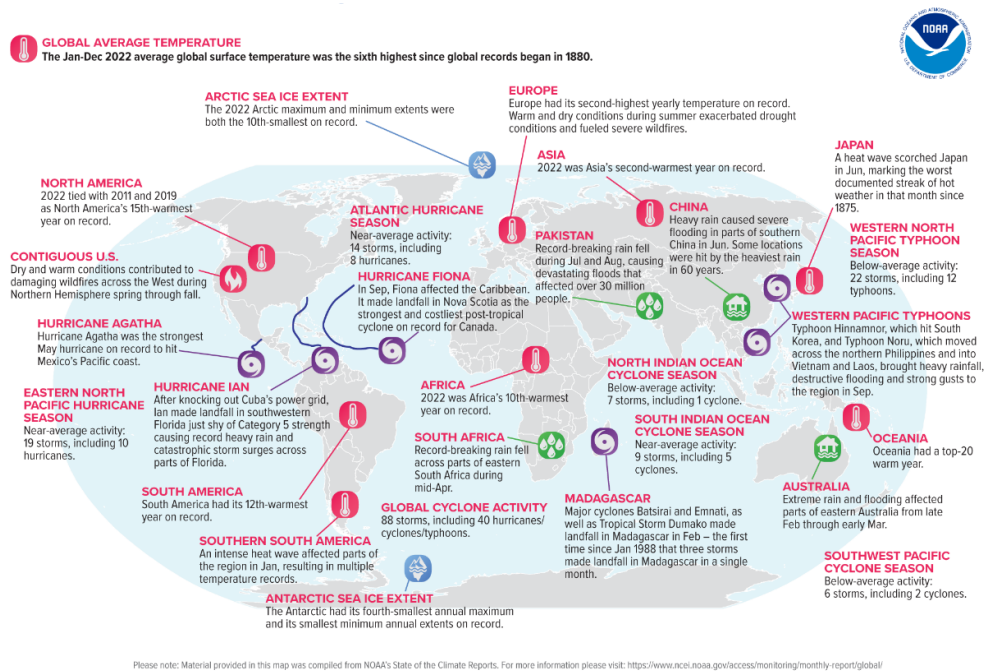


Figure 1-1 Selected significant climate anomalies and events in 2022 (NOAA, 2023)

Indirectly, climate change can give rise to food and water scarcity issues. The consequences of rising global temperatures altered precipitation patterns, and the increased occurrence of extreme weather events linked to climate change can disrupt agricultural systems, resulting in diminished crop yields and strained water resources. As per the IPCC, an increase of 1.5°C in global temperatures above pre-industrial levels could potentially lead to a 5-10% reduction in crop yields, with the most significant impacts affecting staple foods like wheat, rice, and maize, which are crucial for sustaining billions of people. Furthermore, it's worth noting that climate change mitigation policies can also contribute to these challenges. When implemented, these policies may inadvertently affect agricultural practices and food production, potentially exacerbating food and water scarcity concerns. For instance, Hasegawa et al. (2018) found that the implementation of stringent climate mitigation policies, if applied uniformly across all sectors and regions, could potentially have a more significant adverse effect on global hunger and food consumption compared to the direct impacts of climate change.

The relationship between climate change and air quality is inextricably linked, as climate change exacerbates air pollution and vice versa. Rising temperatures, a consequence of climate change, can lead to more frequent and severe heatwaves, which can in turn increase ground-level ozone formation and worsen smog. Additionally, climate change can alter weather patterns, leading to prolonged periods of stagnant air, trapping pollutants and causing particulate matter to accumulate in the atmosphere, further degrading air quality.

Air pollution is one of the most serious issues affecting both human health and the ecosystem (Kampa & Castanas, 2008). It can have direct and harmful consequences on respiratory health, cardiovascular health, and overall well-being for individuals exposed to polluted air. Additionally, it can have devastating effects on ecosystems, including harm to wildlife, damage to vegetation, and the deterioration of air and water quality, all of which can disrupt the delicate balance of our environment.

One of the most significant contributors to air pollution is the combustion of fossil and solid fuels (Kulkarni & Grigg, 2008; Lin et al., 2018). This occurs in energy sector, industrial facilities, residential, and vehicles. When coal, oil, natural gas, and wood are burned, they release a range of

pollutants into the atmosphere, including carbon dioxide (CO₂), sulfur dioxide (SO₂), nitrogen oxides (NO_x), and particulate matter (PM). These emissions have direct and indirect impacts on air quality and human health. Agriculture also plays a role in air pollution (Aneja et al., 2009; Harizanova-Bartos & Stoyanova, 2018; Lichtenberg, 2002). The use of fertilizers, pesticides, and the management of livestock can release ammonia (NH₃), methane (CH₄), and other pollutants into the atmosphere. When disposing of agricultural residual waste through open burning, various pollutants are released into the atmosphere. This process emits CO₂, carbon monoxide (CO), PM, and volatile organic compounds (VOCs). These emissions can have local and regional impacts on air quality and contribute to greenhouse gas emissions. While human activities are significant contributors to air pollution, natural sources also play a role (Colls, 2002; Holman, 1999; Popescu & Ionel, 2010). Events such as volcanic eruptions, wildfires, dust storms, and the release of pollen can introduce natural pollutants and particulate matter into the atmosphere. While these events are beyond human control, they can still impact air quality regionally and even globally.

Fine particulate matter (PM_{2.5}) and Ozone (O₃) are the significant pollutants that affect to human health (Force & Graham, n.d.). PM_{2.5} refers to particles in the air that have a diameter of 2.5 micrometers or smaller. These particles are so small that they can be inhaled deep into the lungs and even enter the bloodstream, posing serious health risks. Particulate Matter (PM) comprises various significant components, including sulfates, nitrates, ammonia, black carbon, mineral dust, sea salt, and water (Philip et al., 2014; Singh & Tripathi, 2021; Van Donkelaar et al., 2019). Many regions across the world concerning levels of PM_{2.5} pollution. According to WHO guideline, they established guidelines for PM_{2.5} pollution to safeguard public health. These guidelines recommend acceptable levels of PM_{2.5} in the air. the WHO PM_{2.5} guidelines were an annual mean of 5 micrograms per cubic meter (µg/m³) and a 24-hour mean of 15 µg/m³. Referring to Figure 1-2, it is evident that the annual PM_{2.5} concentration in the majority of countries worldwide higher than the WHO guideline standards. This disparity is particularly pronounced in regions such as Asia, Africa, and the Middle East. These regions grapple with persistently elevated levels of PM_{2.5} pollution, underscoring the urgent need for comprehensive air quality management and mitigation efforts to protect public health.

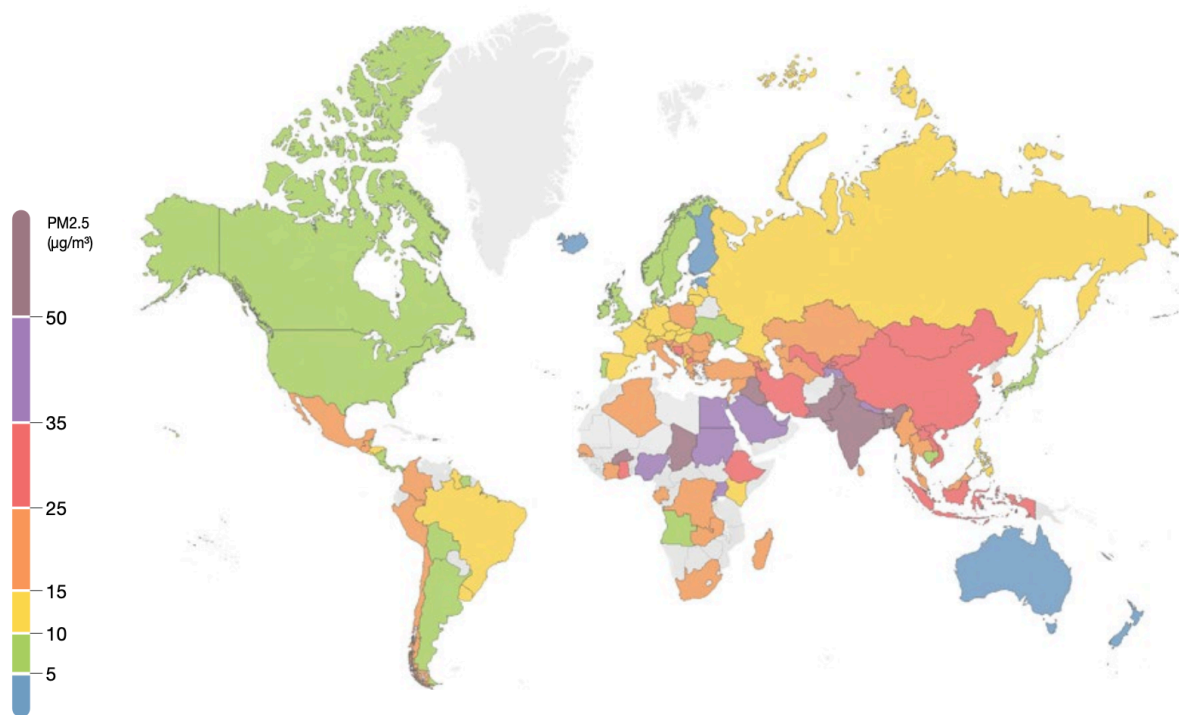


Figure 1-2 Global average PM_{2.5} concentration (IQAir, 2022)

Ground-level ozone, often called bad or tropospheric ozone, is a crucial element of smog and can negatively impact both human health and the environment. Elevated concentrations of ground-level ozone can worsen respiratory problems, particularly in more susceptible individuals, and can also damage plant life. According to WHO, in order to protect public health, the average 8-hour O₃ concentration should not exceed 100 µg/m³ and 60 µg/m³ for average peak season. According to Malashock et al. (2022) study, average population-weighted mean ozone concentration across all cities studied increased by 11%, from 46 ppb (2000) to 51 ppb (2019). Moreover, they also found that the number of cities with ozone concentrations above the WHO peak season ozone standard (60 µg/m³) increased from 89% in 2000 to 96% in 2019.

To address the issue, many countries have developed the clean air act policy. For example, in the UK, since 1956 the first clean air act policy was established to control and reduce air pollution to protect public health and the environment. In 2019, the UK government published a Clean Air Strategy outlining its approach to tackling air pollution (Longhurst et al., 2016). It focused on reducing emissions from transportation, industry, and agriculture, as well as promoting cleaner

technologies and behaviors. In China, the State Council enacted the Air Pollution Prevention and Control Action Plan (APPCAP) in 2013 with the primary objective of reducing particulate matter (PM) levels and addressing air pollution. This plan aims for improving air quality across the country. It sets specific targets for reducing PM_{2.5} concentrations and other key air pollutants in order to safeguard public health and promote environmental sustainability (Zhao & Kim, 2022). In the European Union (EU), the Clean Air Package was introduced to enhance air quality throughout Europe (Amann et al., 2014; Holland, 2014). The primary objectives of this legislative package are to prevent approximately 58,000 premature deaths and protect around 19,000 square kilometers of forest ecosystems from acidification.

1.2 Effect of climate change on air pollution.

Climate change and air quality are intricately linked, as outlined in section 1.1. Climate change can result in shifts in weather patterns and the occurrence of extreme weather events, which, in turn, can influence air pollution levels. Air pollution is often exacerbated by unfavorable meteorological conditions that combine with pollutant emissions (Jacob & Winner, 2009).

According to Reidmiller et al. (2017) study, there are more than 100 million people in USA live in place where air quality is poor. While climate-driven changes in weather conditions, including temperature and precipitation, are expected to increase ground-level ozone and particulate matter. Furthermore, it is not just ambient air pollution that is impacted by climate change; indoor air quality can also be affected. When outdoor air pollution levels rise, it can find its way indoors through various means, including ventilation systems, open windows, and doors.

Temperature changing due to climate change could direct impact to level of secondary fine particulate matter especially sulfate-nitrate-ammonium aerosol (SNA) in the atmosphere. Such impact could be precursor emission rate, chemical reaction, and gas-aerosol partitioning of semi-volatile species. For example, the increasing of surface temperatures can induce heightened gas-phase reaction rates and higher concentrations of oxidants. Consequently, this phenomenon can lead to an induce in sulfate concentration within the atmosphere. Conversely, elevated

temperatures may precipitate a reduction in the mass of nitrate aerosols owing to the partitioning of ammonium and nitrate into the gaseous phase (Dawson et al., 2007; Liao et al., 2006).

According to the IPCC report, during the 21st century under the RCP8.5 scenario, water resources are anticipated to increase in high-latitude regions due to rising precipitation levels, which can directly affect to particulate matter. Previous studies underscore the significant role of precipitation in the enhancement of air quality. Rainfall possesses the capability to efficiently eliminate PM_{2.5} and various airborne pollutants through wash-out process, effectively transporting particulate matter away from the atmosphere. Consequently, this natural process contributes to the reduction of major air pollutants, ultimately resulting in an overarching improvement in air quality (Guo et al., 2016; S. Kim et al., 2014; R. Wang et al., 2023). On the other hand, in presently dry regions, the frequency of drought will likely rise by the end of 21st century resulting by climate change. Thus, the level of fine particulate matter might be increasing. Droughts can lead to soil erosion, reduced vegetation cover, and increased dust emissions, all of which can contribute to higher concentrations of fine particulate matter in the atmosphere (Borlina & Rennó, 2017; Cook et al., 2009; Ginoux et al., 2004; Wu et al., 2021).

In term of O₃ concentration, increasing levels of GHG emissions from sources such as vehicles, power plants, and other anthropogenic activities are driving global warming. This warming effect is expected to lead to an increase in ozone concentrations. It is formed in photochemical reactions, with concentrations affected by weather and the supply of chemical precursors, including nitrogen oxides (NO_x), volatile organic compounds (VOCs), methane (CH₄) and carbon monoxide (CO). Under strong sunlight and high temperature, ozone can undergo various reactions and transformations. For example, ozone can react with other pollutants such as nitrogen oxide, to form smog and other pollutants (Feng et al., 2015). Simultaneously, the emission of VOCs, which are precursors to ozone formation, tends to increase during warmer summers (Langner et al., 2012).

Air pollution plays a significant role in the context of climate change (Seinfeld & Pandis, 2016; Spickett et al., 2011). Aerosols can have a direct radiative forcing effect on the Earth's climate system. Direct radiative forcing refers to the impact of aerosols on the balance of incoming and outgoing solar (shortwave) and infrared (longwave) radiation in the atmosphere. Atmospheric

aerosols can either absorb or scatter incoming solar radiation, leading to changes in ambient temperature (Andreae, 1995; Boucher & Boucher, 2015; Fadnavis et al., 2020). One of the key aerosols capable of absorbing light is black carbon (BC). Black carbon, commonly known as soot, indeed has the ability to absorb sunlight effectively, which leads to a warming effect on the surrounding environment. Furthermore, several studies have identified BC as a significant contributor to the greenhouse gas effect (Kahnert & Devasthale, 2011; Rajesh & Ramachandran, 2018). Its strong capacity to absorb sunlight can contribute to an increase in ambient temperature, contributing to the phenomenon known as global warming.

On the contrary, mineral dust aerosols influence Earth's energy budget by interacting with radiation differently. Due to their light color, they scatter light effectively, which can lead to a reduction in ambient temperature, a phenomenon referred to as the cooling effect. (Kuniyal & Guleria, 2019). According to the Kok et al. (2023) study, the cumulative impact of dust interactions on Earth's overall energy budget is estimated to be approximately $-0.2 \pm 0.5 \text{ W m}^{-2}$ (with a 90% confidence interval). This suggests that, on balance, dust contributes to a cooling effect on the climate.

These complex dynamics highlight the urgent need for comprehensive strategies addressing both climate change mitigation and air quality improvement to safeguard public health and the environment.

1.3 The influencing of agricultural activity on future climate change and air pollution

Agriculture plays a significant role in both climate change and air pollution. On the one hand, modern agricultural practices have contributed to the acceleration of climate change. The use of fertilizers both synthesis and biological, and pesticides release nitrous oxide (N_2O) and CH_4 , potent greenhouse gases, into the atmosphere. Deforestation for expanding farmland further intensifies the issue by releasing stored carbon and reducing the planet's ability to absorb CO_2 .

In addition to these direct emissions, microorganisms in the soil play a crucial role in the release of nitrogen oxides (NO_x). The nitrogen cycle, facilitated by bacteria, includes processes such as nitrification and denitrification. Nitrifying bacteria like *Nitrosomonas* and *Nitrobacter* convert

ammonium (NH_4^+) into nitrite (NO_2^-) and then into nitrate (NO_3^-), releasing nitric oxide (NO) into the atmosphere. Furthermore, certain soil bacteria participate in denitrification, converting nitrate into nitrogen gases, including N_2O , a significant greenhouse gas contributing to climate change.

Livestock, particularly cattle, produce methane during digestion through a process called enteric fermentation. CH_4 is a potent greenhouse gas, with a much higher global warming potential than CO_2 . Additionally, manure management and rice cultivation can release CH_4 . Methane has played a significant role in the increase in global temperatures since the industrial revolution, contributing to approximately 30% of this rise. It is essential to prioritize swift and consistent reductions in methane emissions as a crucial strategy for mitigating near-term warming and enhancing air quality (IEA, 2022). Indeed, methane not only contributes to global warming but also serves as a precursor to the formation of the harmful air pollutant known as tropospheric ozone.

Ground-level ozone, also known as tropospheric ozone, does not originate directly from emissions but is formed through chemical interactions involving oxides of nitrogen (NO_x) and volatile organic compounds (VOC). These reactions occur when pollutants released by various sources such as cars, power plants, industrial boilers, refineries, and chemical plants undergo chemical transformations in the presence of sunlight. Unfavorable ozone levels are more likely to occur on hot, sunny days in urban settings, but elevated levels can still be observed during colder months. Additionally, wind can transport ozone over long distances, leading to high levels even in rural areas. Ozone (O_3) can undergo photolysis, a process where it is broken down by the absorption of light. The photolysis of ozone typically occurs at wavelengths shorter than 370 nanometers (nm). Ultraviolet (UV) radiation, specifically UV-C and shorter wavelengths of UV-B, can provide the energy needed for this reaction. The photolysis of ozone can be represented by the following reaction:



The ground-state oxygen atom will react with oxygen molecules to regenerate ozone,



where M represents a third body (typically an oxygen or nitrogen molecule). At wavelength <0.430 μm , NO_2 is photolyzed represented by the following reaction:



O_3 remove by Nitric oxide reacts with ozone to form NO_2 as shown in 1-4



A cycle of O_3 depletion and creation is created when reactions 1-1 through 1-4 are combined.

In another way, the formation of O_3 occurs in a series of chemical reactions involving free hydroxyl radicals ($\text{OH}\cdot$) and CH_4 in the Earth's atmosphere. This process plays a crucial role in both the regulation of methane concentrations and the production of ozone, which is important for atmospheric chemistry and air quality (Seinfeld & Pandis, 2016). Methane is an important precursor for tropospheric ozone. In the presence of nitrogen oxides (NO_x), tropospheric CH_4 oxidation leads to the formation of O_3 (Crutzen, 1973). The oxidation of methane and other hydrocarbons in the atmosphere is a complex process that involves reactions with hydroxyl radicals (OH) and can contribute to the formation of O_3 .

The oxidation of methane, as well as other hydrocarbons, can lead to the production of O_3 in case of high NO_x emission as shown in Figure 1-3 (Madronich, 1993). The role of NO_x in ozone formation is crucial, as indicated in the statement. When there are high NO_x emissions, it can lead to the production of ozone as a result of the interaction between nitrogen oxides and volatile organic compounds (VOCs), including methane and other hydrocarbons. This process is part of the complex chemistry of the atmosphere. In urban areas, the oxidation of hydrocarbons in the presence of elevated levels of NO_x is a key contributor to the formation of photochemical smog. This smog, characterized by elevated ozone concentrations, is a major air quality concern in cities and urban environments due to its detrimental effects on human health and the environment.

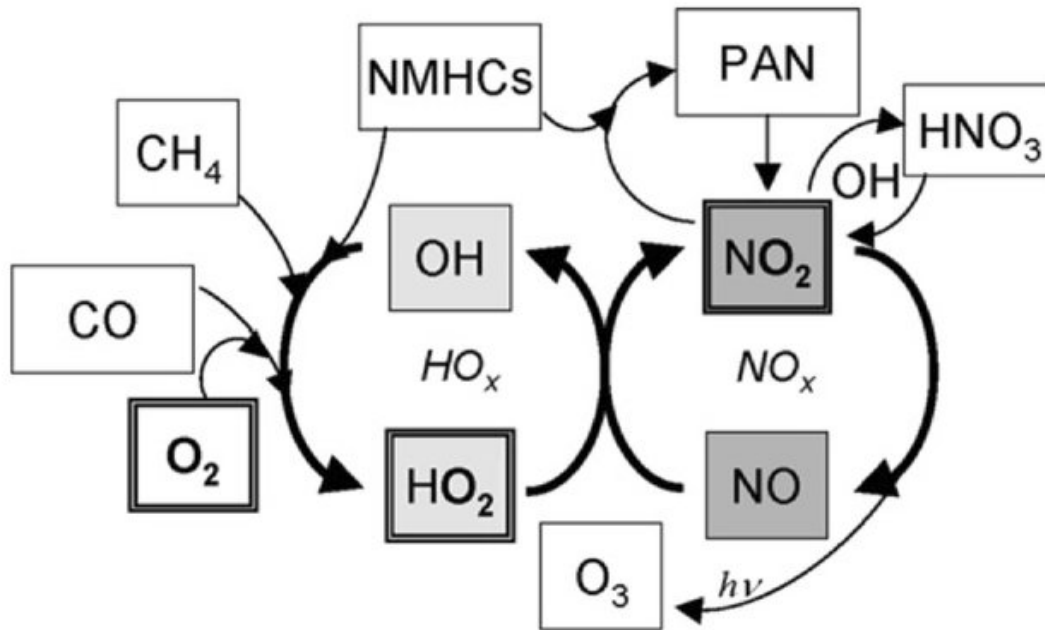


Figure 1-3 Ozone and methane formation/depletion cycle (Koch, 2013)

According to Morgenstern et al. (2013) study, methane increases have a significant impact on surface ozone, leading to an increase in ozone levels, particularly in certain regions and seasons. Methane's influence on ozone is stronger compared to other factors such as climate change and ozone recovery. In EU, CH₄ emission reductions can have a significant impact on reducing ground-level ozone not only in Europe but also worldwide. If global efforts consistently reduce CH₄ emissions to meet climate, air pollution, and other sustainability goals, it is estimated that by 2050, between 70,000 to 130,000 premature deaths annually can be avoided on a global scale. Specifically, within the European Union, this reduction in methane emissions could lead to the prevention of 6,000 to 11,000 premature deaths per year (Van Dingenen et al., 2018).

Ammonia (NH₃) is another emission emitted by the agricultural sector, primarily arising from livestock waste and the application of synthetic fertilizers. Gaseous NH₃ is the most prevalent alkaline and colorless gas present in the atmosphere, composed of nitrogen and hydrogen. As such, ammonia plays a significant role in the formation of atmospheric particulate matter, contributes to visibility degradation, and leads to atmospheric nitrogen deposition in sensitive ecosystems (Gong et al., 2013; Malherbe, L. et al., 2022; Sharma et al., 2007; Wyer et al., 2022). The primary source of this type of pollutant is agricultural activities, including the application of NH₃-based fertilizers.

Currently, global production of nitrogen (N) fertilizers stands at approximately 150 thousand tons of N per year, while the combined supply of ammonia, phosphoric acid, and potash fertilizers from 2015 to 2020 amounted to around 200 thousand tons per year (Food and Agriculture Organization of the United Nations [FAO], 2017).

Agricultural activities are responsible for approximately 81% of global ammonia emissions. In the EU, ammonia contributes to approximately 50% of PM_{2.5} air pollution, while in the United States (US), it accounts for around 30% of PM_{2.5} pollution levels. These statistics underscore the significant role of agriculture in ammonia emissions and its substantial contribution to PM_{2.5} air pollution in these regions (Wyer et al., 2022). Sulfate–Nitrate–Ammonium (SNA) aerosols are the main dominate precursor of the secondary fine particulate matter formation as shown in Figure 1-4. The secondary inorganic aerosols (SIA) components in PM are ammonium (NH₄⁺), nitrate (NO₃), and sulfate (SO₄²⁻), which occur as ammonium nitrate (NH₄NO₃) and ammonium sulfate ((NH₄)₂SO₄), respectively, and are formed by the neutralization of nitric acid (HNO₃) and sulfuric acid (H₂SO₄) with ammonia.

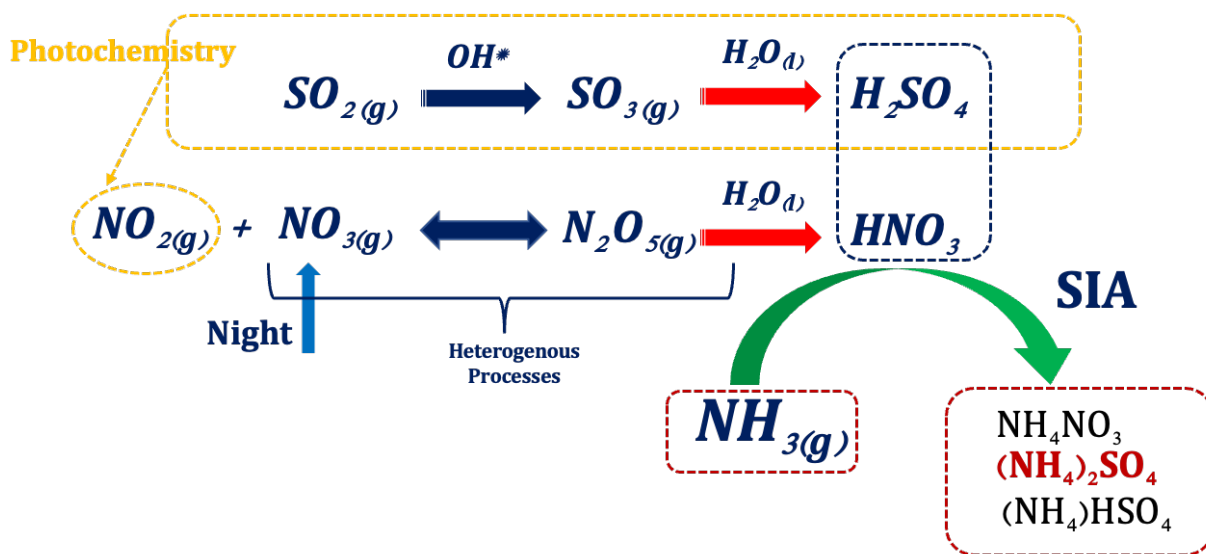


Figure 1-4 Secondary Inorganic Aerosol Formation (Pandis et al., 1992; Seinfeld & Pandis, 2016)

Ammonium sulfate [(NH₄)₂SO₄] is the most stable solid form in the atmosphere because of its low vapor pressure (Scott, W. D., & Cattell, F. C. R. 1979). So, it is a one of the common components of PM_{2.5} in the atmosphere. Moreover, because nitrogen oxides react in the atmosphere to generate

nitric acid vapor, which can combine with ammonia gas to form particulate ammonium nitrate, atmospheric nitrate is essentially secondary. However, when gas phase $\text{SO}_3/\text{H}_2\text{SO}_4/$ acidic particles coexist with NH_4NO_3 particles in the atmosphere, nitric acid will be released and substituted with H_2SO_4 to form acidic ammonium hydrogen sulfate (NH_4HSO_4) particles due to their higher volatilities.

Wang et al. (2013) have simulated sulfate-nitrate-ammonium aerosols over China: Response to 2000-2015 emission changes of sulfur dioxide, nitrogen oxides, and ammonia using a chemical transport model. they found that Annual mean SNA concentrations in China increased by around 60% between 2000 and 2006, owing to increases in SO_2 and NO_x emissions of 60% and 80%, respectively. Sulfate is the main component of SNA over South China (SC) and the Sichuan Basin (SCB) during this era, while nitrate and sulfate contribute equally over North China (NC). However, does not explicitly specify the sources of these emissions, including whether they are from agricultural activities. According to Ye et al. (2019), they found that Annual $\text{PM}_{2.5}$ concentration could be reduced by 5.7% when NH_3 emission from agriculture cut by 47% while to mitigate the ammonia emission could be potential to reduce the level of nitrate in the air.

To address these challenges, sustainable agricultural practices have been promoted to reduce the environmental impact of farming. These include organic farming, reduced pesticide use, improved nutrient management, agroforestry, and no-till farming. Additionally, transitioning to more plant-based diets can reduce the environmental impact of livestock agriculture.

1.4 Global mortality related to ambient air pollution exposure.

According to UNEP report (2021), 99% of global population live in place where the air quality is lower than WHO guideline standard as shown in Figure 1-5. In 2019, approximately four million individuals lost their lives due to exposure fine particulate outdoor air pollution. The regions experiencing the most severe consequences, with the highest mortality rates, were East Asia and Central Europe. $\text{PM}_{2.5}$ air pollution is associated with a range of severe health conditions, with the most life-threatening ones being stroke, heart disease, lung disease, including lower respiratory diseases like pneumonia, and cancer. Furthermore, elevated levels of fine particles can exacerbate

existing health issues such as diabetes. Additionally, this pollution can impede cognitive development in children and also contribute to mental health problems (Mazidi & Speakman, 2017; Requia et al., 2017).

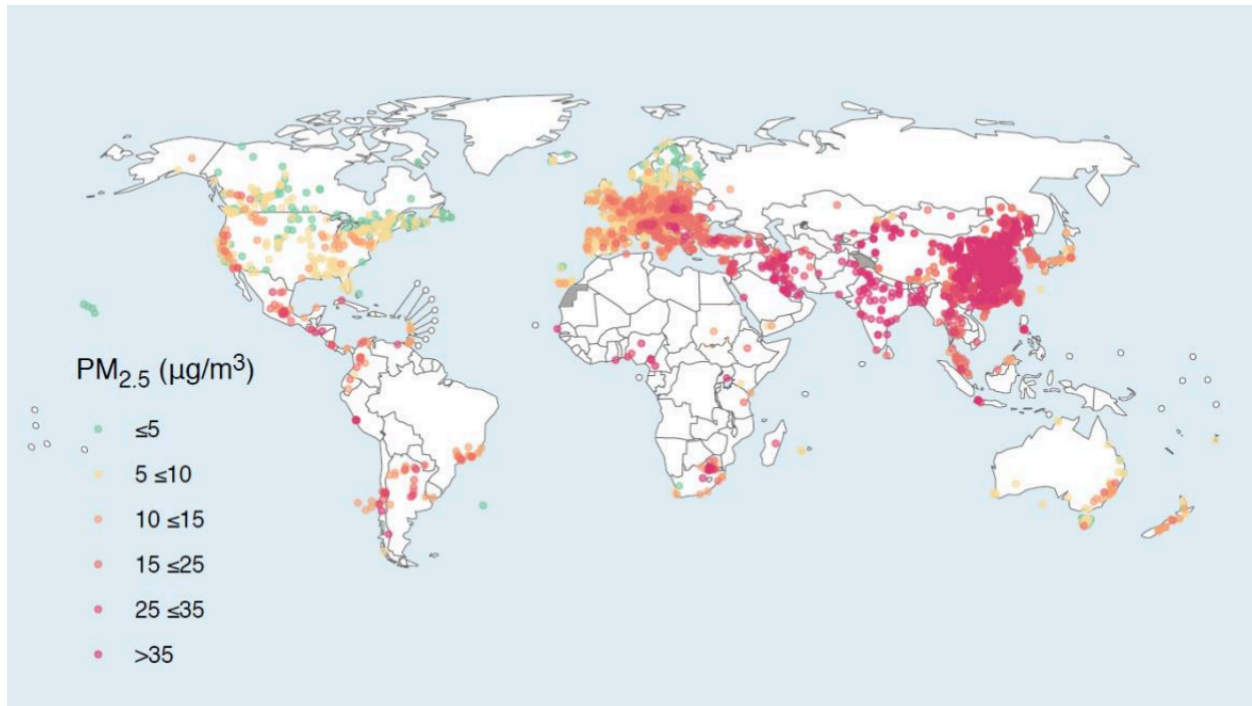


Figure 1-5 Locations settlements with data on PM_{2.5} concentrations, 2010–2019 (WHO, 2023)

Children and the elderly face the most acute impacts of air pollution, with alarming statistics indicating that approximately 17 million infants worldwide are exposed to polluted air, as reported by the United Nations Children's Fund (UNICEF). In the case of newborns, numerous studies have unequivocally demonstrated that exposure to particulate matter (PM) is linked to adverse outcomes, notably including low birth weight and preterm birth (Dugandzic et al., 2006; Pope et al., 2010; Rogers & Dunlop, 2006). Furthermore, such exposure heightens the risk of lower respiratory infections in infants (Colley et al., 1973; Gordon et al., 2014; Smith et al., 2000). Conversely, the elderly population is equally vulnerable to the detrimental effects of air pollution. Prolonged exposure to polluted air over the course of their lives is associated with the development of non-communicable diseases, including but not limited to ischemic heart disease, stroke, chronic obstructive pulmonary disease (COPD), lung cancer, and type 2 diabetes (Bentayeb et al., 2013; Dehghani et al., 2023).

Among low and middle-income countries, the Southeast Asia region suffered the most devastating impact, with a staggering 1,332,000 deaths attributed to ambient air pollution. The Western Pacific region closely followed, recording 1,255,000 deaths. Meanwhile, Africa reported 425,000 premature deaths due to poor air quality, highlighting the severity of the issue on the continent. The Eastern Mediterranean region documented 319,000 such deaths, while Europe and the Americas reported 304,000 and 164,000 deaths, respectively. These figures underscore the dire consequences of inadequate air quality control measures and emphasize the urgent need for targeted interventions in these regions.

In contrast, high-income countries, while not immune to air pollution's adverse effects, experienced relatively lower mortality rates. European high-income nations reported 205,000 deaths due to ambient air pollution, followed by the Americas with 95,000 deaths. The Western Pacific high-income countries registered 82,000 deaths, and the Eastern Mediterranean reported the lowest figure, with 17,000 premature deaths. Though the numbers are comparatively lower in these regions, they should not diminish the global urgency to combat air pollution, which remains a critical public health concern worldwide. Addressing this issue at both local and global levels is imperative to protect the health and well-being of populations around the world.

According to Silva et al. (2017) study about the future global mortality from air pollution associated to climate change. They found that under the RCP8.5 scenario, it has been determined that there will be around 3,340 ozone-related deaths in 2030 and 43,600 ozone-related deaths in 2100 when compared to the climate conditions that existed in the year 2000. As for PM_{2.5}, it is projected that in 2030, approximately 55,600 deaths can be attributed to climate change. By the year 2100, this estimate for PM_{2.5}-related deaths is expected to increase to 215,000, again, when compared to the climate conditions of the year 2000. The estimated premature mortality attributable to climate change is expected to be positive in all regions except for Africa. The highest impact is anticipated in India and East Asia.

1.5 Agricultural implication related to air pollution.

Air pollution can have several significant agricultural implications, as it can directly and indirectly affect crop yields, soil health, and overall farm productivity.

High level of air pollution especially ground surface O₃ could be an important factor which can damage crops production and reduce their yield (Chuwah et al., 2015; Felzer et al., 2007; Pandya et al., 2022). O₃ can reduce crop the net primary production (NPP) leading to reducing the leaf-level photosynthetic rate (Ainsworth et al., 2012; Ren et al., 2007, 2011). Moreover, O₃ can harm plants by entering through the stomata on leaves and oxidizing with the plant tissues during the respiration process. This oxidative process can lead to damage and burning of the leaves (Gheorghe & Ion, 2011).

The table below provides specific examples of responses. Wheat, peas, beans, and onions are among the crops that exhibit sensitivity to ozone with respect to their yield. Potato, barley, and maize are moderately sensitive crops, while oats display lower sensitivity to ozone, as noted by Mills et al. (2011).

Table 1-1 Examples of species-specific responses to O₃

Species	Response	Reference
Wheat	Reduced yield	Pleijel et al. (2006)
Tomato	Reduced yield	Calvo et al. (2007)
Potato	Reduced yield	Vandermeiren et al. (2005)
Lettuce	Visible leaf injury	Goumenaki et al. (2007)
Trifolium repens	Reduced biomass	Hayes et al. (2007)
Maize	Reduced yield	Wedow et al. (2021)
Rice	Reduced yield	Kats et al. (1985)

The influence of O₃ on agricultural outcomes exhibits notable regional disparities attributable to variations in O₃ concentration and climatic conditions (Eitzinger et al., 2013; Lobell & Gourdj, 2012; Meleux et al., 2007). The diversity in O₃ levels across different regions stems from different sources of ozone precursors, such as industrial and traffic emission. Typically, urban and industrial areas exhibit elevated ozone concentrations, posing a heightened risk to crop health. The interaction between O₃ and crop is also influenced by climatic parameters like temperature, humidity, and sunlight, each contributing to the agricultural impacts.

For example, higher temperatures can intensify the rate at which plants assimilate ozone, potentially exacerbating the detrimental effects on crops. Furthermore, the duration of ozone exposure emerges as a pivotal determinant. Prolonged exposure to elevated ozone levels can lead to more substantial agricultural losses, particularly in regions experiencing extended episodes of ozone pollution (L. Emberson, 2020).

Crucially, the developmental stage of the crop also plays a pivotal role in shaping the results of ozone exposure. For instance, the deleterious effects of ozone during critical growth phases, such as flowering and fruiting, can substantially diminish crop yields when compared to damage incurred during the vegetative growth stage (L. D. Emberson et al., 2018; Heagle, 1989). This intricate interplay of regional, climatic, and developmental factors underscores the multifaceted nature of O₃'s impact on agriculture.

In India, which is one of the highly polluted regions, numerous studies have indicated that O₃ can induce crop damage. For instance, Ghude et al. (2014) discovered that the impact of Ozone-induced crop damage in India is substantial, potentially jeopardizing the food supply for up to 94 million people. They also determined that wheat is the crop most severely damaged by ozone (O₃), with an estimated loss of approximately -3.5 ± 0.8 million tons (Mt) during the first decade of the 21st century. In China, Y. Wang et al. (2022) found that during the winter season, national wheat production losses increased by 82% from 2014 to 2017 due to rising levels of O₃. Additionally, a study focusing on maize production revealed that the average annual loss of maize caused by ozone pollution amounted to approximately 4.234 million tons during the period of 2013–2015, representing 1.9% of the average maize output (Yi et al., 2020).

Air pollutants, such as sulfur dioxide (SO₂) and nitrogen oxides (NO_x), can directly harm plant health by interfering with nutrient uptake and photosynthesis. These pollutants can also cause visible symptoms like leaf discoloration and necrosis (Shukla et al., 2008). In addition, SO₂ and NO_x can lead to soil acidification when they are deposited on the ground as acid rain. Acidic soils can inhibit the availability of essential nutrients like calcium, magnesium, and potassium, which are vital for plant growth (Haynes, 1982; McCauley et al., 2009; Sarwar et al., 2010). As a result, plants may struggle to take up these nutrients from the soil, leading to nutrient deficiencies.

Particulate matter (PM) in the atmosphere can have several adverse effects on crops and agricultural systems. For example, it could be lower crop yields by disrupt the photosynthesis process. High concentrations of PM_{2.5} can block sunlight and reduce the amount of light reaching plant leaves (Gheorghe & Ion, 2011). In addition, when the particle attached on the plant leaves, it can interfere with the plant's ability to carry out essential functions, such as transpiration and gas exchange (K. Kim et al., 2022; Li et al., 2019; Ryu et al., 2019). PM_{2.5} can interact with other air pollutants, such as O₃ and NO_x, to create secondary pollutants that can further harm crops and the environment.

1.6 Co-benefit of climate change mitigation policy on future GHGs and air pollution.

Climate change and air pollution are closely interconnected environmental issues that have significant impacts on the planet and human health. Numerous of the same activities that release GHGs also emit air pollutants that can degrade air quality. Climate change and air pollution often interact synergistically. For example, higher temperatures can enhance the formation of ground-level O₃, deteriorating air quality. Additionally, wildfires, exacerbated by climate change, release large amounts of air pollutants, and contribute to unfavorable air quality. Thus, to mitigate climate change, we can simultaneously address air pollution in both direct and indirect way.

Under low-carbon pathways aligned with the objective of limiting global warming to either 2 °C or, preferably, 1.5 °C, it is feasible to simultaneously address the problem of poor air quality. Emissions of pollutants such as SO₂, NO_x, and particulate matter, which primarily result from human activities, can be effectively reduced. According to a study by Rafaj et al. (2021), the trends

in emission reductions under both the 1.5°C and 2°C climate targets show a significant and noteworthy improvement when compared to current emission levels. By the year 2050, emissions of primary PM_{2.5} and their precursors decrease by approximately one-third in the low-carbon scenarios when compared to levels observed in 2015. These reductions more than double when comprehensive decarbonization policies are coupled with ambitious measures aimed at controlling air pollution. In addition, to meet the 1.5 degree limiting target, it is necessary to control the level of CH₄ which is one of the important GHGs. While CO₂ is the most prevalent greenhouse gas emitted by human activities, methane is much more effective at trapping heat in the atmosphere. If CH₄ continues to increase in the atmosphere, it could contribute to temperature rise through its Radiative Forcing (RF) effect (Cain et al., 2022). Changing of CH₄ concentration will affect the level of ground surface O₃ as mentioned in section 1.3.

Dietary change can play a significant role in climate change mitigation (Jarmul et al., 2020; Stehfest et al., 2009). The production and consumption of food has a substantial impact on greenhouse gas emissions and other environmental factors that contribute to climate change. Here are some keyways in which dietary change can contribute to climate change mitigation. The EAT-Lancet Commission, also known as the EAT-Lancet Commission on Healthy Diets from Sustainable Food Systems, is a collaborative effort between the EAT Foundation and The Lancet, a well-respected medical journal. This commission was established to address the interconnected global challenges of achieving a healthy diet for a growing global population while also promoting sustainability and reducing the environmental impact of food production. The EAT-Lancet Commission's work is closely related to addressing climate change through changes in dietary patterns and food systems (Hirvonen et al., 2020).

The production and consumption of food are significant contributors to greenhouse gas emissions, which are a primary driver of climate change (Aleksandrowicz et al., 2016; Bajželj et al., 2014; Vetter et al., 2017). The EAT-Lancet Commission acknowledges that diets rich in animal products, particularly red meat and dairy, have a higher environmental footprint due to the emissions associated with livestock production. By recommending a shift towards plant-based diets and reduced meat consumption, the commission aims to reduce the carbon footprint of the food system. Reducing GHGs from the food system can have indirect benefits for air quality by potentially

reducing some of the emissions associated with livestock farming. According to FAO report, total current emissions from global livestock amount to 7.1 gigatons of CO₂-equivalent per year, which constitutes approximately 14.5 percent of all anthropogenic GHGs (Gerber et al., 2013).

The EAT-Lancet Commission encourages more sustainable agricultural practices, including reduced use of synthetic fertilizers and pesticides (Willett et al., 2019). These practices can help reduce the release of air pollutants associated with agriculture, such as NH₃ and N₂O. These pollutants can contribute to smog formation and acid rain, negatively impacting air quality. They also consider deforestation and land-use change, particularly for expanding agricultural production. Deforestation not only contributes to climate change but can also release particulate matter and other pollutants into the air when forests are cleared through burning or other means. The commission advocates for reducing food waste, which can help lower greenhouse gas emissions associated with food production and disposal. It also indirectly contributes to air quality by reducing the organic waste sent to landfills, where it can generate CH₄, a potent greenhouse gas.

Although the interconnection between climate change and air quality is well-established, a significant research gap exists when it comes to exploring the potential role of agriculture and dietary changes as a crucial policy avenue for promoting a healthier society and reducing mortality rates attributed to poor nutrition. It is surprising that there is a dearth of comprehensive studies delving into the intricate relationship between dietary choices, climate change, and air quality. The majority of existing research primarily focuses on how dietary choices affect greenhouse gas emissions (GHGs) while giving minimal attention to their impact on air quality. Notably, there is limited research available on the role of dietary change in a scenario of climate change mitigation within an integrated policy framework. Thus, further investigation is needed to fill this critical research gap.

1.7 Research objective

The objective of this study is to explore the intricate relationships among climate change mitigation, agricultural practices, and air quality. This investigation will focus on the policy pathway involved and seek to ascertain their respective impacts and potential co-benefits. In this study, our scope will primarily concentrate on significant air pollutants, specifically PM_{2.5} and O₃, while also delving into the investigation of their precursor gases at the global scale. Additionally, this research also places a strong emphasis on the impact of horizontal resolution on the model outcomes. Consequently, we will conduct an in-depth evaluation of model accuracy between high- and low-resolution simulating to define the most appropriate resolution to be employed in the study.

1.8 Chapter organization

This thesis comprises six chapters, and the structure of the thesis, along with the interconnections between the chapters, is illustrated in Figure 1-6. This visualization offers readers a clear perspective on the organization of the thesis and provides guidance on the grouping of the chapters. The summary of the thesis contents is presented as follows:

In Chapter 2, this dissertation presents a comprehensive methodology employed in the study. The central focus of this thesis revolves around the utilization of AIM/Hub and GEOS-Chem as the primary models. Furthermore, an exposure model will be incorporated in our assessment of the impact. This chapter aims to provide a detailed insight into the research methodology, setting the stage for a rigorous investigation.

Chapter 3 will assess the influence of the horizontal resolution in the GEOS-Chem model by analyzing its results in comparison to ground monitoring station data. Additionally, this chapter will explore the implications of air pollution on both agriculture and public health. The findings in Chapter 3 will lay the groundwork for Chapters 4 and 5, as they will evaluate the performance of the GEOS-Chem model under various scenarios.

Chapter 4 delves deeper into the influence of ammonia emissions from the agricultural sector. We will explore this influence under various assumption reduction scenarios and assess its impact on PM_{2.5} and O₃ concentrations. To accomplish this, we will integrate the GEOS-Chem model with meteorological parameters and a health exposure model, offering a more comprehensive understanding of the subject. This chapter providing the foundation and data for understanding a relationship between agriculture and air quality.

Chapter 5 is dedicated to exploring the potential effects of practical recommendations aimed at reducing greenhouse gas emissions resulting from agricultural activities, with a particular focus on dietary changes. In this chapter, we will examine specific dietary modifications and their potential contributions to lowering GHG emissions. Additionally, we will assess how such changes may positively impact air quality and public health, providing valuable insights for policymakers and stakeholders.

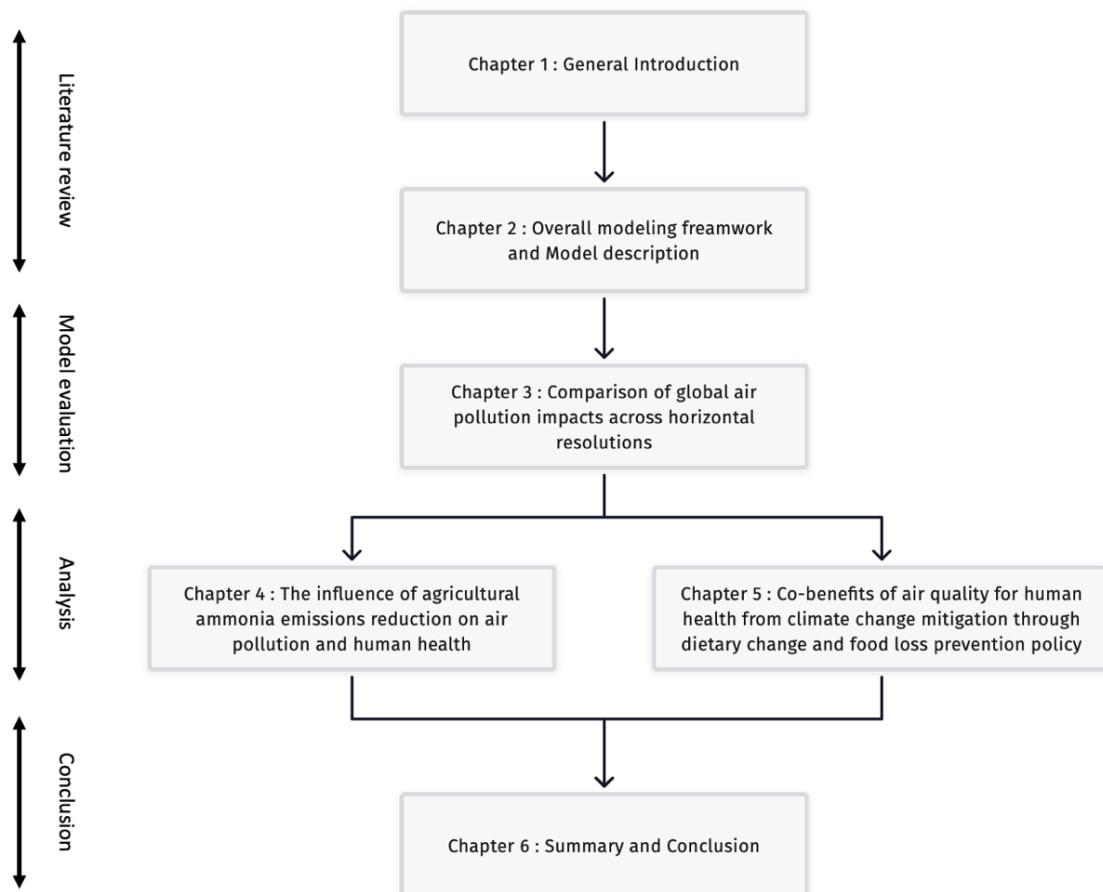


Figure 1-6 Chapter organization

1.9 Reference

- Adler, R. F., Gu, G., Sapiano, M., Wang, J.-J., & Huffman, G. J. (2017). Global precipitation: Means, variations and trends during the satellite era (1979–2014). *Surveys in Geophysics*, 38, 679–699.
- Adler, R. F., Sapiano, M. R., Huffman, G. J., Wang, J.-J., Gu, G., Bolvin, D., Chiu, L., Schneider, U., Becker, A., & Nelkin, E. (2018). The Global Precipitation Climatology Project (GPCP) monthly analysis (new version 2.3) and a review of 2017 global precipitation. *Atmosphere*, 9(4), 138.
- Ainsworth, E. A., Yendrek, C. R., Sitch, S., Collins, W. J., & Emberson, L. D. (2012). The effects of tropospheric ozone on net primary productivity and implications for climate change. *Annual Review of Plant Biology*, 63, 637–661.
- Aleksandrowicz, L., Green, R., Joy, E. J., Smith, P., & Haines, A. (2016). The impacts of dietary change on greenhouse gas emissions, land use, water use, and health: A systematic review. *PloS One*, 11(11), e0165797.
- Amann, M., Borken-Kleefeld, J., Cofala, J., Hettelingh, J.-P., Heyes, C., Höglund-Isaksson, L., Holland, M., Kiese Wetter, G., Klimont, Z., & Rafaj, P. (2014). *The final policy scenarios of the EU Clean Air Policy Package*.
- Andreae, M. O. (1995). Climatic effects of changing atmospheric aerosol levels. *World Survey of Climatology*, 16(06), 347–398.
- Aneja, V. P., Schlesinger, W. H., & Erisman, J. W. (2009). *Effects of agriculture upon the air quality and climate: Research, policy, and regulations*.
- Bajželj, B., Richards, K. S., Allwood, J. M., Smith, P., Dennis, J. S., Curmi, E., & Gilligan, C. A. (2014). Importance of food-demand management for climate mitigation. *Nature Climate Change*, 4(10), 924–929.
- Bentayeb, M., Simoni, M., Norback, D., Baldacci, S., Maio, S., Viegi, G., & Annesi-Maesano, I. (2013). Indoor air pollution and respiratory health in the elderly. *Journal of Environmental Science and Health, Part A*, 48(14), 1783–1789.
- Borlina, C. S., & Rennó, N. O. (2017). The impact of a severe drought on dust lifting in California's Owens Lake Area. *Scientific Reports*, 7(1), 1784.
- Boucher, O., & Boucher, O. (2015). *Atmospheric aerosols*. Springer.

- Cain, M., Jenkins, S., Allen, M. R., Lynch, J., Frame, D. J., Macey, A. H., & Peters, G. P. (2022). Methane and the Paris Agreement temperature goals. *Philosophical Transactions of the Royal Society A*, 380(2215), 20200456.
- Calvo, E., Martin, C., & Sanz, M. (2007). Ozone sensitivity differences in five tomato cultivars: Visible injury and effects on biomass and fruits. *Water, Air, and Soil Pollution*, 186(1–4), 167–181.
- Chuwah, C., van Noije, T., van Vuuren, D. P., Stehfest, E., & Hazeleger, W. (2015). Global impacts of surface ozone changes on crop yields and land use. *Atmospheric Environment*, 106, 11–23.
- Colley, J., Douglas, J., & Reid, D. (1973). Respiratory disease in young adults: Influence of early childhood lower respiratory tract illness, social class, air pollution, and smoking. *Br Med J*, 3(5873), 195–198.
- Colls, J. (2002). *Air pollution*. Taylor & Francis.
- Cook, B. I., Miller, R. L., & Seager, R. (2009). Amplification of the North American “Dust Bowl” drought through human-induced land degradation. *Proceedings of the National Academy of Sciences*, 106(13), 4997–5001.
- Crutzen, P. (1973), A discussion of the chemistry of some minor constituents in the stratosphere and troposphere, *Pure Appl. Geophys.*, 106–108, 1385–1399.
- Dawson, J., Adams, P., & Pandis, S. (2007). Sensitivity of PM 2.5 to climate in the Eastern US: a modeling case study. *Atmospheric Chemistry and Physics*, 7(16), 4295–4309.
- Dehghani, S., Yousefi, S., Oskoei, V., Tazik, M., Moradi, M. S., Shaabani, M., & Vali, M. (2023). Ecological study on household air pollution exposure and prevalent chronic disease in the elderly. *Scientific Reports*, 13(1), 11763.
- Dugandzic, R., Dodds, L., Stieb, D., & Smith-Doiron, M. (2006). The association between low level exposures to ambient air pollution and term low birth weight: A retrospective cohort study. *Environmental Health*, 5, 1–8.
- Eitzinger, J., Trnka, M., Semerádová, D., Thaler, S., Svobodová, E., Hlavinka, P., Šiška, B., Takáč, J., Malatinská, L., & Nováková, M. (2013). Regional climate change impacts on agricultural crop production in Central and Eastern Europe—hotspots, regional differences and common trends. *The Journal of Agricultural Science*, 151(6), 787–812.

- Emberson, L. (2020). Effects of ozone on agriculture, forests and grasslands. *Philosophical Transactions of the Royal Society A*, 378(2183), 20190327.
- Emberson, L. D., Pleijel, H., Ainsworth, E. A., Van den Berg, M., Ren, W., Osborne, S., Mills, G., Pandey, D., Dentener, F., & Büker, P. (2018). Ozone effects on crops and consideration in crop models. *European Journal of Agronomy*, 100, 19–34.
- Fadnavis, S., Mahajan, A. S., Choudhury, A. D., Roy, C., Singh, M., Biswas, M. S., Pandithurai, G., Prabhakaran, T., Lal, S., & Venkatraman, C. (2020). Atmospheric aerosols and trace gases. *Assessment of Climate Change over the Indian Region: A Report of the Ministry of Earth Sciences (MoES), Government of India*, 93–116.
- Felzer, B. S., Cronin, T., Reilly, J. M., Melillo, J. M., & Wang, X. (2007). Impacts of ozone on trees and crops. *Comptes Rendus Geoscience*, 339(11–12), 784–798.
- Feng, Z., Paoletti, E., Bytnerowicz, A., & Harmens, H. (2015). Ozone and plants. *Environmental Pollution*, 202, 215–216.
- Food and Agriculture Organization of the United Nations [FAO]. (2017). *World fertilizer trends and outlook to 2020. Summary Report*.
- Force, C. A. T., & Graham, J. (n.d.). *Fine Particulate Matter (PM_{2.5}) and Ozone (O₃) Air Quality in Western Pennsylvania in the 2000s*.
- Gerber, P. J., Steinfeld, H., Henderson, B., Mottet, A., Opio, C., Dijkman, J., Falcucci, A., & Tempio, G. (2013). *Tackling climate change through livestock: A global assessment of emissions and mitigation opportunities*. Food and Agriculture Organization of the United Nations (FAO).
- Gheorghe, I. F., & Ion, B. (2011). The effects of air pollutants on vegetation and the role of vegetation in reducing atmospheric pollution. *The Impact of Air Pollution on Health, Economy, Environment and Agricultural Sources*, 29, 241–280.
- Ghude, S. D., Jena, C., Chate, D., Beig, G., Pfister, G., Kumar, R., & Ramanathan, V. (2014). Reductions in India's crop yield due to ozone. *Geophysical Research Letters*, 41(15), 5685–5691.
- Ginoux, P., Prospero, J. M., Torres, O., & Chin, M. (2004). Long-term simulation of global dust distribution with the GOCART model: Correlation with North Atlantic Oscillation. *Environmental Modelling & Software*, 19(2), 113–128.

- Gong, L., Lewicki, R., Griffin, R. J., Tittel, F. K., Lonsdale, C. R., Stevens, R. G., Pierce, J. R., Malloy, Q. G., Travis, S. A., & Bobmanuel, L. M. (2013). Role of atmospheric ammonia in particulate matter formation in Houston during summertime. *Atmospheric Environment*, 77, 893–900.
- Gordon, S. B., Bruce, N. G., Grigg, J., Hibberd, P. L., Kurmi, O. P., Lam, K. H., Mortimer, K., Asante, K. P., Balakrishnan, K., & Balmes, J. (2014). Respiratory risks from household air pollution in low and middle income countries. *The Lancet Respiratory Medicine*, 2(10), 823–860.
- Goumenaki, E., Fernandez, I. G., Papanikolaou, A., Papadopoulou, D., Askianakis, C., Kouvarakis, G., & Barnes, J. (2007). Derivation of ozone flux-yield relationships for lettuce: A key horticultural crop. *Environmental Pollution*, 146(3), 699–706.
- Guo, L.-C., Zhang, Y., Lin, H., Zeng, W., Liu, T., Xiao, J., Rutherford, S., You, J., & Ma, W. (2016). The washout effects of rainfall on atmospheric particulate pollution in two Chinese cities. *Environmental Pollution*, 215, 195–202.
- Harizanova-Bartos, H., & Stoyanova, Z. (2018). *Impact of agriculture on air pollution*. 6, 1071–1076.
- Hasegawa, T., Fujimori, S., Havlík, P., Valin, H., Bodirsky, B. L., Doelman, J. C., Fellmann, T., Kyle, P., Koopman, J. F., & Lotze-Campen, H. (2018). Risk of increased food insecurity under stringent global climate change mitigation policy. *Nature Climate Change*, 8(8), 699–703.
- Hayes, F., Jones, M., Mills, G., & Ashmore, M. (2007). Meta-analysis of the relative sensitivity of semi-natural vegetation species to ozone. *Environmental Pollution*, 146(3), 754–762.
- Haynes, R. (1982). Effects of liming on phosphate availability in acid soils: A critical review. *Plant and Soil*, 68, 289–308.
- Heagle, A. S. (1989). Ozone and crop yield. *Annual Review of Phytopathology*, 27(1), 397–423.
- Hirvonen, K., Bai, Y., Headey, D., & Masters, W. A. (2020). Affordability of the EAT–Lancet reference diet: A global analysis. *The Lancet Global Health*, 8(1), e59–e66.
- Holland, M. (2014). *Cost-benefit analysis of final policy scenarios for the EU Clean Air Package*.
- Holman, C. (1999). Sources of air pollution. In *Air pollution and health* (pp. 115–148). Elsevier.
- Huber, D. G., & Gulledege, J. (2011). *Extreme weather and climate change: Understanding the link, managing the risk*. Pew Center on Global Climate Change Arlington.

- IEA. (2022). *Global Methane Tracker 2022*.
- IPCC, S. P. (2019). Climate change and land: An IPCC special report on climate change, desertification, land degradation, sustainable land management, food security, and greenhouse gas fluxes in terrestrial ecosystems. *International Consensus Regarding Land System Impacts of Climate Change as Of*.
- IQAir. (2022). *2022 World Air Quality Report*.
- Jacob, D. J., & Winner, D. A. (2009). Effect of climate change on air quality. *Atmospheric Environment*, 43(1), 51–63.
- Jain, P. (1993). Greenhouse effect and climate change: Scientific basis and overview. *Renewable Energy*, 3(4–5), 403–420.
- Jarmul, S., Dangour, A. D., Green, R., Liew, Z., Haines, A., & Scheelbeek, P. F. (2020). Climate change mitigation through dietary change: A systematic review of empirical and modelling studies on the environmental footprints and health effects of ‘sustainable diets.’ *Environmental Research Letters: ERL [Web Site]*, 15, 123014.
- Kahnert, M., & Devasthale, A. (2011). Black carbon fractal morphology and short-wave radiative impact: A modelling study. *Atmospheric Chemistry and Physics*, 11(22), 11745–11759.
- Kampa, M., & Castanas, E. (2008). Human health effects of air pollution. *Environmental Pollution*, 151(2), 362–367.
- Kats, G., Dawson, P. J., Bytnerowicz, A., Wolf, J. W., Thompson, C. R., & Olszyk, D. M. (1985). Effects of ozone or sulfur dioxide on growth and yield of rice. *Agriculture, Ecosystems & Environment*, 14(1–2), 103–117.
- Kim, K., Jeon, J., Jung, H., Kim, T. K., Hong, J., Jeon, G.-S., & Kim, H. S. (2022). PM_{2.5} reduction capacities and their relation to morphological and physiological traits in 13 landscaping tree species. *Urban Forestry & Urban Greening*, 70, 127526.
- Kim, S., Hong, K.-H., Jun, H., Park, Y.-J., Park, M., & Sunwoo, Y. (2014). Effect of precipitation on air pollutant concentration in Seoul, Korea. *Asian Journal of Atmospheric Environment*, 8(4), 202–211.
- Koch, A. (2013). *Climate impact mitigation potential given by flight profile and aircraft optimization*.

- Kok, J. F., Storelvmo, T., Karydis, V. A., Adebisi, A. A., Mahowald, N. M., Evans, A. T., He, C., & Leung, D. M. (2023). Mineral dust aerosol impacts on global climate and climate change. *Nature Reviews Earth & Environment*, 4(2), 71–86.
- Konisky, D. M., Hughes, L., & Kaylor, C. H. (2016). Extreme weather events and climate change concern. *Climatic Change*, 134, 533–547.
- Kulkarni, N., & Grigg, J. (2008). Effect of air pollution on children. *Paediatrics and Child Health*, 18(5), 238–243.
- Kuniyal, J. C., & Guleria, R. P. (2019). The current state of aerosol-radiation interactions: A mini review. *Journal of Aerosol Science*, 130, 45–54.
- Kweku, D. W., Bismark, O., Maxwell, A., Desmond, K. A., Danso, K. B., Oti-Mensah, E. A., Quachie, A. T., & Adormaa, B. B. (2018). Greenhouse effect: Greenhouse gases and their impact on global warming. *Journal of Scientific Research and Reports*, 17(6), 1–9.
- Langner, J., Engardt, M., Baklanov, A., Christensen, J., Gauss, M., Geels, C., Hedegaard, G. B., Nuterman, R., Simpson, D., & Soares, J. (2012). A multi-model study of impacts of climate change on surface ozone in Europe. *Atmospheric Chemistry and Physics*, 12(21), 10423–10440.
- Li, Y., Wang, Y., Wang, B., Wang, Y., & Yu, W. (2019). The response of plant photosynthesis and stomatal conductance to fine particulate matter (PM 2.5) based on leaf factors analyzing. *Journal of Plant Biology*, 62, 120–128.
- Liao, H., Chen, W., & Seinfeld, J. H. (2006). Role of climate change in global predictions of future tropospheric ozone and aerosols. *Journal of Geophysical Research: Atmospheres*, 111(D12).
- Lichtenberg, E. (2002). Agriculture and the environment. *Handbook of Agricultural Economics*, 2, 1249–1313.
- Lin, C., Huang, R.-J., Ceburnis, D., Buckley, P., Preissler, J., Wenger, J., Rinaldi, M., Facchini, M. C., O’Dowd, C., & Ovadnevaite, J. (2018). Extreme air pollution from residential solid fuel burning. *Nature Sustainability*, 1(9), 512–517.
- Lobell, D. B., & Gourdji, S. M. (2012). The influence of climate change on global crop productivity. *Plant Physiology*, 160(4), 1686–1697.
- Longhurst, J., Barnes, J., Chatterton, T., Hayes, E., & Williams, W. (2016). Progress with air quality management in the 60 years since the UK clean air act, 1956. Lessons, failures,

- challenges and opportunities. *International Journal of Sustainable Development and Planning*, 11(4), 491–499.
- Madronich, S. (1993). Tropospheric photochemistry and its response to UV changes. In *The role of the stratosphere in global change* (pp. 437–461). Springer.
- Mahmoud, S. H., & Gan, T. Y. (2018). Impact of anthropogenic climate change and human activities on environment and ecosystem services in arid regions. *Science of the Total Environment*, 633, 1329–1344.
- Malashock, D. A., Delang, M. N., Becker, J. S., Serre, M. L., West, J. J., Chang, K.-L., Cooper, O. R., & Anenberg, S. C. (2022). Global trends in ozone concentration and attributable mortality for urban, peri-urban, and rural areas between 2000 and 2019: A modelling study. *The Lancet Planetary Health*, 6(12), e958–e967.
- Malherbe, L., German, R., Couvidat, F., Zanatta, L., Blannin, L., James, A., Létinois, L., Schucht, S., Berthelot, B., & Raoult, J. (2022). *Emissions of ammonia and methane from the agricultural sector. Emissions from livestock farming (Eionet Report—ETC HE 2022/21)*. European Topic Centre on Human Health and the Environment.
- Mazidi, M., & Speakman, J. R. (2017). Ambient particulate air pollution (PM_{2.5}) is associated with the ratio of type 2 diabetes to obesity. *Scientific Reports*, 7(1), 9144.
- McBean, G. (2004). Climate change and extreme weather: A basis for action. *Natural Hazards*, 31, 177–190.
- McCauley, A., Jones, C., & Jacobsen, J. (2009). Soil pH and organic matter. *Nutrient Management Module*, 8(2), 1–12.
- Meleux, F., Solmon, F., & Giorgi, F. (2007). Increase in summer European ozone amounts due to climate change. *Atmospheric Environment*, 41(35), 7577–7587.
- Mills, G., Hayes, F., Norris, D., Hall, J., Coyle, M., Cambridge, H., Cinderby, S., Abott, J., Cooke, S., & Murrells, T. (2011). *Impacts of ozone pollution on food security in the UK: a case study for two contrasting years, 2006 and 2008*.
- Morgenstern, O., Zeng, G., Luke Abraham, N., Telford, P. J., Braesicke, P., Pyle, J. A., Hardiman, S. C., O'Connor, F. M., & Johnson, C. E. (2013). Impacts of climate change, ozone recovery, and increasing methane on surface ozone and the tropospheric oxidizing capacity. *Journal of Geophysical Research: Atmospheres*, 118(2), 1028–1041.

- NOAA National Centers for Environmental Information, Monthly Global Climate Report for Annual 2022, published online January 2023, retrieved on January 18, 2024 from <https://www.ncei.noaa.gov/access/monitoring/monthly-report/global/202213>.
- Pandis, S. N., Harley, R. A., Cass, G. R., & Seinfeld, J. H. (1992). Secondary organic aerosol formation and transport. *Atmospheric Environment. Part A. General Topics*, 26(13), 2269–2282.
- Pandya, S., Gadekallu, T. R., Maddikunta, P. K. R., & Sharma, R. (2022). A study of the impacts of air pollution on the agricultural community and yield crops (Indian context). *Sustainability*, 14(20), 13098.
- Philip, S., Martin, R. V., van Donkelaar, A., Lo, J. W.-H., Wang, Y., Chen, D., Zhang, L., Kasibhatla, P. S., Wang, S., & Zhang, Q. (2014). Global chemical composition of ambient fine particulate matter for exposure assessment. *Environmental Science & Technology*, 48(22), 13060–13068.
- Pleijel, H., Eriksen, A. B., Danielsson, H., Bondesson, N., & Selldén, G. (2006). Differential ozone sensitivity in an old and a modern Swedish wheat cultivar—Grain yield and quality, leaf chlorophyll and stomatal conductance. *Environmental and Experimental Botany*, 56(1), 63–71.
- Pope, D. P., Mishra, V., Thompson, L., Siddiqui, A. R., Rehfuss, E. A., Weber, M., & Bruce, N. G. (2010). Risk of low birth weight and stillbirth associated with indoor air pollution from solid fuel use in developing countries. *Epidemiologic Reviews*, 32(1), 70–81.
- Popescu, F., & Ionel, I. (2010). Anthropogenic air pollution sources. *Air Quality*, 1–22.
- Rafaj, P., Kieseewetter, G., Krey, V., Schoepp, W., Bertram, C., Drouet, L., Fricko, O., Fujimori, S., Harmsen, M., & Hilaire, J. (2021). Air quality and health implications of 1.5° C–2° C climate pathways under considerations of ageing population: A multi-model scenario analysis. *Environmental Research Letters*, 16(4), 045005.
- Rajesh, T., & Ramachandran, S. (2018). Black carbon aerosols over urban and high altitude remote regions: Characteristics and radiative implications. *Atmospheric Environment*, 194, 110–122.
- Reidmiller, D. R., Avery, C. W., Easterling, D. R., Kunkel, K. E., Lewis, K. L., Maycock, T. K., & Stewart, B. C. (2017). *Impacts, risks, and adaptation in the United States: Fourth national climate assessment, volume II*.

- Ren, W., Tian, H., Chen, G., Liu, M., Zhang, C., Chappelka, A. H., & Pan, S. (2007). Influence of ozone pollution and climate variability on net primary productivity and carbon storage in China's grassland ecosystems from 1961 to 2000. *Environmental Pollution*, *149*(3), 327–335.
- Ren, W., Tian, H., Tao, B., Chappelka, A., Sun, G., Lu, C., Liu, M., Chen, G., & Xu, X. (2011). Impacts of tropospheric ozone and climate change on net primary productivity and net carbon exchange of China's forest ecosystems. *Global Ecology and Biogeography*, *20*(3), 391–406.
- Requia, W. J., Adams, M. D., & Koutrakis, P. (2017). Association of PM_{2.5} with diabetes, asthma, and high blood pressure incidence in Canada: A spatiotemporal analysis of the impacts of the energy generation and fuel sales. *Science of the Total Environment*, *584*, 1077–1083.
- Rogers, J. F., & Dunlop, A. L. (2006). Air pollution and very low birth weight infants: A target population? *Pediatrics*, *118*(1), 156–164.
- Ryu, J., Kim, J. J., Byeon, H., Go, T., & Lee, S. J. (2019). Removal of fine particulate matter (PM_{2.5}) via atmospheric humidity caused by evapotranspiration. *Environmental Pollution*, *245*, 253–259.
- Sarwar, N., Saifullah, Malhi, S. S., Zia, M. H., Naeem, A., Bibi, S., & Farid, G. (2010). Role of mineral nutrition in minimizing cadmium accumulation by plants. *Journal of the Science of Food and Agriculture*, *90*(6), 925–937.
- Scott, W. D., & Cattell, F. C. R. (1979). Vapor pressure of ammonium sulfates. *Atmospheric Environment* (1967), *13*(2), 307–317.
- Seinfeld, J. H., & Pandis, S. N. (2016). *Atmospheric chemistry and physics: From air pollution to climate change*. John Wiley & Sons.
- Sharma, M., Kishore, S., Tripathi, S., & Behera, S. (2007). Role of atmospheric ammonia in the formation of inorganic secondary particulate matter: A study at Kanpur, India. *Journal of Atmospheric Chemistry*, *58*(1), 1–17.
- Shukla, S. K., Nagpure, A., Kumar, V., Baby, S., Shrivastava, P., Singh, D., & Shukla, R. (2008). Impact of dust emission on plant vegetation in the vicinity of cement plant. *Environmental Engineering and Management Journal*, *7*(1), 31–35.
- Silva, R. A., West, J. J., Lamarque, J.-F., Shindell, D. T., Collins, W. J., Faluvegi, G., Folberth, G. A., Horowitz, L. W., Nagashima, T., Naik, V., Rumbold, S. T., Sudo, K., Takemura, T.,

- Bergmann, D., Cameron-Smith, P., Doherty, R. M., Josse, B., MacKenzie, I. A., Stevenson, D. S., & Zeng, G. (2017). Future global mortality from changes in air pollution attributable to climate change. *Nature Climate Change*, 7(9), 647–651. <https://doi.org/10.1038/nclimate3354>
- Singh, K., & Tripathi, D. (2021). Particulate matter and human health. *Environmental Health*.
- Smith, K. R., Samet, J. M., Romieu, I., & Bruce, N. (2000). Indoor air pollution in developing countries and acute lower respiratory infections in children. *Thorax*, 55(6), 518–532.
- Spickett, J. T., Brown, H., & Rumchev, K. (2011). Climate change and air quality: The potential impact on health. *Asia Pacific Journal of Public Health*, 23(2_suppl), 37S-45S.
- Stehfest, E., Bouwman, L., Van Vuuren, D. P., Den Elzen, M. G., Eickhout, B., & Kabat, P. (2009). Climate benefits of changing diet. *Climatic Change*, 95(1–2), 83–102.
- United Nations Environment Programme. (2021). *Actions on air quality: A global summary of policies and programmes to reduce air pollution*.
- Van Dingenen, R., Crippa, M., Anssens-Maenhout, G., Guizzardi, D., & Dentener, F. (2018). Global trends of methane emissions and their impacts on ozone concentrations. *JRC Science for Policy Report*.
- Van Donkelaar, A., Martin, R. V., Li, C., & Burnett, R. T. (2019). Regional estimates of chemical composition of fine particulate matter using a combined geoscience-statistical method with information from satellites, models, and monitors. *Environmental Science & Technology*, 53(5), 2595–2611.
- Vandermeiren, K., Black, C., Pleijel, H., & De Temmerman, L. (2005). Impact of rising tropospheric ozone on potato: Effects on photosynthesis, growth, productivity and yield quality. *Plant, Cell & Environment*, 28(8), 982–996.
- Vetter, S. H., Sapkota, T. B., Hillier, J., Stirling, C. M., Macdiarmid, J. I., Aleksandrowicz, L., Green, R., Joy, E. J., Dangour, A. D., & Smith, P. (2017). Greenhouse gas emissions from agricultural food production to supply Indian diets: Implications for climate change mitigation. *Agriculture, Ecosystems & Environment*, 237, 234–241.
- Wang, R., Cui, K., Sheu, H.-L., Wang, L.-C., & Liu, X. (2023). Effects of Precipitation on the Air Quality Index, PM_{2.5} Levels and on the Dry Deposition of PCDD/Fs in the Ambient Air. *Aerosol and Air Quality Research*, 23(4), 220417.

- Wang, Y., Wild, O., Ashworth, K., Chen, X., Wu, Q., Qi, Y., & Wang, Z. (2022). Reductions in crop yields across China from elevated ozone. *Environmental Pollution*, 292, 118218.
- Wang, Y., Zhang, Q., He, K., Zhang, Q., & Chai, L. (2013). Sulfate-nitrate-ammonium aerosols over China: Response to 2000–2015 emission changes of sulfur dioxide, nitrogen oxides, and ammonia. *Atmospheric Chemistry and Physics*, 13(5), 2635–2652.
- Weart, S. (2008). The carbon dioxide greenhouse effect. *The Discovery of Global Warming. American Institute of Physics*.
- Wedow, J. M., Burroughs, C. H., Rios Acosta, L., Leakey, A. D., & Ainsworth, E. A. (2021). Age-dependent increase in α -tocopherol and phytosterols in maize leaves exposed to elevated ozone pollution. *Plant Direct*, 5(2), e00307.
- WHO. (2023). *WHO Ambient Air Quality Database (update 2023)* (Version 6.0). World Health Organization.
- Willett, W., Rockström, J., Loken, B., Springmann, M., Lang, T., Vermeulen, S., Garnett, T., Tilman, D., DeClerck, F., & Wood, A. (2019). Food in the Anthropocene: The EAT–Lancet Commission on healthy diets from sustainable food systems. *The Lancet*, 393(10170), 447–492.
- Wu, Y., Wen, B., Li, S., & Guo, Y. (2021). Sand and dust storms in Asia: A call for global cooperation on climate change. *The Lancet Planetary Health*, 5(6), e329–e330.
- Wyer, K. E., Kelleghan, D. B., Blanes-Vidal, V., Schaubberger, G., & Curran, T. P. (2022). Ammonia emissions from agriculture and their contribution to fine particulate matter: A review of implications for human health. *Journal of Environmental Management*, 323, 116285.
- Ye, Z., Guo, X., Cheng, L., Cheng, S., Chen, D., Wang, W., & Liu, B. (2019). Reducing PM_{2.5} and secondary inorganic aerosols by agricultural ammonia emission mitigation within the Beijing-Tianjin-Hebei region, China. *Atmospheric Environment*, 219, 116989.
- Yi, F., Feng, J., Wang, Y., & Jiang, F. (2020). Influence of surface ozone on crop yield of maize in China. *Journal of Integrative Agriculture*, 19(2), 578–589.
- Zhao, Y., & Kim, B. (2022). Environmental regulation and chronic conditions: Evidence from China's air pollution prevention and control action plan. *International Journal of Environmental Research and Public Health*, 19(19), 12584.

Chapter 2

Model Description

2.1 Overall modeling framework

In this study, AIM/Hub and GEOS-Chem serve as the fundamental models. These models are employed to estimate GHGs and air pollutants across various scenarios. The AIM/Hub model is applied in conjunction with SSPs and social assumption data to predict emissions. Subsequently, these emissions are spatially represented using the AIM/DS model, which is based on sources and emission data, and this information is then integrated with the GEOS-Chem model. The GEOS-Chem model is utilized to evaluate air quality by simulating the concentrations of pollutants. Finally, the outcomes pertaining to air quality from these models are utilized to assess their impact on both human health and agriculture. In this chapter the detailed of each of these models would be described.

2.2 AIM/Hub

The Asia-Pacific Integrated Model (AIM/Hub) framework is a novel economic modeling paradigm that integrates components from two distinct methodological approaches: Integrated Assessment Modeling (IAM) and Computable General Equilibrium Modeling (CGE). This novel synthesis is generally applicable to the evaluation of complicated policy developments, notably in the fields of climate change and environmental policy. By utilizing the synergistic potential of these multidimensional methodologies, AIM/CGE permits an in-depth analysis of the delicate interplay between economic dynamics and environmental considerations, thereby producing nuanced insights into the effects of diverse policy interventions. AIM/CGE can evaluate a variety of policy kinds. This model's primary policies can include climate policy (mitigation and adaptation), energy policy, land use and agricultural policy, among others.

AIM/Hub is intended to examine the climate change countermeasure policies and climate change impacts on environmental, economic, and social sector. In this model, the energy system is broken down into energy supply and demand, and land usage is disaggregated so that the land base

mitigation treatment may be comprehended. Additionally, this model is flexible for global analysis. As seen in Table 2-1, the spatial component of the model currently encompasses seventeen socioeconomic regions.

Table 2-1 Socioeconomic region codes

Region Code	Region
BRA	Brazil
CAN	Canada
CHN	China
CIS	Former Soviet Union
IND	India
JPN	Japan
TUR	Turkey
USA	United States of America
XAF	Sub-Saharan
XER	Europe (excluding the European Union)
XE25	European Union (EU25)
XLM	Latin America
XME	Middle East
XNF	North Africa
XOC	Oceania
XSA	Rest of Asia
XSE	Southeast Asia

Complex relationships between the economy, energy systems, environment, and climate change are studied using IAMs. These models combine numerous subsystems, including as energy production, consumption, land use, emissions, and climate dynamics, to provide a holistic view of how various policies and external events (such as technology breakthroughs or population expansion) may interact and influence the future. CGE models are utilized to evaluate the economic behavior and market interactions of an economy. These models depict the economy as a series of equations describing production, consumption, trade, and other economic processes.

CGE models explore how changes in one sector or policy might affect prices, wages, and output levels throughout the entire economy.

In AIM/Hub, the Shared Socio-economic Pathways (SSPs) created by O’Neill et al. (2014), which supplied the primary economic driver including population and GDP, would be utilized as socio-economic drivers. SSPs are a collection of future socioeconomic and environmental scenarios used in climate change research. These scenarios are intended to assist academics and policymakers in comprehending how different socioeconomic factors may impact greenhouse gas emissions, climate change impacts, and potential mitigation and adaptation options. There are five SSPs, each representing a distinct future development scenario as shown in Figure 2-1.



Figure 2-1 SSPs mapped in the challenges to mitigation/adaptation space (O’Neill et al., 2017)

SSP1: This scenario predicts a future with a significant emphasis on sustainable growth, international cooperation, and attempts to address social and environmental challenges. Slowing population growth and technical developments lead to more effective resource utilization and less environmental problems.

SSP2: Middle-of-the-Road - This scenario depicts a world in which economic growth continues at a moderate rate, with modest increases in living standards, but where inequality and environmental management remain persistent concerns. It reflects a "business as usual" trajectory devoid of notable deviations from current trends.

This scenario envisions a future in which regional competitiveness and strife take precedence over international cooperation. Uneven economic growth and persistent socioeconomic disparities result in fragmented efforts to address environmental concerns.

SSP4: Inequality - In this scenario, high levels of inequality and limited social development result in slower economic progress. Weak environmental regulations have caused environmental degradation and made underprivileged groups more vulnerable.

SSP5: Fossil-Powered Growth - This scenario envisions a future in which fossil fuels continue to dominate the energy mix, leading to significant greenhouse gas emissions. Prioritizing economic expansion over environmental concerns results in more severe climatic impacts.

2.2.1 Model Structure

The AIM/Hub model employs a comprehensive approach, utilizing a Social Accounting Matrix (SAM) to characterize both national and global economies. This facilitates a detailed examination of energy commodity transactions and greenhouse gas (GHG) emissions. The following section outlines the model's classification of SAM according to factors, activities, commodities, and institutions. Notably, the model incorporates a carbon tax to address carbon emissions constraints, serving as a complementary variable. The solution methodology involves employing Mixed Complementary Problems (MCP) to effectively resolve these complex interactions. The core of

the model relies on a fundamental equation with fixed parameters to project individual behaviors across various scenarios. Employing nonlinear functions, the model forecasts decisions related to population production and consumption. These predictions are driven by the objective of maximizing earnings and utility. Furthermore, the equations encompass a set of system-wide constraints, such as macroeconomic balance and balance of payments, which must be upheld holistically, even if not explicitly prioritized by individual actors. A visual representation of this structural framework is provided in Figure 2-2.

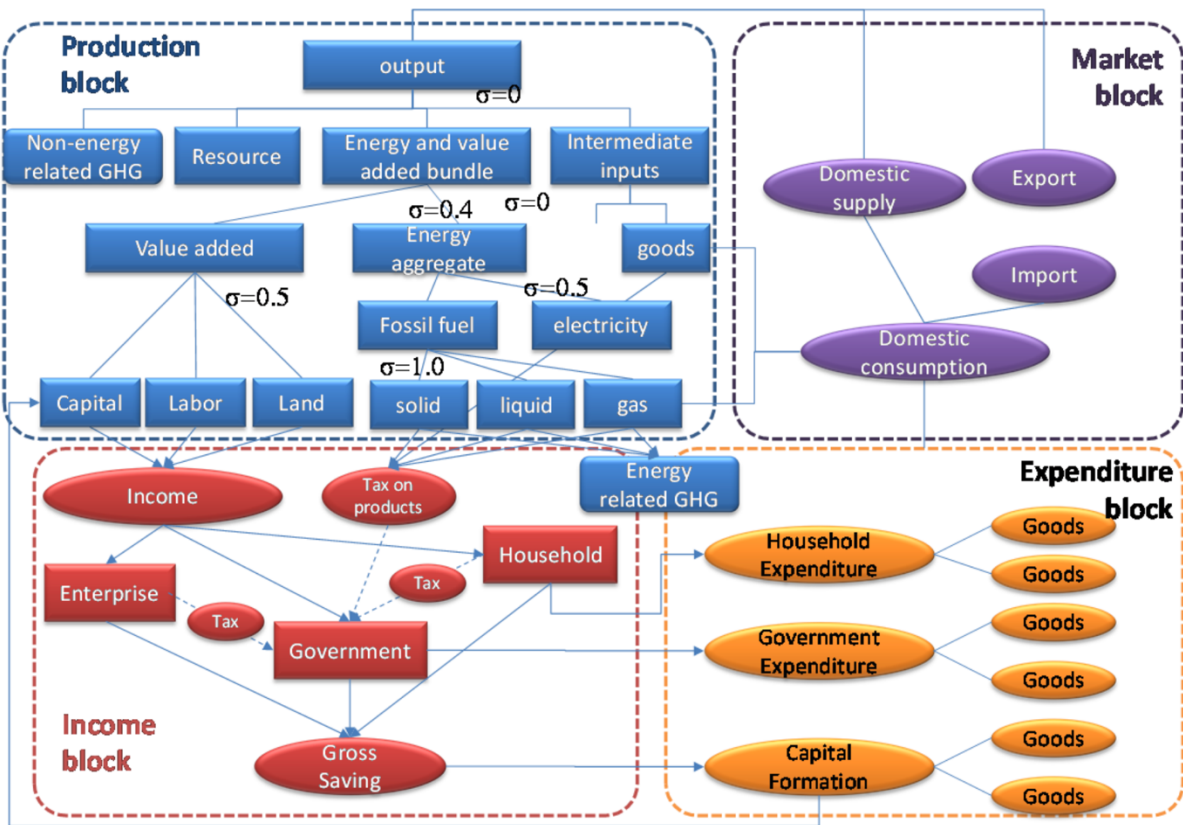


Figure 2-2 The AIM/Hub overview model structure (Fujimori et al., 2012)

The AIM/Hub model divides the structure of the model into four blocks: production, income distribution, end consumption, and market. The production block is used to present the production function's structure. A nested CES function is used to describe the production activity in numerous nested CES, while the incomes are separated into the three main institutional sectors, namely businesses, governments, and households. Taxation is the primary source of government revenue. Third, the items are consumed as ultimate consumption by businesses, governments, and

households. Government expenditure and capital formation are defined as constant coefficient functions inside this model. The Linear Expenditure System (LES) function is utilized to calculate household expenditures. Finally, the CES function is applied to imports and the CET function is applied to exports. Consumption and supply of products are in equilibrium on each market.

The CGE model is used to track GHG emissions and air pollutants, such as CO (Carbon Monoxide), NH₃ (Ammonia), NMVOC (Non-Methane Volatile Organic Compounds), NO_x (Nitrogen Oxides), SO₂ (Sulfur Dioxide), BC (Black Carbon), OC (Organic Carbon), CO₂ (Carbon Dioxide), CH₄ (Methane), and N₂O (Nitrous Oxide). The emission source is divided into two primary sources. First, the emission from fuel combustion that is proportional to the amount of energy consumed, and second, the emission proportional to the level of activity. For instance, CO₂ emissions from cement manufacture are proportional to the degree of activity. Table 2-2 lists the emission sources and their respective groupings. In addition, the use of biomass is accounted for in this model to predict air pollutants.

Table 2-2 Emission sources in AIM/Hub

Emission source related to activity level		Emission source related to fuel combustion	
IPCC category	Explanation	IPCC category	Explanation
2A	Production of minerals	1A1a	Public electricity and heat production
2A1	Cement production	1A1be	Other Energy Industries
2A2	Lime production	1A2	Manufacturing Industries and Construction
2B	Production of chemicals	1A3a	Domestic aviation
2C	Production of metals	1A3b	Road transportation
2D	Production of pulp / paper / food / drink	1A3c	Rail transportation
2G	Non - energy use of lubricants / waxes (CO ₂)	1A3d	Inland navigation
3A	Solvent and other product use: paint	1A3e	Other transportation
3B	Solvent and other product use: degrease	1A4	Residential and other sectors
3C	Solvent and other product use: chemicals	1A1a	Public electricity and heat production
3D	Solvent and other product use: other	1A1be	Other Energy Industries
4A	Enteric fermentation	1A2	Manufacturing Industries and Construction
4B	Manure management	1A3a	Domestic aviation
4C	Rice cultivation	1A3b	Road transportation
4D1	Direct soil emissions	1A4	Residential and other sectors
4D2	Manure in pasture / range / paddock		
4D3	Indirect N ₂ O from agriculture		
4D4	Other direct soil emissions		
4E	Savanna burning		

Table 2-2 Emission sources in AIM/Hub, Continued

Emission source related to activity level		Emission source related to fuel combustion	
IPCC category	Explanation	IPCC category	Explanation
4F	Agricultural waste burning		
5A	Forest fires		
5C	Grassland fires		
5F2	Forest Fires - Post burn decay		
6A	Solid waste disposal on land		
6B	Wastewater handling		
6C	Waste incineration		
6D	Other waste handling		

2.3 AIM/Downscaling

The AIM/DS algorithm is a tool to downscaling aggregate emission from AIM/CGE model outcome which regionally aggregate into a grid with have 0.5x0.5 degree developed by Fujimori et al. (2017). The method for downscaling would depend on sector and sources of emission which would be segregated into three groups as shown in Table 2-3.

Table 2-3 Downscaling algorithm emission source groups and weight used (Fujimori et al., 2017).

Sector	Group	Weight
Energy	1	GDP
Industry	1	GDP
Inland transport	1	GDP
Building	1	Population
Solvent	1	GDP
Waste	1	Population
Agricultural	2	
Agricultural waste	2	
Land use change	2	
Savana burning	2	
International navigation	3	
Aviation	3	

As illustrated in the table above, Gross Domestic Product (GDP) and Population emerge as the principal catalysts behind emissions within the ambit of group 1. Within this framework, it is conjectured that the energy facet intertwined with emission dynamics could plausibly demonstrate an interconnection with either GDP or Population. The second group was established in proportion to the base year (2015). The third group was downscaled in proportion to the total global emissions from the base year's geographic distribution and was applied to aviation emissions. The methodology for analyzing group 1, focusing on emissions from energy, solvent, and waste sectors, encompasses two primary factors: convergence and inertia as illustrated in Equation (2-1). The fundamental for the calculation methodology draws from the framework established by van Vuuren et al. Emissions' intensity tends to converge among countries belonging to the same aggregated region. The concept of inertia, on the other hand, can be interpreted as the prevailing technological level, legislative measures, or sectoral configurations existing in the base year.

$$EMG_{i,t} = \sum_{r \in RI} \alpha_t \cdot EI_{r,t} \cdot DV_{i,t} + (1 - \alpha_t) \cdot EMG_{i,t-1} \quad (2-1)$$

where $EMG_{i,t}$ is emissions in grid i and year t ; $EI_{r,t}$ is the emissions intensity in country r and year t ; and $DV_{i,t}$ is the driver in country r and year t (e.g., population and GDP). The factors α and $(1 - \alpha)$ are the weighting coefficients between the convergence and inertia factors; α ranges from 0 to 1. If the factor is thought to be stronger than the inertia factor, the weight should be close to 1. A significant convergence factor suggests that the emissions efficiency (such as emissions per unit of GDP) for individual geographical cells tends to approach a specific value associated with a larger region. For instance, if a cell is located within Indonesia, its emissions efficiency might gradually align with the average emissions efficiency of the entire Southeast Asia region. In contrast, a substantial inertia factor indicates that the differences in emissions efficiency from the base year remain prominent. As an example, if a cell is situated in Indonesia, its emissions efficiency might persist at the same level as the deviation from the regional average that was observed in the initial year. The parameter α is utilized to distinguish between these two approaches. The function RI maps a collection of countries r to specific grid cells i . The term $DV_{i,t}$ represents an external parameter that can vary over time, and $EMG_{i,t-1}$ signifies emissions data from the preceding year.

Equation (2-2) represent the parameter $EI_{r,t}$ which is the product of two term. The first one is the country specific emission intensity associated with the average emissions intensity change ratio in the aggregated region. Second is emission intensity specific in aggregate region.

$$EI_{r,t} = \left(EI_{r,t_0} \cdot \frac{\sum_{(r.rag) \in RM} EIAG_{rag,t}}{\sum_{(r.rag) \in RM} EIAG_{rag,t_0}} \right)^{\beta_t} \cdot \sum_{(r.rag) \in RM} EIAG_{rag,t}^{(1-\beta_t)} \quad (2-2)$$

where $EIAG_{rag,t}$ is the average emissions intensity of the aggregated region rag (AIM/CGE; 17 regions) in year t, β is a parameter that represents the convergence of each region, RM is a mapping for the AIM/CGE-aggregated region to which the country belongs, and t0 is the base year (2005). If $\beta = 0$, all countries that belong to an aggregated region converge to the regional average intensity. We assumed that β was 1 in 2100 and 0 in the base year. The intermediate periods were connected linearly. Summing up the emissions data calculated directly from Equation (2-2) for each individual country and then aggregating them into the initial set of 17 AIM/CGE regions resulted in conflicting figures for the total emissions within these aggregated regions. As a solution, the values of $EMG_{i,t}$ were adjusted by employing scaling according to the formula stated in Equation (2-3).

$$EMG_{i,t}^* = \sum_{r \in RI} EM_{r,t} \cdot \frac{EMG_{i,t}}{\sum_{r \in RI} EMG_{ii,t}} \quad (2-3)$$

where $EMG_{i,t}^*$ is the updated emissions in grid i and year t, and $EM_{r,t}$ is the emissions in aggregated region r and year t.

To create spatially distributed populations and GDPs, national-level data encompassing populations, urbanization rates, and GDP was employed. The dataset used was the 2.5x2.5° data from the Gridded Population of the World. By utilizing 0.5x0.5° population grid data, we generated population distributions within the 2.5x2.5° grid cells as initial values. Additionally, initial population data and national urban population data were applied to urban areas. Population density thresholds were established based on the original populations in the 0.5x0.5° data, enabling alignment with national urban populations. Grid cells exceeding the threshold were designated as urban cells, while those below were categorized as rural cells. For the 30x30° grid cells, we used

urban population/area ratios as the urban index. The Greenhouse Gas Initiative database provided by the International Institute for Applied Systems Analysis was the source of this data. To estimate urban grid cell populations, we employed the rank-size rule—a statistical principle utilized to approximate past city populations, which is also adaptable for future population estimations. The allocation of GDP distributions was fundamentally linked to the populations, while considering geographical factors such as mountains, water bodies, and urban expansion.

2.4 GEOS-Chem

GEOS-Chem stands as a comprehensive global 3-D atmospheric chemistry model, seamlessly integrated with meteorological input sourced from NASA's Goddard Earth Observing System (GEOS) via the Global Modeling and Assimilation Office. This model caters to both regional and global scales of atmospheric composition simulation. Notably, it encompasses not only climate data from NASA but also facilitates real-time online simulations, achieved through the amalgamation of a chemical module with weather and climate models.

The off-line atmospheric composition simulation capability is accessible across a broad time span, ranging from 1979 to the present day, through the utilization of NASA's continuous global GEOS data archive that comes bundled with GEOS-Chem. This data resource encompasses two primary datasets: the GEOS-Forward Processing product (GEOS-FP) applicable from 2012 to the present, boasting a horizontal resolution of 0.25° latitude by 0.3125° longitude; and the MERRA-2 reanalysis product available from 1979 onwards, characterized by a horizontal resolution of 0.5° latitude by 0.625° longitude. Both datasets offer 72 vertical levels, rendering them highly adaptable for integration within the simulation process. Furthermore, the off-line version offers users the flexibility to tailor simulations according to their specific objectives. The overview of model framework illustrated in Figure 2-3.

GC-Classic operates on a rectilinear grid, utilizing OpenMP for shared-memory parallelization, which suits the single-node mode of GEOS-Chem modeling. On a different note, the GEOS-Chem High Performance (GCHP) version employs MPI for distributed-memory parallelization, enabling simulations on a cubed-sphere grid. This version caters to users seeking to harness the

computational power of multiple nodes within their computing infrastructure. GEOS-Chem simulations maintain the capability to encompass global scenarios, maintaining either the original grid resolution or a lower resolution as chosen by the user. Additionally, simulations can be confined to designated user-defined regions, either in a dynamic nested mode with adaptable boundary conditions, or in a stretched-grid mode that allows zooming in on specific regions of interest.

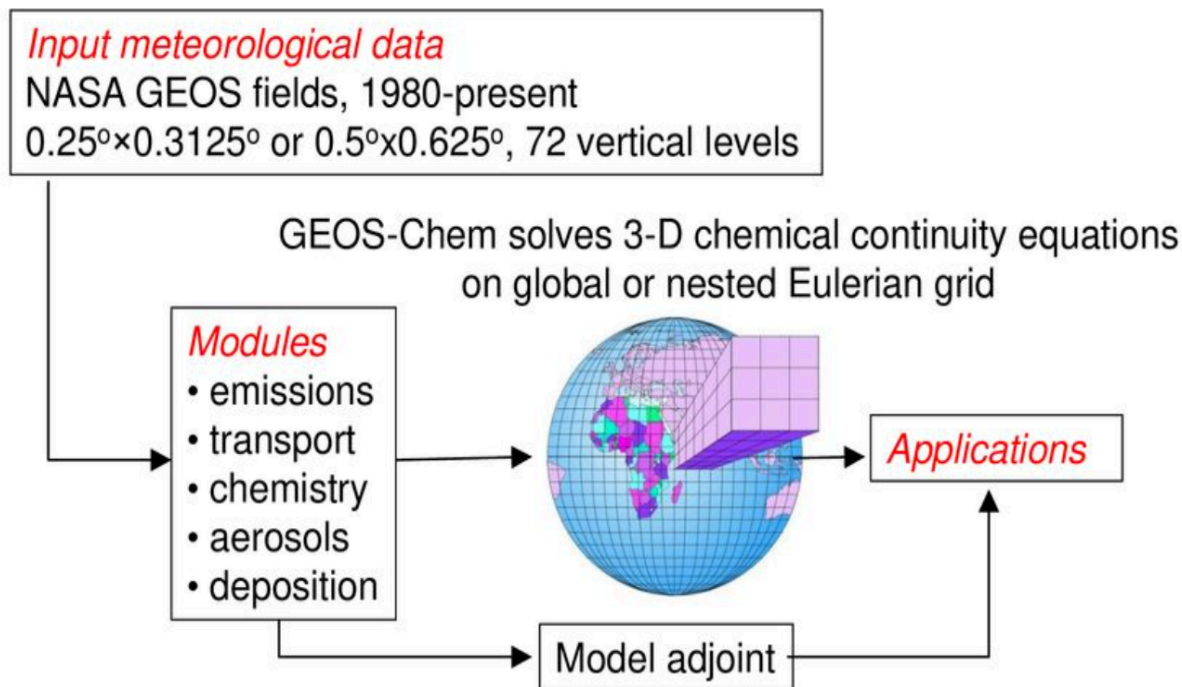


Figure 2-3 GEOS-Chem model framework (Daniel J. Jacob, 2017)

2.4.1 GEOS-Chem chemistry mechanisms

The GEOS-Chem model is a widely used global 3D chemical transport model that simulates the composition of the Earth's atmosphere. One crucial aspect of the GEOS-Chem model is its representation of chemical processes through various chemistry mechanisms. These mechanisms are sets of chemical reactions and processes that describe how different trace gases and pollutants interact, transform, and influence atmospheric composition. In the context of GEOS-Chem, chemistry mechanisms serve as the foundation for understanding the complex interplay between natural and anthropogenic emissions, transport, and chemical reactions that determine the distribution of atmospheric species. These mechanisms encompass a wide range of chemical

reactions, including photochemical reactions, gas-phase chemistry, aerosol formation, and heterogeneous processes occurring on the surfaces of aerosols and clouds.

The GEOS-Chem model offers flexibility in the choice of chemistry mechanisms as present in Table 2-4, allowing researchers to tailor the model's simulations to specific research questions and objectives. Different versions of the model may incorporate various levels of chemical complexity, reflecting the current state of scientific understanding and the specific focus of the investigation.

Table 2-4 Information about the available chemistry mechanisms in GEOS-Chem

Simulation type	Description
Full Chemistry	Standards NO _x + O _x + Br + Cl + I + aerosols chemistry in the troposphere and stratosphere
	Benchmark The process of validating and evaluating the performance of the GEOS-Chem atmospheric model against a variety of observational data and reference datasets.
	Complex SOA This scheme combines the volatility-based scheme (VBS) of Pye et al. (2010) for all SOA components with the aqueous-phase irreversible reactive uptake schemes of Marais et al. (2016) for isoprene SOA and Fisher et al. (2016) for organonitrogen SOA.
	Marine POA Composed of organic compounds that are directly emitted from the ocean surface into the atmosphere. These compounds can originate from various biological activities, such as phytoplankton blooms, as well as from other processes like sea spray emissions.
	Acid uptake on dust The process by which acidic gases in the atmosphere, such as sulfur dioxide (SO ₂) and nitrogen dioxide (NO ₂), are absorbed onto aerosol particles and other surfaces. This process can have significant implications for atmospheric chemistry, air quality, and the behavior of aerosols.
	TOMAS The Two-Moment Aerosol Sectional (TOMAS) microphysics package was originated at Carnegie Mellon University for integration into GEOS-Chem. Employing a dynamic sectional and moment-oriented methodology, TOMAS effectively monitors two distinct parameters (quantity and mass) of the aerosol size spectrum across numerous discrete size segments.

Table 2-4 Information about the available chemistry mechanisms in GEOS-Chem, Continued

Simulation type	Description
Full Chemistry	<p>APM</p> <p>The Advanced Particle Microphysics (APM) package was originally created for seamless integration into GEOS-Chem at the State University of New York (SUNY) by Yu & Luo (2009). The APM model is finely tuned to precisely emulate the genesis of secondary particles (SP), comprising sulfate, nitrate, ammonium, and secondary organic aerosols (SOA) and their growth to CCN sizes, with a higher size resolution for the size range of importance.</p>
	<p>RRTMG</p> <p>The GEOS-Chem model with online radiative transfer calculations (referred to as GCRT) was developed to allow GEOS-Chem users to produce gas and aerosol direct radiative effect (DRE) output for both the longwave and shortwave. This alternative to offline coupling allows better temporal resolution in the RT calculations and provides a consist platform for GEOS-Chem users with the widely used radiative transfer package RRTMG (Heald et al., 2013)</p>
Aerosols only	<p>The aerosol simulation is conducted offline and specifically targets aerosol tracers. It utilizes archived monthly mean concentrations of OH, NO₃, O₃, and total nitrate from a previous extensive full-chemistry simulation. It also incorporates production and loss rates for H₂O₂. Notably, this simulation does not possess the capacity for "tagged" functionalities, but instead trims down the range of tracers available in the full chemistry simulation.</p>
CH ₄	<p>The GEOS-Chem model employs various atmospheric and chemical data inputs to simulate the transport, chemistry, and sources/sinks of methane. This allows for a comprehensive understanding of CH₄ dynamics and its interactions with other components of the atmosphere.</p>
CO ₂	<p>The CO₂ simulation employs the GEOS-Chem model to study the behavior and distribution of carbon dioxide (CO₂) within the atmosphere. This simulation provides insights into the movement of CO₂ emissions, its interactions with other atmospheric components, and its overall impact on the Earth's climate system.</p>
Hg	<p>The mercury (Hg) simulation is carried out using the GEOS-Chem model. This simulation is designed to investigate the behavior, distribution, and fate of mercury within the atmosphere.</p>

Table 2-4 Information about the available chemistry mechanisms in GEOS-Chem, Continued

Simulation type	Description
POPs	The Persistent Organic Pollutants (POPs) simulation is executed using the GEOS-Chem model.
Tagged CH ₄	The tagged CH ₄ is specifically tailored to investigate methane (CH ₄) concentrations while allowing for source attribution through tagging. By employing archived data from a prior comprehensive simulation, including monthly mean OH concentrations, the model enables the identification of specific source regions or types contributing to CH ₄ concentrations.
Tagged CO	The tagged CO simulation is an independent computational process designed exclusively for calculating concentrations of carbon monoxide (CO). It relies on archived monthly average OH concentrations from a preceding comprehensive full-chemistry simulation (further elaborated below). Utilizing a linear approach, this simulation enables the tagging of CO based on its source region or type.
Tagged O ₃	The tagged O ₃ simulation offers the advantage of utilizing stored ozone production and loss rates to execute a simulation focusing on geographically specific ozone tracers. This targeted approach eliminates the need for running a comprehensive full-chemistry simulation.
Transport Tracers	The standard Rn-Pb-Be simulation uses the following tracers: <ul style="list-style-type: none"> ○ Rn²²², which is emitted naturally from soils. ○ Pb²¹⁰, which is the primary decay product of Rn²²². ○ Be⁷, which is produced by cosmic rays in the stratosphere and upper atmosphere. ○ Be¹⁰, which is produced by cosmic rays in the stratosphere and upper atmosphere.
Trace metals	The trace metals simulation employs the GEOS-Chem model to investigate the behavior and distribution of various trace metals within the atmosphere.
Carbon	The carbon mechanism is a comprehensive representation of the processes governing the behavior of carbon compounds within the atmosphere. This mechanism encompasses the complex interactions, reactions, and transformations of various carbon-containing species, such as carbon dioxide (CO ₂), methane (CH ₄), volatile organic compounds (VOCs), and more.

2.4.2 GEOS-Chem emissions

The Harmonized Emissions Component (HEMCO) manages emissions in GEOS-Chem. A dynamic software called HEMCO is used to efficiently manage emissions from a wide variety of sources, areas, and species while perfectly lining up with user-defined grids. Beyond its core obligation to provide emissions data, HEMCO also provides the ability to combine and improve baseline inventories by using scaling factors. This flexible programmed can be used both independently for in-depth investigations and in conjunction with atmospheric models for a thorough investigation of the effects of emissions on the atmosphere.

2.4.2.1 Anthropogenic emissions

GEOS-Chem model uses the anthropogenic emission from several sources to simulate the atmospheric condition. Global anthropogenic emissions from the Community Emissions Data System (CEDS) inventory and Emissions Database for Global Atmospheric Research (EDGAR) anthropogenic emissions inventories are currently supported in GEOS-Chem 13.4.0 and later. CEDS provide species include aerosol (BC, OC) and aerosol precursor and reactive compounds (SO₂, NO_x, NH₃, CH₄, CO, NMVOC) and CO₂ for 1750-2019. The primary dataset was sourced from <https://esgf-node.llnl.gov/search/input4mips/> to obtain the requisite data. The emission sources accessible for the CEDS are comprehensively documented in Table 2-5.

Table 2-5 Emission sources for CEDS (Hoesly et al., 2018)

Emission source	Description
Energy Production (ENE)	Emissions from the combustion of fossil fuels for electricity and heat generation, encompassing coal, oil, and natural gas sources.
Transportation (TRA)	Emissions arising from road vehicles, aviation, shipping, and rail transport, involving the release of pollutants and greenhouse gases.
Industrial Processes (IND)	Emissions originating from industrial activities, such as manufacturing, chemical production, and cement production, which release a range of pollutants and trace gases.

Table 2-5 Emission sources for CEDS (Hoesly et al., 2018), Continued

Emission source	Description
Residential and Commercial Activities (RCO)	Emissions resulting from the use of energy in homes and businesses, including heating, cooking, and the consumption of electricity.
Agriculture (AGR)	Emissions from agricultural practices, such as enteric fermentation in livestock, use of synthetic fertilizers, and rice paddies, releasing greenhouse gases and other compounds.
Waste Management (WST)	Emissions associated with the management and disposal of waste, including landfills, waste incineration, and wastewater treatment.
Chemical Solvent Use (SLV)	Emissions from the use of volatile organic compounds (VOCs) in products like paints, adhesives, and cleaning agents.
International Ship (SHP)	Emissions from international shipping activities including the pollutants and greenhouse gases released into the atmosphere from vessels engaged in maritime transportation across international waters.

In term of aircraft emission, GEOS-Chem utilize the Aircraft Emissions Inventory Code (AEIC) developed at MIT (Simone et al., 2013). The total fuel consumed, the distance flown, and the pollutant emissions for both landing and takeoff (LTO) and non-LTO flight, including cruise, are estimated in this inventory.

2.4.2.2 Natural emissions

The local meteorological conditions affect the emissions of dust aerosol, lightning NO_x, biogenic VOCs, soil NO_x, and sea salt aerosol. These emissions are calculated off-line using the GEOS meteorological data's native resolution, and they are then archived and used as input for GEOS-Chem.

Lightning-generated nitrogen oxides (NO_x) emissions hold a critical role within the GEOS-Chem model, serving as a cornerstone for comprehending atmospheric chemistry and air quality

dynamics. Nitric oxide (NO) and nitrogen dioxide (NO₂), engendered by electrical discharge mechanisms during thunderstorms and lightning occurrences, collectively constitute "lightning NO_x emissions." The model incorporates these emissions, guided by variables such as lightning flash frequencies, altitude profiles, and regional attributes. GEOS-Chem model use NO_x from soil emission developed by Hudman et al. (2012). This inclusion enriches the model's representation of NO_x sources, encompassing emissions stemming from soil processes and interactions, thus contributing to a more accurate portrayal of atmospheric chemistry and its intricate dynamics. Furthermore, the Model of Emissions of Gases and Aerosols from Nature version 2.1 (MEGAN2.1), developed by Guenther et al. (2012), finds application within the GEOS-Chem framework for biogenic emissions provisioning. These emissions, encompassing reactive volatile organic compounds (VOCs), exert notable influence on atmospheric chemistry. Their impact resonates across air quality and climate domains, signifying their pivotal contribution to the intricate web of atmospheric processes.

In order to capture the presence of mineral dust within the GEOS-Chem model, two distinct approaches have been integrated. The scheme by Ginoux et al. (2004), denoted as G04, originally developed for the GOCART CTM, has been employed alongside the dust entrainment and deposition (DEAD) scheme formulated by Zender et al. (2003). Both schemes share a common characteristic: they model the vertical dust flux by establishing a proportional relationship with the horizontal saltation flux. Sea salt aerosols within the GEOS-Chem model are a crucial component of the atmospheric simulation, effectively capturing the complex interactions between the ocean surface and the atmosphere. These aerosols originate from the sea's surface due to the physical processes of wind-driven sea spray and bubble bursting. They encompass a range of particle sizes and chemical compositions, impacting both regional and global atmospheric dynamics. The treatment of sea salt aerosols in current version of GEOS-Chem is based on Jaeglé et al. (2011) study. Emissions originating from volcanic activity spanning the years 1978 to 2019 were sourced from NASA/GMAO. This dataset serves as a vital resource, offering insights into the intricate interplay between volcanic emissions and atmospheric dynamics across this extensive timeframe.

2.5 Human health exposure model

Individuals can come into contact with contaminated substances through various pathways, encompassing ingestion of tainted food, inhalation of polluted air, consumption of impure water, interaction with polluted soil, or even through the utilization of everyday products. There are two factors which determine the nature and extent of exposure.

The human factor encompasses a spectrum of elements, spanning individual or collective behaviors, social dynamics, and physical attributes. These factors can exert both direct and indirect influences on an individual's susceptibility to receiving contaminants. Behavior plays a paramount role in determining the extent of substance exposure, as it reflects the quantity of substances encountered. Simultaneously, activity patterns serve as a representation of the timing and location of exposure instances. Another factor is the concentrations of a pollutant in the exposure media that influence the level of exposure that individuals experience. These concentrations directly affect the potential health risks associated with exposure. When the pollutant concentrations are high, the likelihood of adverse health effects also increases. Conversely, lower pollutant concentrations generally result in lower risks. For example, a group of children is playing in a park located near a busy road. The road experiences heavy traffic, emitting a significant amount of vehicular exhaust containing PM_{2.5} particles. As the children engage in active play, they are running around, breathing more rapidly, and spending several hours outdoors. So, they could be exposed to PM_{2.5} in high level compared with children who play in the indoor.

Human exposure modeling establishes a connection between pollutant concentrations in broader environmental settings and the pollutant concentrations encountered by a human population in their immediate surroundings. These models typically replicate the movement of either individuals or groups based on their activity patterns through specific settings known as microenvironments within a defined geographical or administrative area, often referred to as exposure districts. As these individuals or groups traverse through these microenvironments, they come into contact with pollutants present at varying concentrations.

This interplay between human movement and pollutant distribution facilitates potential interactions between individuals or groups and pollutants. Consequently, this modeling approach

enables the estimation of the exposure levels experienced by diverse individuals or groups within the population concerning the pollutants under consideration. In essence, human exposure modeling provides insights into how pollutants are encountered in real-world scenarios, aiding in the assessment of the associated health risks and the formulation of effective mitigation strategies.

The Integrated Exposure-Response Model (IER) and the Global Exposure Mortality Model (GEMM) have emerged as prominent tools for delving into the intricate relationship between human health and air quality, particularly concerning pollutants like PM_{2.5} and O₃. These models serve as robust frameworks that enable researchers to unravel the complex interplay between exposure to these pollutants and their potential impacts on human well-being. By seamlessly integrating exposure assessments with the nuanced dose-response dynamics, IER and GEMM illuminate the potential health risks posed by air pollutants. These models play a pivotal role in providing insights that drive evidence-based policies, fostering a safer and healthier environment for communities worldwide.

2.5.1 The Integrated Exposure-Response Model (IER)

The Integrated Exposure–Response (IER) function (Equation 2-4) was developed by Burnett et al. (2014). IER developed the relative risk (RR) across the entire world exposure range for the cause of mortality in adults including ischemic heart disease (IHD), cerebrovascular disease (stroke), chronic obstructive pulmonary disease (COPD), lung cancer (LC), and lower respiratory infection (LRI). The IER was defined for PM_{2.5} concentrations exceeding C₀ (7.5 µg m⁻³) because the concentration which lower than 7.5 is not observed related mortality in cohort study.

$$RR_j(C_i) = 1 + a(1 - \exp(-\beta(C_i - C_0)^\delta)) \quad (2 - 4)$$

where ‘ α ’, ‘ β ’, and ‘ δ ’ are bare constants in the IER that are age- and disease-specific (j) as shown in Table 2-6 (Burnett et al., 2014).

Table 2-6 Integrated Exposure–Response (IER) parameter estimates by cause of death.

Cause of Death	Age	Alpha (α)	Beta (β)	Delta (δ)	C ₀
LRI	25+	2.2023	0.0028	1.1830	7.2834
	25+	15.2237	0.0009	0.6839	7.3744
COPD	25	4.8248	0.0562	0.4176	7.5931
	30	4.1553	0.0607	0.4150	7.5791
	35	3.5727	0.0652	0.4119	7.5572
	40	3.0606	0.0702	0.4053	7.5402
	45	2.7991	0.0747	0.3486	7.6417
	50	2.2853	0.0782	0.3587	7.6121
	55	1.8853	0.0823	0.3591	7.5850
	60	1.5540	0.0869	0.3676	7.5337
	65	1.2631	0.0910	0.3733	7.5221
	70	1.0079	0.0965	0.3762	7.5221
	75	0.7844	0.1035	0.3835	7.4994
	80	0.5869	0.1102	0.3824	7.4946
IHD	25+	1.4273	0.0476	0.3762	7.4624
	25+	114.7418	0.0001	0.7409	7.3799
LC	25	5.8878	0.0157	0.6513	7.5558
	30	5.0565	0.0157	0.6839	7.5199
	35	4.2831	0.0167	0.6991	7.4571
	40	3.6171	0.0170	0.8078	7.5048
	45	3.0363	0.0165	0.9211	7.4904
	50	2.5199	0.0166	0.9570	7.5142
	55	2.0829	0.0172	0.9809	7.5168
	60	1.7075	0.0173	0.9945	7.4893
	65	1.4035	0.0222	0.8975	7.4893
	70	1.1060	0.0206	0.9612	7.4446
	75	0.8472	0.0198	1.0279	7.4371
	80	0.6250	0.0190	1.0900	7.4034
STROKE	25+	1.2641	0.0072	1.3137	7.3875

2.5.2 The Global Exposure Mortality Model (GEMM)

The Global Exposure Mortality Mode (GEMM) function developed by Burnett et al. (2018) was used to estimate the number or premature mortality related to PM_{2.5} and O₃, considered five health outcomes: stroke, IHD, COPD, LC, and acute respiratory lung infection (ALRI) as shown in the following equation.

$$RR(z)_j = \exp \left[\frac{\theta \log \left(\frac{1+z}{\alpha} \right)}{1 + \exp \left\{ - \left(\frac{z - \mu}{v} \right) \right\}} \right] \quad (2 - 5)$$

where ‘θ’, ‘α’, ‘μ’, ‘v’, are constants in the GEMM that are age- and disease-specific (j) shown in Table 2-7 and 2-8 (Burnett et al., 2018). ‘z’ is excess PM_{2.5} concentration above the threshold to which the population is exposed, $z = \max(0, PM_{2.5} - 2.4 \mu g/m^3)$.

Table 2-7 GEMM parameter estimates by cause of death, with inclusion of Chinese Male Cohort

Cause of Death	Age Range (years)	θ	standard error θ	α	μ	v
NCD+LRI	>25	0.1430	0.01807	1.6	15.5	36.8
	27.5	0.1585	0.01477	1.6	15.5	36.8
	32.5	0.1577	0.01470	1.6	15.5	36.8
	37.5	0.1570	0.01463	1.6	15.5	36.8
	42.5	0.1558	0.01450	1.6	15.5	36.8
	47.5	0.1532	0.01425	1.6	15.5	36.8
	52.5	0.1499	0.01394	1.6	15.5	36.8
	57.5	0.1462	0.01361	1.6	15.5	36.8
	62.5	0.1421	0.01325	1.6	15.5	36.8
	67.5	0.1374	0.01284	1.6	15.5	36.8
	72.5	0.1319	0.01234	1.6	15.5	36.8
	77.5	0.1253	0.01174	1.6	15.5	36.8
85	0.1141	0.01071	1.6	15.5	36.8	
LRI	>25	0.4468	0.11735	6.4	5.7	8.4
COPD	>25	0.2510	0.06762	6.5	2.5	32

Table 2-7 GEMM parameter estimates by cause of death, with inclusion of Chinese Male Cohort,
Continued

Cause of Death	Age Range (years)	θ	standard error θ	α	μ	ν
IHD	>25	0.2969	0.01787	1.9	12	40.2
	27.5	0.5070	0.02458	1.9	12	40.2
	32.5	0.4762	0.02309	1.9	12	40.2
	37.5	0.4455	0.02160	1.9	12	40.2
	42.5	0.4148	0.02011	1.9	12	40.2
	47.5	0.3841	0.01862	1.9	12	40.2
	52.5	0.3533	0.01713	1.9	12	40.2
	57.5	0.3226	0.01564	1.9	12	40.2
	62.5	0.2919	0.01415	1.9	12	40.2
	67.5	0.2612	0.01266	1.9	12	40.2
	72.5	0.2304	0.01117	1.9	12	40.2
	77.5	0.1997	0.00968	1.9	12	40.2
	85	0.1536	0.00745	1.9	12	40.2
Stroke	>25	0.2720	0.07697	6.2	16.7	23.7
	27.5	0.4513	0.11919	6.2	16.7	23.7
	32.5	0.4240	0.11197	6.2	16.7	23.7
	37.5	0.3966	0.10475	6.2	16.7	23.7
	42.5	0.3693	0.09752	6.2	16.7	23.7
	47.5	0.3419	0.09030	6.2	16.7	23.7
	52.5	0.3146	0.08307	6.2	16.7	23.7
	57.5	0.2872	0.07585	6.2	16.7	23.7
	62.5	0.2598	0.06863	6.2	16.7	23.7
	67.5	0.2325	0.06190	6.2	16.7	23.7
	72.5	0.2051	0.05418	6.2	16.7	23.7
	77.5	0.1778	0.04695	6.2	16.7	23.7
	85	0.1368	0.03611	6.2	16.7	23.7
Lung Cancer	>25	0.2942	0.06147	6.2	9.3	29.8

Table 2-8 GEMM parameter estimates by cause of death, without inclusion of Chinese Male Cohort

Cause of Death	Age Range (years)	θ	standard error θ	α	μ	ν
NCD+LRI	>25	0.1231	0.01797	1.5	10.4	25.9
	27.5	0.1358	0.01326	1.5	10.4	25.9
	32.5	0.1353	0.01321	1.5	10.4	25.9
	37.5	0.1348	0.01315	1.5	10.4	25.9
	42.5	0.1338	0.01304	1.5	10.4	25.9
	47.5	0.1317	0.01283	1.5	10.4	25.9
	52.5	0.1288	0.01255	1.5	10.4	25.9
	57.5	0.1256	0.01225	1.5	10.4	25.9
	62.5	0.1221	0.01194	1.5	10.4	25.9
	67.5	0.1181	0.01157	1.5	10.4	25.9
	72.5	0.1133	0.01112	1.5	10.4	25.9
	77.5	0.1077	0.01058	1.5	10.4	25.9
	85	0.0979	0.00964	1.5	10.4	25.9
IHD	>25	0.2543	0.04589	4.9	-21.1	17.7
	27.5	0.3996	0.03016	4.9	-21.1	17.7
	32.5	0.3796	0.02834	4.9	-21.1	17.7
	37.5	0.3512	0.02651	4.9	-21.1	17.7
	42.5	0.327	0.02468	4.9	-21.1	17.7
	47.5	0.3027	0.02285	4.9	-21.1	17.7
	52.5	0.2785	0.02103	4.9	-21.1	17.7
	57.5	0.2543	0.0192	4.9	-21.1	17.7
	62.5	0.2301	0.01737	4.9	-21.1	17.7
	67.5	0.2059	0.01554	4.9	-21.1	17.7
	72.5	0.1816	0.01371	4.9	-21.1	17.7
	77.5	0.1574	0.01188	4.9	-21.1	17.7
	85	0.1211	0.00914	4.9	-21.1	17.7

Table 2-8 GEMM parameter estimates by cause of death, without inclusion of Chinese Male Cohort, Continued

Cause of Death	Age Range (years)	θ	standard error θ	α	μ	ν
Stroke	>25	0.1873	0.08431	6.2	14.5	14.4
	27.5	0.3177	0.11625	6.2	14.5	14.4
	32.5	0.2985	0.1092	6.2	14.5	14.4
	37.5	0.2792	0.10216	6.2	14.5	14.4
	42.5	0.26	0.09511	6.2	14.5	14.4
	47.5	0.2407	0.08807	6.2	14.5	14.4
	52.5	0.2214	0.08102	6.2	14.5	14.4
	57.5	0.2011	0.07398	6.2	14.5	14.4
	62.5	0.1829	0.06693	6.2	14.5	14.4
	67.5	0.1637	0.05988	6.2	14.5	14.4
COPD	>25	0.2095	0.06725	7.2	2	14.7
	>25	0.2626	0.07849	6.7	11	16.5
Lung Cancer	>25	0.2626	0.07849	6.7	11	16.5
LRI	>25	NA	NA	NA	NA	NA

2.5.3 Log-linear function

The log-linear function for assessing the relative risk associated with O₃ exposure is a mathematical model that captures the relationship between different levels of O₃ exposure and the corresponding increase in the risk of adverse health outcomes. This type of function is commonly used to analyze the dose-response relationship between O₃ concentrations and health effects. The Peak Seasonal (six-month) Maximum of Daily 8-hour Average (PSMDA8) ozone concentrations of ozone in ambient air were used to calculate It can be represented as follows:

$$RR_j(C_i) = \exp [((PSMDA8 - TMREL) \times \beta) - 1] \quad (2-6)$$

where $\beta = 0.007696$, TMREL is the theoretical minimum risk exposure level which is estimated 29.1~35.7 ppb in GBD study. In this study, we applied the beta coefficient (β) from Turner et al. (2016) for relative risk computing and TMREL is 32.4 for all region and people ppb as median value referring to Malashock et al. (2022).

2.6 The Lund–Potsdam–Jena managed land 2 crop model

The Lund-Potsdam-Jena Managed Land (LPJmL) Crop Model is a sophisticated agricultural modeling tool that has been developed collaboratively by researchers from Lund University in Sweden, the Potsdam Institute for Climate Impact Research in Germany, and the Friedrich Schiller University in Jena, German (Bondeau et al., 2007). This model is designed to simulate and analyze various aspects of crop production and land use changes within managed agricultural landscapes as shown in Figure 2-4.

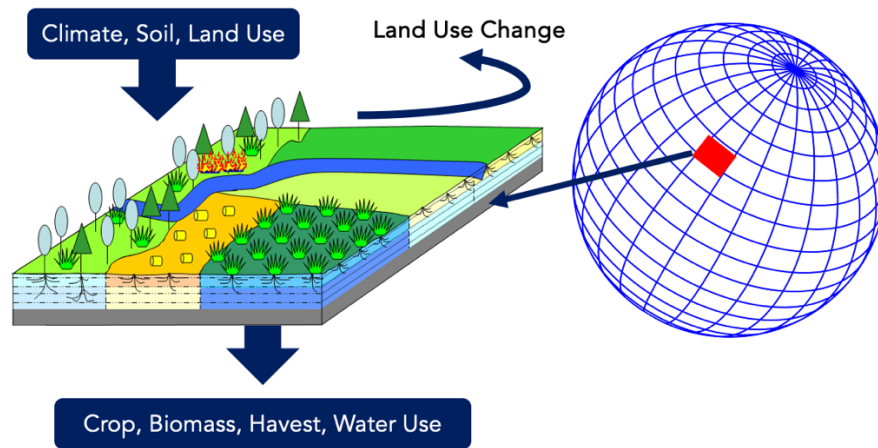


Figure 2-4 The Lund-Potsdam-Jena Managed Land (LPJmL) Crop Model conceptual framework. Adapted from Bondeau et al. (2007)

The LPJmL Crop Model integrates complex interactions between climate, soil, and management practices to project how different agricultural systems might respond to changing environmental conditions and human interventions. The model takes into account factors such as temperature,

precipitation, soil type, cropping patterns, irrigation practices, and nutrient inputs to simulate crop growth, yields, and land use changes over time. The source code of the model is available under the AGPLv3 license at <https://github.com/PIK-LPJmL/LPJmL>. Key features of the LPJmL Crop Model include:

2.6.1 Crop Growth Simulation

The model simulates the growth of different crops (e.g., wheat, maize, rice) based on inputs such as climate data, soil properties, and management practices. It considers factors like photosynthesis, water availability, and nutrient uptake to estimate crop yields.

2.6.2 Land Use Dynamics

LPJmL captures changes in land use over time, including shifts between cropland, pasture, and other land uses. This helps analyze how agricultural activities might impact land cover and ecosystem services.

2.6.3 Climate Change Impact Assessment

The model is often used to assess the potential effects of climate change on agricultural systems. By incorporating future climate scenarios, it can project how changing temperature and precipitation patterns might influence crop productivity and land use.

2.6.4 Policy Analysis

Researchers and policymakers use LPJmL to explore the potential outcomes of different agricultural policies and management strategies. This can include evaluating the impacts of changes in irrigation practices, fertilizer use, and other interventions.

2.6.5 Regional and Global Applications

LPJmL can be applied at various scales, from regional to global. It contributes to understanding how agriculture interacts with broader environmental and societal changes.

2.7 Reference

- Bondeau, A., Smith, P. C., Zaehle, S., Schaphoff, S., Lucht, W., Cramer, W., Gerten, D., LOTZE-CAMPEN, H., Müller, C., & Reichstein, M. (2007). Modelling the role of agriculture for the 20th century global terrestrial carbon balance. *Global Change Biology*, *13*(3), 679–706.
- Burnett, R., Chen, H., Szyszkowicz, M., Fann, N., Hubbell, B., Pope III, C. A., Apte, J. S., Brauer, M., Cohen, A., & Weichenthal, S. (2018). Global estimates of mortality associated with long-term exposure to outdoor fine particulate matter. *Proceedings of the National Academy of Sciences*, *115*(38), 9592–9597.
- Burnett, R. T., Pope III, C. A., Ezzati, M., Olives, C., Lim, S. S., Mehta, S., Shin, H. H., Singh, G., Hubbell, B., & Brauer, M. (2014). An integrated risk function for estimating the global burden of disease attributable to ambient fine particulate matter exposure. *Environmental Health Perspectives*, *122*(4), 397–403.
- Daniel J. Jacob. (2017). *GEOS-Chem model overview*. IGC8, Harvard. <https://slideplayer.com/slide/15062576/>
- Fujimori, S., Masui, T., & Matsuoka, Y. (2012). AIM/CGE [basic] manual. *Center for Social and Environmental Systems Research, NIES: Tsukuba, Japan*.
- Ginoux, P., Prospero, J. M., Torres, O., & Chin, M. (2004). Long-term simulation of global dust distribution with the GOCART model: Correlation with North Atlantic Oscillation. *Environmental Modelling & Software*, *19*(2), 113–128.
- Guenther, A., Jiang, X., Heald, C. L., Sakulyanontvittaya, T., Duhl, T. any, Emmons, L., & Wang, X. (2012). The Model of Emissions of Gases and Aerosols from Nature version 2.1 (MEGAN2. 1): An extended and updated framework for modeling biogenic emissions. *Geoscientific Model Development*, *5*(6), 1471–1492.
- Heald, C., Ridley, D., Kroll, J., Barrett, S., Cady-Pereira, K., Alvarado, M., & Holmes, C. (2013). Beyond direct radiative forcing: The case for characterizing the direct radiative effect of aerosols. *Atmos. Chem. Phys. Discuss*, *13*, 32925–32961.
- Hoesly, R. M., Smith, S. J., Feng, L., Klimont, Z., Janssens-Maenhout, G., Pitkanen, T., Seibert, J. J., Vu, L., Andres, R. J., & Bolt, R. M. (2018). Historical (1750–2014) anthropogenic emissions of reactive gases and aerosols from the Community Emissions Data System (CEDS). *Geoscientific Model Development*, *11*(1), 369–408.

- Hudman, R., Moore, N., Martin, R., Russell, A., Mebust, A., Valin, L., & Cohen, R. (2012). A mechanistic model of global soil nitric oxide emissions: Implementation and space based-constraints. *Atmospheric Chemistry & Physics Discussions*, *12*(2).
- Jaeglé, L., Quinn, P., Bates, T., Alexander, B., & Lin, J.-T. (2011). Global distribution of sea salt aerosols: New constraints from in situ and remote sensing observations. *Atmospheric Chemistry and Physics*, *11*(7), 3137–3157.
- Malashock, D. A., Delang, M. N., Becker, J. S., Serre, M. L., West, J. J., Chang, K.-L., Cooper, O. R., & Anenberg, S. C. (2022). Global trends in ozone concentration and attributable mortality for urban, peri-urban, and rural areas between 2000 and 2019: A modelling study. *The Lancet Planetary Health*, *6*(12), e958–e967.
- O'Neill, B. C., Kriegler, E., Riahi, K., Ebi, K. L., Hallegatte, S., Carter, T. R., Mathur, R., & Van Vuuren, D. P. (2014). A new scenario framework for climate change research: The concept of shared socioeconomic pathways. *Climatic Change*, *122*, 387–400.
- Simone, N. W., Stettler, M. E., & Barrett, S. R. (2013). Rapid estimation of global civil aviation emissions with uncertainty quantification. *Transportation Research Part D: Transport and Environment*, *25*, 33–41.
- Turner, M. C., Jerrett, M., Pope III, C. A., Krewski, D., Gapstur, S. M., Diver, W. R., Beckerman, B. S., Marshall, J. D., Su, J., & Crouse, D. L. (2016). Long-term ozone exposure and mortality in a large prospective study. *American Journal of Respiratory and Critical Care Medicine*, *193*(10), 1134–1142.
- Yu, F., & Luo, G. (2009). Simulation of particle size distribution with a global aerosol model: Contribution of nucleation to aerosol and CCN number concentrations. *Atmospheric Chemistry and Physics*, *9*(20), 7691–7710.
- Zender, C. S., Bian, H., & Newman, D. (2003). Mineral Dust Entrainment and Deposition (DEAD) model: Description and 1990s dust climatology. *Journal of Geophysical Research: Atmospheres*, *108*(D14).

Chapter 3

Comparison of global air pollution impacts across horizontal resolutions.

3.1 Abstract

The impact of ambient air pollution on human health, especially fine particulate matter (PM_{2.5}) and tropospheric ozone (O₃), is a significant global environmental concern. Atmospheric chemical transport models (CTMs) have been used to determine the concentrations of air pollutants at which health concerns arise. It is therefore critically important to fully understand the limitations of these atmospheric CTMs. There is a lack of consensus on how the resolution of a CTM in the horizontal direction affects the accuracy with which it predicts changes in air pollution levels. Low-spatial-resolution and high-spatial-resolution domains for estimating O₃ and PM_{2.5} concentrations were created to examine the impact of nested-grid simulations on model outputs. We compared modeling outcomes and observations to validate the accuracy of each resolution and assessed the changes in agricultural and health implications. The model validation demonstrated that increasing the resolution improved the reproducibility of the observation regionally but did not necessarily improve the overall global results. Moreover, the differences in the changes of global agricultural and health effects were minor and comparable to the uncertainty associated with emissions inventories and CTMs. Some of the regional variations were larger than the global total, which could be a significant issue in some contexts or for specific objectives. Although improvements in the resolution of the CTM could potentially alter the predicted effects of air pollution in certain regions, the influence on the overall study was deemed to be small.

Keywords: Air pollution, Atmospheric chemistry transport model, Climate change, GEOS-Chem, Horizontal resolution, O₃, PM_{2.5}

3.2 Introduction

The impact of climate change is one of the most pressing global issues confronting modern human society. In addition, climate change and local air quality are subject to a wide range of complex interactions. Air quality management policies may reduce the emissions of greenhouse gases (GHGs), while climate change mitigation initiatives such as the phase-out of fossil fuels may reduce air pollution (Jiang et al., 2013; Nemet et al., 2010; Thurston & Bell, 2021; Vandyck et al., 2018; West et al., 2013). Air pollution has detrimental consequences on human health and agricultural production, and reducing these impacts is essential to climate change mitigation efforts (Agrawal, 2005; Ashmore, 1991; Brunekreef & Holgate, 2002). High GHG emissions from automobiles, power plants, agriculture, and other anthropogenic activities have resulted in increases in atmospheric fine particulate matter (PM_{2.5}) and tropospheric ozone (O₃) in highly polluted regions (Ajijere & Nwaerema, 2020; Hata et al., 2023).

Chemical transport models (CTMs) and source receptor models have been used to convert the emissions of air pollutants into atmospheric concentrations of the air pollutants (Askariyeh et al., 2020). Then, impact assessment models have been used to examine the impacts of air pollutants such as PM_{2.5} and tropospheric O₃, which are associated with human health risks and agricultural losses (Anenberg et al., 2010; Chuwah et al., 2015; Cissé et al., 2022; Cohen et al., 2017; Xiong et al., 2022). One of the advantages of using source receptor models is that they require little computation load and time, while CTMs are better equipped to account for nonlinear, complex chemical-transport interactions requiring substantial computing power and resources. Thus, given current global CTM conditions and computer resources, the horizontal resolution may need to be limited to explore the global outcomes.

One potential solution to this situation is the use of nested-grid simulations (Chen et al., 2009; Protonotariou et al., 2010; Zhang et al., 2011), which constrains the target simulation area but has a finer resolution. However, the effects of CTM horizontal resolution on the outcomes of simulations is poorly understood. It is critically important to better understand the extent to which nested-grid simulations can be applied to determine the impacts of global air pollution on human health and crop production. If nested-grid simulations provide much better insights of global air

pollution than a global simulation with a relatively coarse spatial resolution, the running of a series of nested-grid simulations should be seriously considered in addition to the global simulation. Otherwise, using single global model results without nested-grid simulations could provide an unacceptable approximation of the implications of global air pollution.

This study aimed to investigate the potential advantages and/or disadvantages of employing a nested-grid simulation over a non-nested-grid simulation, and to assess how the use of a nested-grid simulation may impact both human health and agricultural productivity. Our hypothesis posits that any differences in resolution between the two simulation methods would not significantly impact the overall social and environmental implications being studied. To examine the influence of horizontal resolution on the global simulation outcomes using a CTM, we employed a global three-dimensional model of atmospheric chemistry, GEOS-Chem, driven by meteorological inputs from the NASA Global Modeling and Assimilation Office with gridded emissions from an Integrated Assessment Model (IAM), the Asia-Pacific Integrated Model (AIM) tool, to estimate global concentrations at fine ($0.5^\circ \times 0.625^\circ$) and coarse ($4^\circ \times 5^\circ$) resolutions.

Future climate change policies and their effects on air quality can be predicted by integrating IAMs with the GEOS-Chem model, which was another goal of this study. Then, we compared both the simulation results for the $PM_{2.5}$ and O_3 concentrations with observations and determined the health impacts and crop yield changes associated with these air pollutants and evaluated the differences between the two types of simulation. If the hypothesis of this paper is valid, it would be significantly beneficial to carry out studies that explore the air pollution implications associated with climate change counter measure policy impacts to for IAMs because we could quickly provide using a global simulation of air quality based on IAM when a new climate change policy is released without relying on intensive computer resources.

3.3 Methodology

We used the GEOS-Chem model to predict the ground surface concentrations of PM_{2.5} and O₃ using an air pollution emission inventory and meteorological data as inputs in the simulations with (0.5° × 0.625°) and without (4° × 5°) nested grids (Figure 3-1). We implemented several future emissions scenarios derived from AIM so that the validity of the nested-grid simulation could be tested under multiple plausible future scenarios. We conducted two types of assessment. First, we compared the simulated PM_{2.5} and O₃ concentrations with monitoring data to confirm the validity of the simulation results at both resolutions. Second, crop production losses caused by O₃, and the mortality changes due to PM_{2.5} exposure were used to evaluate how the resolution would change the implications for the human social system.

3.3.1 Target area and spatial resolution

In this study, a customized nested configuration was adopted in response to resource limitations. This approach was strategically chosen to differentiate it from the pre-provided developer configuration, with the primary goal of optimizing resource allocation. By tailoring the nested setup to match the precise requirements of the study, significant computational resources were effectively conserved. To assess model accuracy across distinct horizontal spatial distributions, we judiciously selected varied regions within the nested-grid GEOS-Chem simulation, taking into account a range of influencing factors. The first was the scale of anthropogenic emissions, which was the source of PM_{2.5} and tropospheric O₃ precursors. In addition, we also considered the population and area of agricultural land because we assessed the impact on agriculture and human health. The final target area is shown in Figure 2. The United States, Canada, European Union, Japan, China, Thailand, Singapore, and Brazil are examples of the selected regions to represent the geographical distribution of global concentrations, ground surface concentrations obtained from nested-grid simulations in each region and the global concentration data simulated by the non-nested-grid model would be combined. Here, we used the boundary condition outcome from the global simulation to be a condition for nested grid simulation to improve the accuracy and model results at finer spatial scales by representing the accurate information about how the atmosphere is changing at its outer boundaries.

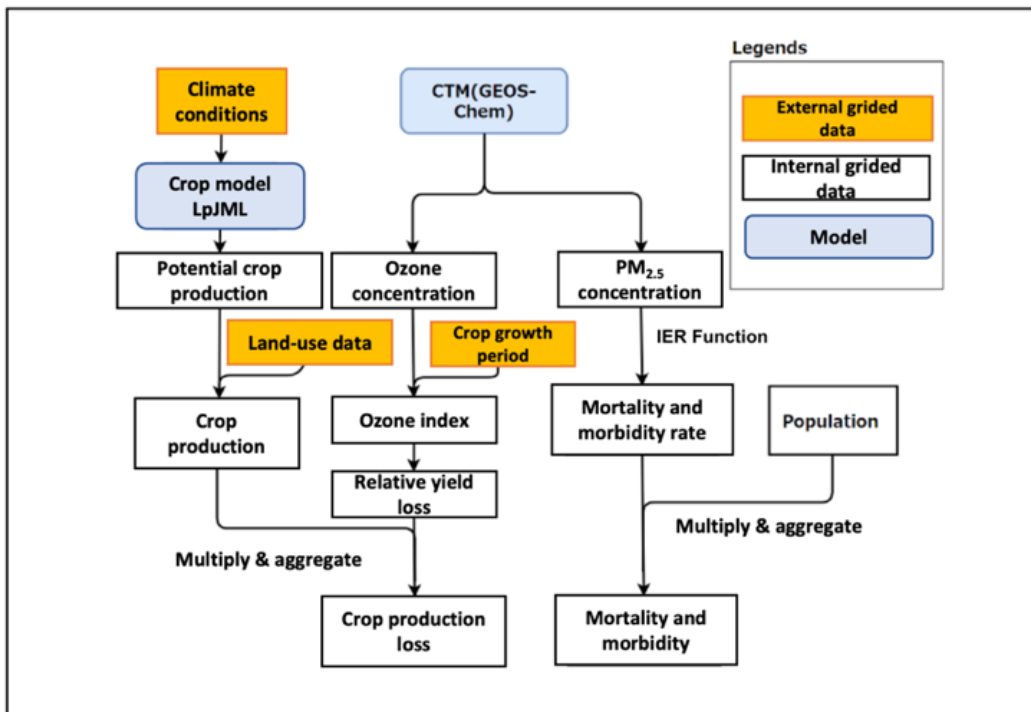
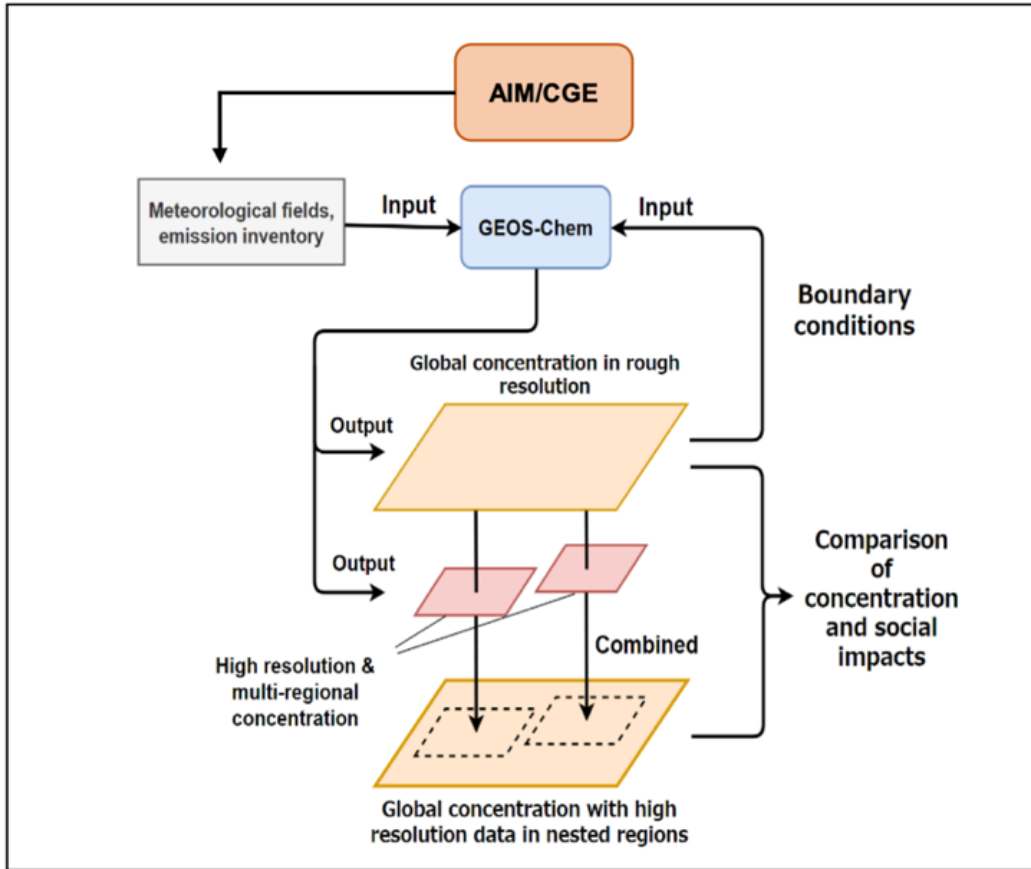


Figure 3-1 The framework of GEOS-Chem simulations (top) and the impact assessment (bottom).

We assessed the health and agricultural effects arising from the model outputs of the global and nested-grid simulations. Consequently, the spatial distribution of each pollutant was aggregated to a resolution of $0.5^\circ \times 0.5^\circ$, which corresponded to the data inputs from other sources. The first-order conservative remapping technique was applied as a mapping method.

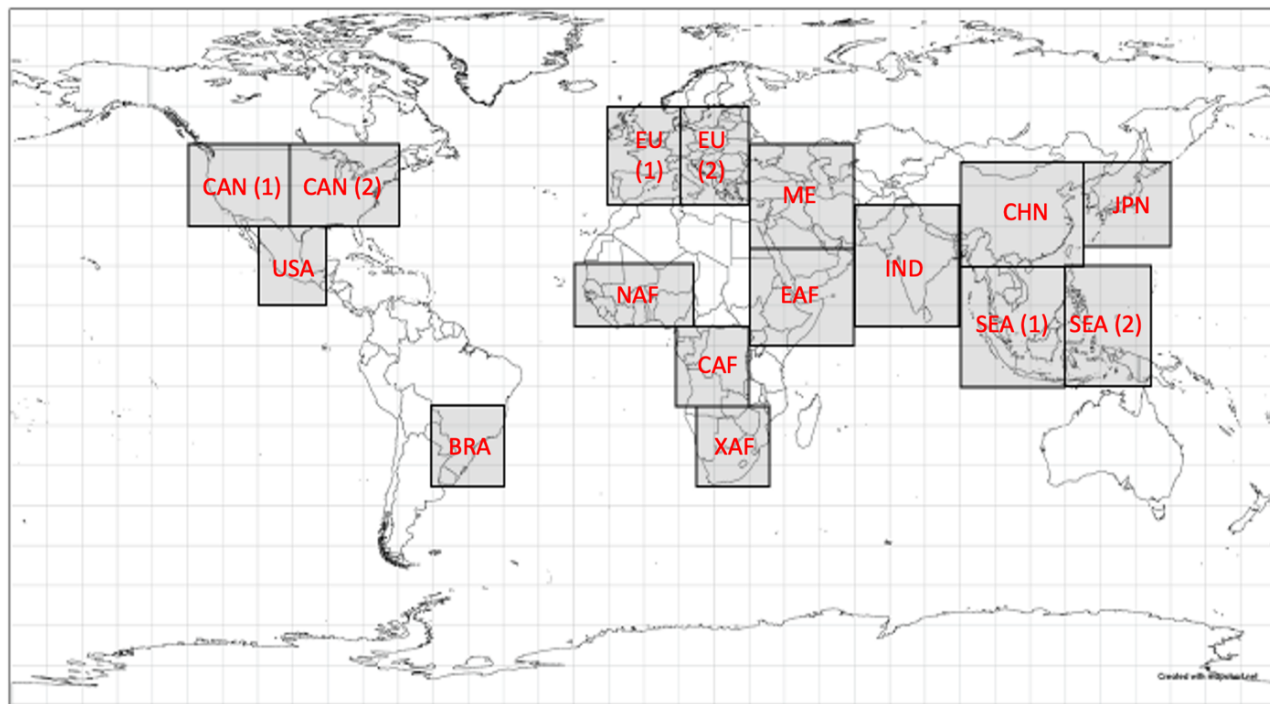


Figure 3-2 GEOS-Chem nested-grid domain ($0.5^\circ \times 0.625^\circ$) for the target area. BRA = Brazil; CAN = Canada; CHN = China; EU=Europe; IND = India; JPN = Japan; USA = United States of America; ME = Middle East; SEA = Southeast Asia; NAF = North Africa; EAF = East Africa; CAF = Central Africa; XAF = South Africa.

3.3.2 Emission scenarios

The future of air quality may depend critically on the rate of economic expansion and the effectiveness of strategies to combat climate change. Thus, to examine the impact of different anthropogenic emissions conditions on air quality, the baseline scenario with high GHG emissions and the mitigation scenario with low GHG emissions were applied. In this study, the mitigation scenario was roughly corresponding to the emissions scenarios by limiting the global average temperature increase to 1.5°C while baseline is a sort of scenarios that extends the historical

socioeconomic situation which yields relatively higher GHG and air pollution emissions. By evaluating the model using future scenarios, we may determine the performance of its predictions under conditions that have not yet occurred. This enables us to detect any biases or limits in the model before policy decision or future research are based on it. Note that the climate change impacts such as temperature and precipitation changes were not included in these two scenarios and thus the meteorological condition is same among the scenarios and years. The emissions were then entered into the GEOS-Chem model. We selected the years 2015, 2030, 2050, and 2100 for CTM simulations to examine the immediate, medium-term, and long-term effects.

Here we can see the rough scenario conditions from the global total major GHG and air pollutant emissions. Compared to the baseline scenario, the GHG emissions were substantially reduced under the mitigation policy scenario. By 2100, the total emissions of Kyoto Protocol-regulated gases under the mitigation scenario decreased by approximately 95 Gt CO₂ eq/year. The NO_x and SO_x emissions were also predicted to decrease significantly due to the assumption of air pollutant control measures in SSP2 (Rao et al., 2017), whereas the differences in other pollutants were not pronounced.

3.3.3 Comparison of model outputs with monitoring station observations

To evaluate the results of the GEOS-Chem model, observation data from developed and developing countries (Table 3-1) were compared using 2015 as the baseline year. Due to restricted access to data from ground monitoring stations in certain locations observational data were highly limited.

When the observations were compared to the modeled concentrations, the observation point in the target region of the nested grid was associated with the nearest 0.5° × 0.5° grid. We used the monthly average concentration data to determine the model accuracy by calculating the mean absolute error (MAE) and correlation coefficient (R) between the observed and modeled concentrations.

Table 3-1 Sources of air quality monitoring data and number of observations.

Country	Organization (Data sources)	Number of observations	
		PM _{2.5}	O ₃
United States	Clean Air Status and Trends Network	396	396
Canada	Ministry of the Environment, Conservation and Parks	39	39
Europe	European Environment Agency	2021	2700
Japan	National Institute for Environmental Studies	1021	1185
China	China National Environmental Monitoring Centre	1482	-
Thailand	Air4Thai	12	-
Singapore	Pollution Central Department	5	-
Korea	Air Korea	12	-
Brazil	Environmental Company of the State of São Paulo	14	-

3.3.4 Agricultural impacts

We selected the five main global crops, i.e., sugar cane, maize, soybeans, rice, and wheat, to assess the crop production losses due to O₃ exposure. These crops were selected based on the major crop categories used in the AIM/Hub model.

Equation 3-1 was used to quantify O₃ exposure in each grid. For the assessment of crop production losses, the accumulated dose of ozone over a threshold of 40 ppb (AOT40) was used to indicate the accumulated O₃ exposure during the daytime in the 3 months before harvesting (Sacks et al., 2010; Tai et al., 2014). AOT40 was estimated over the time period of 08:00 until 19:59 UTC for the vast areas of agricultural land in temperate and tropical zones.

$$AOT40(\text{ppb}) = \sum_{t=1}^n \max([O_3]_t - 40, 0) \quad (t \in 08:00 - 19:59) \quad (3 - 1)$$

While the response function (Equation 3-2) is used to depict the dose–response relationship between the relative crop yield and O₃ exposure to determine the relative crop yield from AOT40. Different coefficients (a and b) were allocated to different crops as shown in table 3-2 (Mills et al., 2007).

$$y = ax + b \quad (3 - 2)$$

where x is AOT40 in ppmh and y is the relative yield.

The Lund–Potsdam–Jena managed land 2 crop model was used for the calculation of the potential production volume and regional consolidation, and potential harvestability and land-use data for the major crops in 2015 from Fujimori et al. (2018) were applied. First, the grid yield was calculated by multiplying the production volume grid by the relative yield. The grid yield was then determined by country and divided into 17 regions. The relative yields by country were then calculated by comparing aggregated yields with and without O₃ effects.

Table 3-2 the impact function coefficients (a, b) for each crop in the study

Species	<i>a</i>	<i>b</i>
Rice	0.0039	-0.06
Wheat	0.0161	-0.01
Maize	0.0036	0.02
Soybeans	0.0116	0.02
Sugar crops	0.016	0.07

3.3.5 Mortality due to PM_{2.5} exposure

We also studied the human health impact of PM_{2.5} exposure using the integrated exposure–response (IER) function established by Burnett et al. (2014) as shown in Chapter 2. The IER function is a nonlinear function that calculates excess mortality due to long-term exposure to ambient PM_{2.5}. Mortality was calculated using the RR from Equation (3-3) by using following formula (Apte et al., 2015).

$$Mortality = \frac{RR(z) - 1}{RR(z)} \times Pop \times B \quad (3 - 3)$$

where z is the $PM_{2.5}$ concentration ($\mu g/m^3$), Pop is grid population (number of people), and B is the baseline mortality rate by country (%).

Gridded population estimates were based on the SSP2 baseline scenario (Jones & O'Neill, 2016). The number of deaths calculated per grid was aggregated by regional divisions as well as agricultural impacts, and the number of deaths for each disease were combined to obtain the estimated number of deaths attributable to $PM_{2.5}$ exposure for all diseases.

3.4 Results

3.4.1 Spatial distribution of tropospheric O_3 and $PM_{2.5}$ concentrations representation in nested-grid simulations.

The spatial distribution patterns of both pollutants were similar in the nested-grid and non-nested-grid simulations; however, in the territorial waters of the European Union and Japan, the O_3 concentration was higher in the nested-grid than non-nested-grid simulation (Figure 3-3a and 3-3b). In 2015, an annual average O_3 concentration of 30 ppbv or more was observed in the Northern Hemisphere's mid-latitudes and a large area of Africa, while an annual average of 60 ppbv was observed in the Tibetan Plateau and parts of central Africa. The high O_3 concentration in the Tibetan Plateau was likely caused by the high atmospheric column resulting from this region's high altitude and susceptibility to the effects of ultraviolet rays. The high O_3 concentration in central Africa was due to the volatile organic compounds emitted from the open burning of vegetation from both anthropogenic and natural sources.

Some regions of Asia and Africa had annual average $PM_{2.5}$ concentrations of $30 \mu g/m^3$ or more per year, whereas China and India had concentrations of $100 \mu g/m^3$ or higher. In addition, high concentrations were estimated even in desert regions such as Africa because naturally derived emissions were included in this study.

3.4.2 Model validation

The monthly mean average data for the grids ($0.5^\circ \times 0.5^\circ$) corresponding to the observation points were used to compare the observation data to the modeling outcomes; however, in the European Union and Brazil, only annual average observation data could be obtained due to the limited data accessibility. The observed O_3 (left) and $PM_{2.5}$ (right) concentrations on a monthly scale are shown in Figure 3-c.

The nested-grid simulation for tropospheric ozone provided a modest enhancement in the performance of the model. As shown in Table 3-3, the Mean Absolute Error (MAE) was reduced while the correlation coefficient (R) was marginally improved in all regions. In Japan, the nested grid simulation leads to a slight decline in MAE and a marginally increase in R for both monthly and daily estimation. However, in Canada, while the nested grid simulation results in a slightly lower MAE, there is no notable improvement in R for daily. The efficiency of the nested-grid simulation in enhancing the performance of the model for $PM_{2.5}$ estimation varied by region. While some locations showed tremendous improvement, others displayed little or no change (Table 3-4). In the United States, the nested grid simulation resulted in a marginally reduced MAE for both monthly and daily estimates, but in R, no meaningful improvement was observed (Figure 3-3c). Even if Canada's MAE was reduced, R did not improve substantially. Nevertheless, nested-grid simulation does not significantly improve the model's overall performance in compared to non-nested grid simulation. Moreover, in many regions, such as China, Japan, and Korea, the R was improving while the MAE was declining.

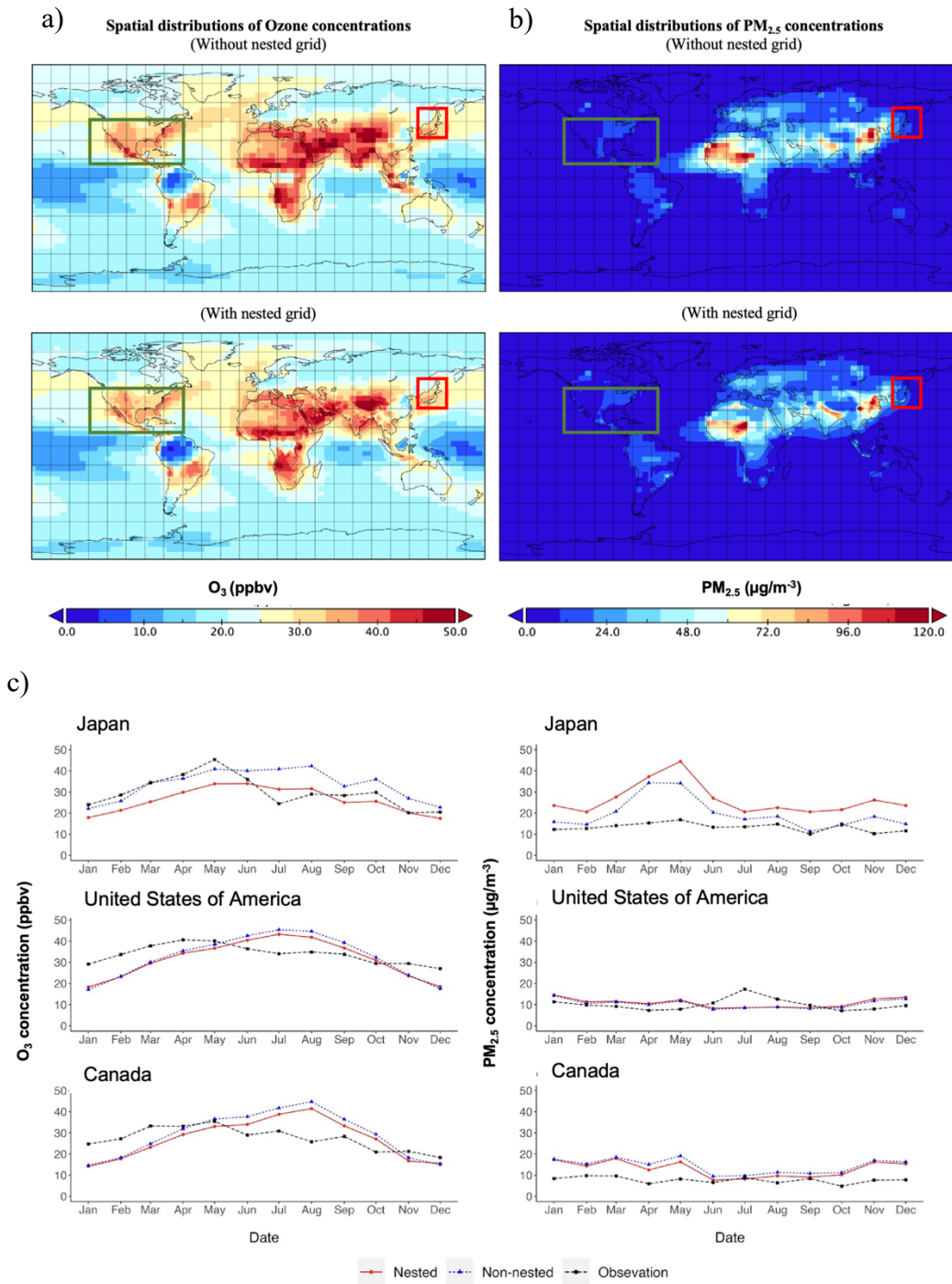


Figure 3-3 Spatial distributions of the O₃ (a) and PM_{2.5} (b) concentrations for cases simulated without (upper) and with (lower) a nested grid ; the red box represents Japan, while the green box corresponds to the USA and Canada. And a comparison between model outcome (red: nested; blue: Non-nested) and observation (black) data in Japan, Canada, and USA (c)

Table 3-3 Changes in the MAE due to the nested-grid simulation of the modeled/observed O₃ concentrations (ppbv).

Region	Monthly				Daily			
	Without nested grid		With nested grid		Without nested grid		With nested grid	
	MAE	R	MAE	R	MAE	R	MAE	R
United States	9.5	0.31	8.1	0.44	11.2	0.26	10.6	0.31
Japan	6.8	0.50	6.7	0.57	10.9	0.26	10.8	0.32
Canada	7.7	0.44	7.0	0.50	10.3	0.29	9.7	0.30
European Union*	6.1	0.29	5.8	0.33	-	-	-	-

*Annual average

Table 3-4 Changes in the MAE due to the nested-grid simulation of the modeled/observed PM_{2.5} concentration (µg/m³).

Region	Monthly				Daily			
	Without nested grid		With nested grid		Without nested grid		With nested grid	
	MAE	R	MAE	R	MAE	R	MAE	R
United States	5.6	0.20	5.5	0.20	6.2	0.11	6.4	0.13
Japan	5.3	0.42	13.2	0.45	10.0	0.26	15.3	0.21
Canada	8.1	0.59	5.4	0.59	8.3	0.19	7.5	0.20
China	44.4	0.33	37.1	0.55	45.48	0.13	57.17	0.2
Thailand	12.9	0.61	13.2	0.54	15.1	0.36	17.2	0.38
Singapore	14.1	0.27	13.9	0.39	14.4	0.05	14.3	0.20
Korea	13.4	0.05	27.1	0.14	-	-	-	-
European Union*	12.2	0.37	9.7	0.38	-	-	-	-
Brazil*	15.2	0.44	19.3	0.46	-	-	-	-

*Annual average

3.4.3 PM_{2.5} exposure and mortality

Figure 3-4a shows a comparison of premature deaths caused by PM exposure in simulations with and without nested grids. The results indicate that in the baseline year, the global mortality rate was around 5 million, which decreased to approximately 3 million when the mitigation scenario was implemented. The nested-grid simulations yielded a higher mortality rate than the non-nested-grid simulations. Specifically, while mortality due to PM_{2.5} exposure was only slightly different in 2015 between the nested-grid and non-nested-grid simulations, the differences became significant in 2050 and 2100. The distinctions in the mitigation scenario were even more pronounced.

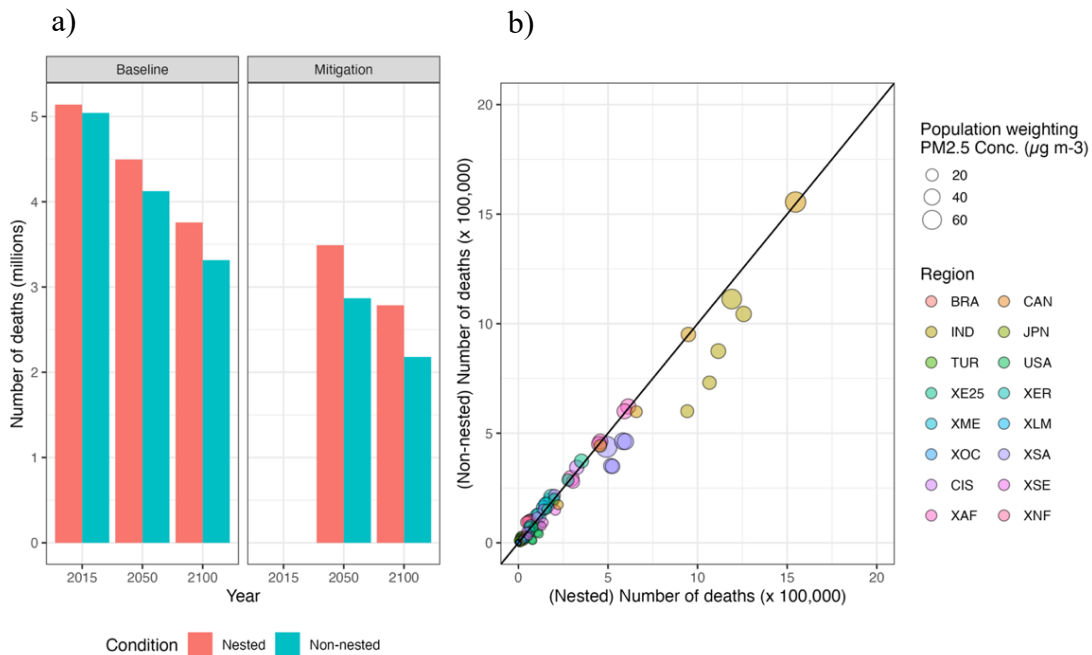


Figure 3-4 (a) Comparison of the number of worldwide premature deaths attributable to exposure to PM_{2.5} in the simulations with and without nested grids. (b) Changes in the number of deaths by region due to the application of the nested-grid simulation (the black diagonal represents the 1:1 line). BRA = Brazil; CAN = Canada; CHN = China; CIS = Former Soviet Union; IND = India; JPN = Japan; TUR= Turkey; USA = United States of America; XAF = Sub-Saharan; XER = Europe (excluding the European Union); XE25 = European Union (EU25); XLM = Latin America; XME = Middle East; XNF = North Africa; XOC = Oceania; XSA = Rest of Asia; XSE = Southeast Asia

Figure 3-4b presents a scatterplot comparing the number of deaths by region as calculated in the simulations with and without nested grids. The number of premature deaths attributable to PM_{2.5} exposure was determined using the IER function. The number of deaths from all diseases in all Asian countries was highest in the scenario with the lowest emissions due to the changes in the spatial distribution of the pollutants. The IER function was extremely sensitive to the concentration intervals used to express the pollutant levels.

3.4.4 Crop production losses due to O₃ exposure

In the base year of 2015, the relative global yield loss was approximately 7%, while in the mitigation scenario, the loss was approximately 3%. Figure 3-5a depicts the relative yield losses for 2015 by region, alongside a comparison of the nested-grid and non-nested-grid simulations.

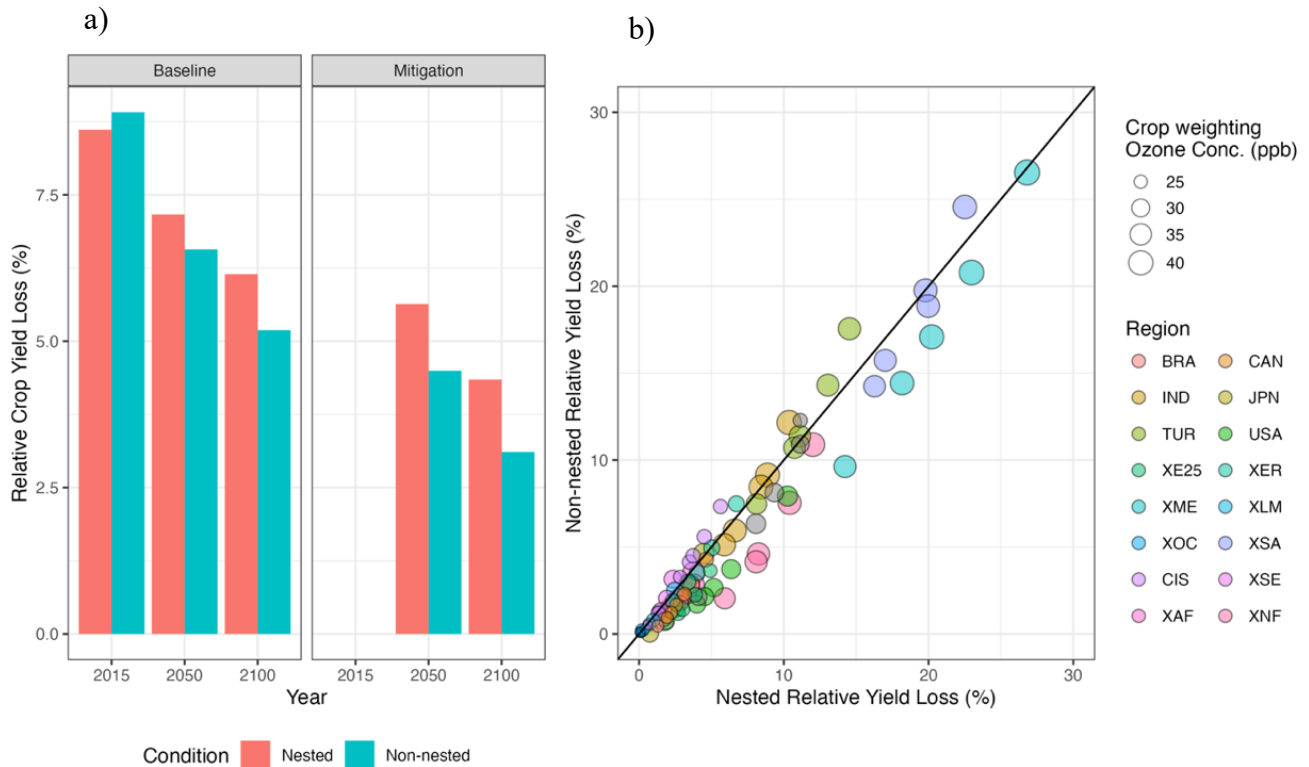


Figure 3-5 (a) Comparison of the worldwide crop production loss due to O₃ exposure in the simulations with and without nested grids. (b) Changes in crop production loss by region due to the application of the nested-grid simulation (the black diagonal represents the 1:1 line).

When the nested-grid simulation was used, losses tended to reduce in Asia, but they increased in the Middle East. In the United States and the European Union, which have high production volumes, yield losses increased by 1–2 percent, but this increase was offset by a decrease in yield losses in Asia; thus, the global yield loss changed minimally, whereas in 2050 and 2100, the gap between nesting and non-nesting is greater than in the base year in both scenarios.

Figure 3-5b presents a scatterplot comparing the crop production loss by region as calculated in the simulations with and without nested grids. When the nested-grid simulation was implemented, there was a 7% increase in losses in the Middle East, and a similar trend was observed in neighboring Turkey and North Africa. There was a change of 5% or less in all other regions. AOT40 was used as an indicator of crop losses. The correlation between the weighted concentration and yield loss was weak, and the change in crop production loss due to the application of the nested-grid simulation tended to increase in proportion to the region's yield loss. The change in the O₃ concentration due to the application of the nested-grid simulation was reflected in the relative yield loss in areas where the O₃ concentration was relatively high.

3.5 Discussion

3.5.1 Model evaluation

With the application of the nested-grid simulation, the estimated tropospheric O₃ and PM_{2.5} concentrations in the 2015 data set had a tendency to be overestimated compared to the observations. The O₃ concentration was overestimated by around 3.5 ppbv (11.8%) on a monthly basis, whereas the PM_{2.5} concentration was overestimated by approximately 20.9 µg/m³. For daily investigations, the result was a 12% (3.6 ppbv) overestimation of the O₃ concentration and a 97.7% (13.0 µg/m³) overestimation of the PM_{2.5} concentration. This result is related to Travis et al. (2016) study. Their study revealed that the CTM model's surface ozone concentrations exhibited an overestimation, attributed to a combination of heightened vertical mixing and net ozone production within the model's boundary layer. In the context of PM_{2.5} concentration, the GEOS-Chem model demonstrates a tendency to overstate levels of nitrate, elemental carbon (EC), and organic carbon (OC). This overestimation collectively contributes to an overall exaggeration in PM_{2.5} concentration estimates. (Lee et al., 2017).

In terms of seasonal variation, the reproducibility of the O₃ concentration was generally good and the geographical characteristics were also well reproduced. However, in the nested-grid simulation, the estimated concentration was close to the observed data only in Japan and the European Union, while there was a decrease in the MAE in all regions. The influence of the nested-grid simulation on the validity of the modeled concentrations was therefore considered to be limited.

The seasonal repeatability of PM_{2.5} was equivalent to that of O₃. The MAEs of the estimated and observed concentrations were lowest in Canada, Singapore, and the European Union, with values of 2.7 µg/m³ for monthly data and 0.8 µg/m³ for daily data. In contrast to the overestimation that occurred in the majority of locations, the difference between the modeled and observed concentration and the MAE were minor when the nested-grid simulation was applied. Despite the fact that nested grid could improve the result's precision in comparison to non-nested grid, the overall performance of both models is poor. The models may not adequately represent the complexity of atmospheric processes that influence air quality, which is the leading cause of model uncertainty such as regional meteorological pattern.

3.5.2 Impact assessment

When the agricultural impact assessment of this study was compared with that of Van Dingenen et al. (2009), the relative crop yield loss trend was largely consistent when the target year and crop definitions were taken into account. However, it was necessary to take into account the fact that crop production losses in the Middle East and adjacent regions increased due to the high emission loads since 2005. In addition, when the nested-grid calculation was conducted, the relative yield loss in the agricultural impact analysis differed from that of Van Dingenen et al. (2009) by 1% for the global average and by 7% for the regional area. Although the change in relative crop yield loss on a global basis was relatively small when compared to the uncertainty range of the relative crop yield loss, this change could impact the food supply and economic system on a regional scale. In terms of health impacts, we found that mortality related to PM_{2.5} exposure was overestimated for both nested and non-nested simulations. Our model's results indicated an overestimate of 5.2 million for nested calculation and 5 million for non-nested calculation compared to the World

Health Organization's report of 4.2 million deaths in 2015 due to exposure to PM_{2.5}. Therefore, non-nested simulation is more reliable in producing results closer to observation data than nesting.

3.5.3 Limitation

The modeled O₃ and PM_{2.5} concentrations tended to be overestimations compared to the observed levels, regardless of the application of a nested-grid or non-nested-grid simulation. Consequently, the accuracy of the modeled concentration was considered to be a limitation of the impact of the nested-grid simulation. It was concluded that the nested-grid simulation did not significantly impact the model's precision. In addition, the global and regional impacts on the calculation of health effects were less significant than the agricultural impact. It is likely that considerable regional changes will occur in the future. When assessing the regional effects of air pollution on agriculture, it is vital to consider the impact of model uncertainty on the conclusions. The results demonstrated that even at a low resolution, the global evaluation of air pollution did not compromise the dependability of the results. In addition, as shown in Table 3-3 and 3-4, global models are ill-suited for replicating daily data but are suitable for demonstrating temporal trends. Observations made when simulating future situations indicate that nested-grid simulations have a stronger impact on impact assessment outcomes than non-nested computations. This trend is found not just for future scenarios, but also for baseline scenarios for 2050 and 2100, due to the fact that high spatial resolution meteorological data can capture atmospheric processes and mixing better than low spatial resolution data, which leads to high concentrations.

Finally, some caveats to this study should be noted. First, the findings were dependent on the GEOS-Chem parameters used in the calculations. Although GEOS-Chem's meteorological conditions and terrain are very precise in high-resolution computations within nested regions, it is not possible to simulate all the atmospheric phenomena that could potentially occur. Second, the series of simulations in this study did not include the interactions between air pollutants and meteorological conditions. GEOS-Chem uses meteorological data as an input, which are not influenced by air pollutants. Interactions such as the process by which aerosols resulting from chemical processes in the atmosphere block solar radiation were not taken into account. Third, when performing high-resolution computations in the nested region, low-resolution concentrations

were used as boundary conditions. It is possible that the concentration within the nested zone depends on the transboundary effects outside the target area. Both PM_{2.5} and NO_x, which is an O₃ precursor, contribute to the formation of smog. Due to atmospheric transport from regions with large emission sources, secondary pollutants formed outside the boundary may flow into the nested zone and pollutant concentrations may be increased.

Additionally, with regard to the emission inventory used in our study, particularly when considering the long-term implications of land cover and land use changes, it's important to note that the downscaling method employed to derive emissions from the AIM/Hub model may introduce uncertainties. In this downscaling approach, emissions are scaled down in proportion to the total regional emissions within the agricultural sector based on CEDS emission grid, which is recognized as a significant source of PM_{2.5} and O₃. This downscaling method may not fully capture the intricacies of land cover and land use changes over time. By scaling emissions based on regional totals, it may not account for localized variations and specific land use dynamics, potentially contributing to uncertainties in our emissions inventory data.

3.6 Summary and conclusions

The low-spatial distributions and high-spatial distributions of O₃ and PM_{2.5} were calculated using the GEOS-Chem model, with multiple future emissions scenarios. We also assessed the impact of air pollution on the agricultural sector and human health. The results showed that the nested-grid simulation had little influence on the accuracy of the model concentrations, and the agricultural and health implications are not so different among the different horizontal resolution while minor differences can be observed in the base year. When comparing the observed and modeled data, the nested-grid simulation improved the accuracy on a monthly and daily scale. In the United States and European Union, the spatial distributions of PM_{2.5} and tropospheric O₃ were improved because the nested-grid simulations reproduced topography more correctly than the non-nested-grid simulations.

The estimated yield loss and mortality rate in this study in 2015 were consistent with the literature. When the nested-grid simulation was applied, global mortality increased by 10,000. Both the yield

loss and mortality rate were within the margin of error; thus, there was a negligible difference between the nested-grid and non-nested-grid simulation results, and there was no tendency for the values to depend on emissions. Although the number of deaths on a regional scale in India and other regions of Asia varied by up to 500,000, such small proportions of the overall population were unlikely to alter the conclusions obtained for health consequences. In the agricultural impact scenario, the relative global yield loss decreased to around 7% in the nested-grid simulation. Furthermore, the nested-grid simulation revealed that there were decreased losses in Asia, but increased losses in the Middle East. Although yield losses in the United States and European Union, which have substantial production volumes, increased by 1-2%, there was a decline in Asia, resulting in only a slight change in the overall global yield loss value.

Despite the modest effect of CTM resolution, yield losses and deaths were lower when the nested-grid simulation was not used both baseline and mitigation scenario. Moreover, in mitigation scenario, the gaps between nested and non-nested is largest; thus, when examining the cost-effectiveness of mitigation strategies, it is important to take nested-grid simulations and model uncertainty into account.

3.7 Reference

- Agrawal, M. (2005). Effects of air pollution on agriculture: An issue of national concern. *Natl Acad Sci Lett*, 28(3/4), 93–106.
- Ajiere, S., & Nwaerema, P. (2020). Climate change and air pollution: Implication for human health and environment in rivers state. *International Journal of Research and Innovation in Social Science (IJRISS)*, 4, 276–279.
- Anenberg, S. C., Horowitz, L. W., Tong, D. Q., & West, J. J. (2010). An estimate of the global burden of anthropogenic ozone and fine particulate matter on premature human mortality using atmospheric modeling. *Environmental Health Perspectives*, 118(9), 1189–1195.
- Apte, J. S., Marshall, J. D., Cohen, A. J., & Brauer, M. (2015). Addressing global mortality from ambient PM_{2.5}. *Environmental Science & Technology*, 49(13), 8057–8066.
- Ashmore, M. (1991). Air pollution and agriculture. *Outlook on Agriculture*, 20(3), 139–144.
- Askariyeh, M. H., Khreis, H., & Vallamsundar, S. (2020). Air pollution monitoring and modeling. In *Traffic-Related Air Pollution* (pp. 111–135). Elsevier.
- Bey, I., Jacob, D. J., Yantosca, R. M., Logan, J. A., Field, B. D., Fiore, A. M., Li, Q., Liu, H. Y., Mickley, L. J., & Schultz, M. G. (2001). Global modeling of tropospheric chemistry with assimilated meteorology: Model description and evaluation. *Journal of Geophysical Research: Atmospheres*, 106(D19), 23073–23095.
- Brunekreef, B., & Holgate, S. T. (2002). Air pollution and health. *The Lancet*, 360(9341), 1233–1242.
- Burnett, R. T., Pope III, C. A., Ezzati, M., Olives, C., Lim, S. S., Mehta, S., Shin, H. H., Singh, G., Hubbell, B., & Brauer, M. (2014). An integrated risk function for estimating the global burden of disease attributable to ambient fine particulate matter exposure. *Environmental Health Perspectives*, 122(4), 397–403.
- Chen, D., Wang, Y., McElroy, M. B., He, K., Yantosca, R. M., & Le Sager, P. (2009). Regional CO pollution and export in China simulated by the high-resolution nested-grid GEOS-Chem model. *Atmospheric Chemistry and Physics*, 9(11), 3825–3839.
- Chuwah, C., van Noije, T., van Vuuren, D. P., Stehfest, E., & Hazeleger, W. (2015). Global impacts of surface ozone changes on crop yields and land use. *Atmospheric Environment*, 106, 11–23.

- Cissé, G., McLeman, R., Adams, H., Aldunce, P., Bowen, K., Campbell-Lendrum, D., Clayton, S., Ebi, K., Hess, J., & Huang, C. (2022). Health, wellbeing, and the changing structure of communities. *Climate Change*.
- Cohen, A. J., Brauer, M., Burnett, R., Anderson, H. R., Frostad, J., Estep, K., Balakrishnan, K., Brunekreef, B., Dandona, L., & Dandona, R. (2017). Estimates and 25-year trends of the global burden of disease attributable to ambient air pollution: An analysis of data from the Global Burden of Diseases Study 2015. *The Lancet*, 389(10082), 1907–1918.
- Environmental Company of the State of São Paulo. (n.d.). *Air quality report in the State of São Paulo*. Retrieved April 19, 2022, from <https://cetesb.sp.gov.br/ar/publicacoes-relatorios/>
- European Environment Agency. (n.d.). *Air quality statistics calculated by the EEA*. Retrieved April 15, 2022, from <http://aidef.apps.eea.europa.eu>
- Fountoukis, C., & Nenes, A. (2007). ISORROPIA II: a computationally efficient thermodynamic equilibrium model for K⁺–Ca²⁺–Mg²⁺–NH₄⁺–Na⁺–SO₄²⁻–NO₃⁻–Cl⁻–H₂O aerosols. *Atmospheric Chemistry and Physics*, 7(17), 4639–4659.
- Fritz, T. M., Eastham, S. D., Emmons, L. K., Lin, H., Lundgren, E. W., Goldhaber, S., Barrett, S. R., & Jacob, D. J. (2022). Implementation and evaluation of the GEOS-Chem chemistry module version 13.1.2 within the Community Earth System Model v2.1. *EGUsphere*, 1–54.
- Fujimori, S., Abe, M., Kinoshita, T., Hasegawa, T., Kawase, H., Kushida, K., Masui, T., Oka, K., Shiogama, H., & Takahashi, K. (2017). Downscaling global emissions and its implications derived from climate model experiments. *PloS One*, 12(1), e0169733.
- Fujimori, S., Hasegawa, T., Ito, A., Takahashi, K., & Masui, T. (2018). Gridded emissions and land-use data for 2005–2100 under diverse socioeconomic and climate mitigation scenarios. *Scientific Data*, 5(1), 1–13.
- Hata, H., Inoue, K., Yoshikado, H., Genchi, Y., & Tsunemi, K. (2023). Impact of introducing net-zero carbon strategies on tropospheric ozone (O₃) and fine particulate matter (PM_{2.5}) concentrations in Japanese region in 2050. *Science of The Total Environment*, 891, 164442.
- Jiang, P., Chen, Y., Geng, Y., Dong, W., Xue, B., Xu, B., & Li, W. (2013). Analysis of the co-benefits of climate change mitigation and air pollution reduction in China. *Journal of Cleaner Production*, 58, 130–137.

- Jo, D. S., Emmons, L. K., Callaghan, P., Tilmes, S., Woo, J., Kim, Y., Kim, J., Granier, C., Soulié, A., & Doumbia, T. (2023). Comparison of Urban Air Quality Simulations During the KORUS-AQ Campaign With Regionally Refined Versus Global Uniform Grids in the Multi-Scale Infrastructure for Chemistry and Aerosols (MUSICA) Version 0. *Journal of Advances in Modeling Earth Systems*, *15*(7), e2022MS003458.
- Jones, B., & O'Neill, B. C. (2016). Spatially explicit global population scenarios consistent with the Shared Socioeconomic Pathways. *Environmental Research Letters*, *11*(8), 084003.
- Korea Environment Corporation. (n.d.). *AirKorea*. Retrieved April 20, 2022, from https://www.airkorea.or.kr/web/detailViewDown?pMENU_NO=125
- Lee, H.-M., Park, R. J., Henze, D. K., Lee, S., Shim, C., Shin, H.-J., Moon, K.-J., & Woo, J.-H. (2017). PM_{2.5} source attribution for Seoul in May from 2009 to 2013 using GEOS-Chem and its adjoint model. *Environmental Pollution*, *221*, 377–384.
- Lin, H., Feng, X., Fu, T.-M., Tian, H., Ma, Y., Zhang, L., Jacob, D. J., Yantosca, R. M., Sulprizio, M. P., & Lundgren, E. W. (2020). WRF-GC (v1. 0): Online coupling of WRF (v3. 9.1. 1) and GEOS-Chem (v12. 2.1) for regional atmospheric chemistry modeling—Part 1: Description of the one-way model. *Geoscientific Model Development*, *13*(7), 3241–3265.
- Lin, H., Jacob, D., Lundgren, E. W., Payer Sulprizio, M., Keller, C., Fritz, T., Eastham, S. D., Goldhaber, S., & Emmons, L. K. (2020). *Development of the Harmonized Emissions Component (HEMCO) 3.0 as a general emissions component for atmospheric models. 2020, A022-04.*
- Mao, J., Paulot, F., Jacob, D. J., Cohen, R. C., Crouse, J. D., Wennberg, P. O., Keller, C. A., Hudman, R. C., Barkley, M. P., & Horowitz, L. W. (2013). Ozone and organic nitrates over the eastern United States: Sensitivity to isoprene chemistry. *Journal of Geophysical Research: Atmospheres*, *118*(19), 11–256.
- Mills, G., Buse, A., Gimeno, B., Bermejo, V., Holland, M., Emberson, L., & Pleijel, H. (2007). A synthesis of AOT40-based response functions and critical levels of ozone for agricultural and horticultural crops. *Atmospheric Environment*, *41*(12), 2630–2643.
- Ministry of the Environment, Conservation and Parks. (n.d.). *Air Pollutant Data*. Air Quality Ontario; Government of Ontario, Ministry of the Environment. Retrieved April 13, 2022, from <http://www.airqualityontario.com/history/>

- Ministry of the Environment, Government of Japan. (n.d.). *PM2.5 monitoring data (overseas)*. Retrieved April 18, 2022, from <http://www2.env.go.jp/pm25monitoring/download.html>
- National Environment Agency. (n.d.). *Historical 1-hr PM2.5*. Data.Gov.Sg. Retrieved April 19, 2022, from <https://data.gov.sg/dataset/historical-1-hr-pm2-5>
- National Institute for Environmental Studies. (n.d.). *Environmental Numerical Database*. Retrieved April 15, 2022, from <https://www.nies.go.jp/igreen/index.html>
- Nemet, G. F., Holloway, T., & Meier, P. (2010). Implications of incorporating air-quality co-benefits into climate change policymaking. *Environmental Research Letters*, 5(1), 014007.
- Parrella, J., Jacob, D. J., Liang, Q., Zhang, Y., Mickley, L. J., Miller, B., Evans, M., Yang, X., Pyle, J., & Theys, N. (2012). Tropospheric bromine chemistry: Implications for present and pre-industrial ozone and mercury. *Atmospheric Chemistry and Physics*, 12(15), 6723–6740.
- Pollution Control Department, Thailand. (n.d.). *Air4Thai: Historical data*. Retrieved April 18, 2022, from <http://www.air4thai.com/webV2/history/>
- Protonotariou, A., Tombrou, M., Giannakopoulos, C., Kostopoulou, E., & Le Sager, P. (2010). Study of CO surface pollution in Europe based on observations and nested-grid applications of GEOS-CHEM global chemical transport model. *Tellus B: Chemical and Physical Meteorology*, 62(4), 209–227.
- Pye, H., Chan, A., Barkley, M., & Seinfeld, J. (2010). Global modeling of organic aerosol: The importance of reactive nitrogen (NO_x and NO₃). *Atmospheric Chemistry and Physics*, 10(22), 11261–11276.
- Rao, S., Klimont, Z., Smith, S. J., Van Dingenen, R., Dentener, F., Bouwman, L., Riahi, K., Amann, M., Bodirsky, B. L., & van Vuuren, D. P. (2017). Future air pollution in the Shared Socio-economic Pathways. *Global Environmental Change*, 42, 346–358.
- Sacks, W. J., Deryng, D., Foley, J. A., & Ramankutty, N. (2010). Crop planting dates: An analysis of global patterns. *Global Ecology and Biogeography*, 19(5), 607–620.
- Schwantes, R. H., Lacey, F. G., Tilmes, S., Emmons, L. K., Lauritzen, P. H., Walters, S., Callaghan, P., Zarzycki, C. M., Barth, M. C., & Jo, D. S. (2022). Evaluating the impact of chemical complexity and horizontal resolution on tropospheric ozone over the conterminous US with a global variable resolution chemistry model. *Journal of Advances in Modeling Earth Systems*, 14(6), e2021MS002889.

- Tai, A. P., Martin, M. V., & Heald, C. L. (2014). Threat to future global food security from climate change and ozone air pollution. *Nature Climate Change*, *4*(9), 817–821.
- Thurston, G. D., & Bell, M. L. (2021). The human health co-benefits of air quality improvements associated with climate change mitigation. In *Climate Change and Global Public Health* (pp. 181–202). Springer.
- Travis, K. R., Jacob, D. J., Fisher, J. A., Kim, P. S., Marais, E. A., Zhu, L., Yu, K., Miller, C. C., Yantosca, R. M., & Sulprizio, M. P. (2016). Why do models overestimate surface ozone in the Southeast United States? *Atmospheric Chemistry and Physics*, *16*(21), 13561–13577.
- U.S. Environmental Protection Agency Clean Air Markets Division. (n.d.). *Clean Air Status and Trends Network (CASTNET)*. Hourly Ozone, Hourly PM_{2.5}. Retrieved April 13, 2022, from www.epa.gov/castnet
- Van Dingenen, R., Dentener, F. J., Raes, F., Krol, M. C., Emberson, L., & Cofala, J. (2009). The global impact of ozone on agricultural crop yields under current and future air quality legislation. *Atmospheric Environment*, *43*(3), 604–618.
- Vandyck, T., Keramidas, K., Kitous, A., Spadaro, J. V., Van Dingenen, R., Holland, M., & Saveyn, B. (2018). Air quality co-benefits for human health and agriculture counterbalance costs to meet Paris Agreement pledges. *Nature Communications*, *9*(1), 1–11.
- West, J. J., Smith, S. J., Silva, R. A., Naik, V., Zhang, Y., Adelman, Z., Fry, M. M., Anenberg, S., Horowitz, L. W., & Lamarque, J.-F. (2013). Co-benefits of mitigating global greenhouse gas emissions for future air quality and human health. *Nature Climate Change*, *3*(10), 885–889.
- Xiong, Y., Partha, D., Prime, N., Smith, S. J., Mariscal, N., Salah, H., & Huang, Y. (2022). Long-term trends of impacts of global gasoline and diesel emissions on ambient PM_{2.5} and O₃ pollution and the related health burden for 2000–2015. *Environmental Research Letters*, *17*(10), 104042.
- Zhang, L., Jacob, D. J., Downey, N. V., Wood, D. A., Blewitt, D., Carouge, C. C., van Donkelaar, A., Jones, D. B., Murray, L. T., & Wang, Y. (2011). Improved estimate of the policy-relevant background ozone in the United States using the GEOS-Chem global model with $1/2 \times 2/3$ horizontal resolution over North America. *Atmospheric Environment*, *45*(37), 6769–6776.

Chapter 4

The influence of agricultural ammonia emissions reduction on air pollution and human health

4.1 Abstract

The use of nitrogen fertilizers for food production could limit global warming to 2-degree Celsius above pre-industrial levels. An essential source of human activity is the agricultural sector. About 40% of total methane emissions are attributed to FAOSTAT, while nitrous oxide emissions account for 60% of total emissions. This study uses the GEOS-chem model meteorological parameter to examine the impact of ammonia emissions from the agricultural sector, particularly fine particulate matter (PM_{2.5}) and ozone (O₃), and assess health burden from air pollution. The result can show that the changes in the annual average PM_{2.5} concentrations according to the ammonia (NH₃) emission changes in the world ranging from 0.0 to -64.9 percent (0.0 to -46.5 µg/m³) at Manmade-ammonia emission reduction at 100% while the 50% ammonia reduction scenarios, the ranged was from 0.0 to -24.0 percentage (0.0 to -24.7 µg/m³). However, when focusing on reducing ammonia, only the agricultural sector found that PM_{2.5} concentrations decreased by approximately 23.8 µg/m³ and 45.8 µg/m³ when reducing ammonia emissions at 50% and 100%, respectively. In addition, the comparison between changes in PM_{2.5} concentration changes due to emission inventory changes found that the concentration was significantly declined in the area with high agricultural emission rates, such as Asia, Europe, and North America. Regarding O₃ concentrations, when we examined scenarios with zero ammonia emissions, we observed a significant increase in O₃ concentration. Specifically, in China, the O₃ concentration rose by up to 9.3%, and in the European Union, it experienced a 7.4% increase. In ammonia reduction scenarios, at both 50% and 100% levels, we project a significant reduction in mortality, ranging from about 3.17% to 13.51%. Additionally, when NH₃ and NO_x reduction strategies are combined, mortality decreases substantially, ranging from 5.95% to 15.85% for 50% emission reduction and complete emission eradication, respectively.

Keywords: Ammonia, Fine Particulate Matter, Fertilizer, Agricultural, Air Pollution

4.2 Introduction

NH_3 is an inorganic compound composed of nitrogen and hydrogen. It is a colorless gas that is primarily released from various sources in the agricultural sector. These sources include livestock manure, synthetic fertilizers, and other agricultural practices. According to the EEA 2018 report, agriculture is responsible for a significant portion, approximately 92%, of volatile ammonia emissions in Europe. Within the agricultural sector, livestock and manure are the main contributors to ammonia emissions, accounting for approximately 64% of the total emissions. The use of nitrogen fertilizers is another significant source, contributing around 17% of ammonia emissions. The remaining 19% of ammonia emissions come from other sources within the agricultural sector (EEA, 2018). Ammonia, a compound with environmental impacts, can contribute to air pollution and disturbances in ecosystems. It exhibits the ability to move between the Earth's surface and the atmosphere, with its transport influenced by several factors, including meteorological conditions and soil characteristics. The transfer of NH_3 gas takes place through two main fluid layers: the laminar layer at the liquid-air interface, where molecular diffusion aids its movement, and the turbulent layer, where turbulent diffusion allows NH_3 to disperse into the surrounding environment. In this process, ammonia can react with other gases, leading to the formation of secondary pollutants such as $\text{PM}_{2.5}$ and O_3 (Behera et al., 2013).

$\text{PM}_{2.5}$ emissions are predominantly of anthropogenic origin, arising from diverse human activities (Gelencsér et al., 2007; Querol et al., 2001; X. Wang et al., 2020). These include the industrial sector, vehicular traffic, and uncontrolled wildfires, while agricultural practices also contribute to some extent. Depending on their origins, $\text{PM}_{2.5}$ is categorized as primary or secondary. Primary $\text{PM}_{2.5}$ constitutes particles that are directly released into the atmosphere from various sources. These particles are initially in solid or liquid form and may undergo transformations in the atmosphere due to various physical and chemical processes. Secondary $\text{PM}_{2.5}$, on the other hand, forms in the atmosphere as a result of complex chemical reactions involving gaseous precursors emitted from anthropogenic sources. For instance, short-lived gaseous ammonia can react with other atmospheric constituents to produce more persistent fine particulates that can impact air quality in regions far from their agricultural origins (Koziel et al., 2006; Von Schneidemesser et al., 2015).

Sulfate–Nitrate–Ammonium (SNA) aerosols are the main dominate precursor of the secondary fine particulate matter formation in many region of the world (Heald et al., 2012; Long et al., 2014; Y. Wang et al., 2023; Zhang et al., 2021). The secondary inorganic aerosols (SIA) components in PM are ammonium (NH_4^+), nitrate (NO_3^-), and sulfate (SO_4^{2-}), which occur as ammonium nitrate ($\text{NH}_4 \text{NO}_3$) and ammonium sulfate ($(\text{NH}_4)_2\text{SO}_4$), respectively, and are formed by the neutralization of nitric acid (HNO_3) and sulfuric acid (H_2SO_4) with ammonia in the atmosphere. For example, Wang et al. (2013) have simulated sulfate-nitrate-ammonium aerosols over China: Response to 2000-2015 emission changes of sulfur dioxide, nitrogen oxides, and ammonia using a chemical transport model. they found that Annual mean SNA concentrations in China increased by around 60% between 2000 and 2006, owing to increases in SO_2 and NO_x emissions of 60% and 80%, respectively. Sulfate is the main component of SNA over South China (SC) and the Sichuan Basin (SCB) during this era, while nitrate and sulfate contribute equally over North China (NC).

Air pollution stands as an undeniable and alarming threat to both human health and environmental well-being (Kampa & Castanas, 2008; Mabahwi et al., 2014; Manisalidis et al., 2020). Among the various pollutants, ambient air pollution, especially $\text{PM}_{2.5}$ and O_3 , has emerged as a major contributor to the devastation. According to a World Health Organization (WHO) report, approximately 4.2 million people succumb to premature deaths each year worldwide due to the impacts of ambient air pollution. This staggering toll highlights the urgency of addressing this global challenge. Consequently, numerous studies have been undertaken to investigate the sources of pollution emissions, aiming to find effective solutions to mitigate this pressing issue. Understanding the origins of these pollutants is crucial in formulating targeted strategies to safeguard public health and preserve environmental quality for future generations.

This study we aim to understand the influencing of ammonia emissions from the agricultural sector in each assumption reduction scenarios on $\text{PM}_{2.5}$ and O_3 concentration using GEOS-Chem model collaborating with meteorological parameter and health exposure model to determine the number of avoided deaths from the reduction scenario.

4.3 Methodology

4.3.1 Air pollution simulations

In this study we applied a global 3-D model of atmospheric chemistry driven by meteorological input from the Goddard Earth Observing System (GEOS-Chem) version 12.9.3 of the NASA Global Modeling and Assimilation Office (<http://www-as.harvard.edu/chemistry/trop/geos>) to simulate the concentrations of fine particulate matter and ozone due to ammonia emission from agricultural changing (Bey et al., 2001). The GEOS-Chem simulations use a global resolution of 4° latitude by 5° longitude with 72 vertical layers and the sulfate-nitrate-ammonium aerosol system in conjunction with gas-phase chemistry to provide the aerosol species. While the total ammonia and nitric acid partitioning between gas and particle phase was determined using ISORROPIA II thermodynamic equilibrium model to provide the inorganic aerosol formation and calculate aerosol concentrations correspond to PM_{2.5} concentrations.

4.3.2 Sensitivity Analysis of Ammonia Emission Reduction on Air Pollution and Human Health

In this study, the researchers aimed to investigate the influence of agricultural emission focus on NH₃ and NO_x emission reduction on air pollution and human health. The Anthropogenic gridded emission inventories (0.5 degrees) from 12 sectors, including agriculture, agricultural burning, energy, forest burning, industry, domestic, inland transport, air transport, savanna burning, shipping, solvent, and waste from the AIM-SSP/RCP Gridded Emissions developed by Fujimori et al. (2018) was used to be as an input emission inventory in the GEOS-chem model. The baseline scenario chosen was SSP2 in 2015 without considering climate change. To understand the effects of ammonia emission reduction, several assumption scenarios were formulated based on different emission reduction levels as shown in Table 4-1.

In order to determine the sensitivity of ammonia and nitrogen oxide emission reduction, we designed an experiment to ascertain the relationship between changes in ammonia emissions and PM_{2.5} and O₃ concentrations. By comparing the different scenarios and their corresponding effects on PM_{2.5} concentrations, the researchers could draw conclusions about the impact of ammonia

emission reductions on air pollution and human health. This information could be valuable for policymakers and stakeholders in formulating strategies to mitigate air pollution and its associated health risks.

Table 4-1 Scenario description

Scenario Name	Species	Emission Reduction (%)	Sector
Scenario 0		Baseline (Business as Usual)	
Scenario 1		50	All sectors*
Scenario 2		100	
Scenario 3	Ammonia (NH ₃)	50	
Scenario 4		100	
Scenario 5	Nitrogen Oxide	50	Agriculture
Scenario 6	(NO _x)	100	
Scenario 7		50	
Scenario 8	NH ₃ and NO _x	100	

*All sectors including Transportation, Resident, Industry, Solvent, International Ship, Energy, Waste disposal, Agriculture

We evaluated the outcomes of an air pollution simulation utilizing ten air pollution monitoring stations distributed globally. The selection of these monitoring stations was guided by land use data, with a predominant focus on locating them within or in close proximity to agricultural regions. This approach allows us to effectively demonstrate the influence of agricultural activities on air pollution. The chosen locations for these monitoring stations include Thailand, South Korea, China, Japan, Canada, Singapore, Brazil, the United States of America, South Africa, and India as shown in Table 4-2.

Table 4-2 Air pollution monitoring station locations based on agricultural land use.

Station	Country	Latitude	Longitude
Nakhon Sawan, THA	Thailand	15.68	100.11
Jeonbuk, KOR	Korean	35.614	127.286
Luoyang, CHN	China	34.61	112.454
Sendai, JPN	Japan	38.26	140.869
Fort Saskatchewan, CAN	Canada	53.698	-113.222
Central, SIG	Singapore	1.366	103.8
Taubate, BRA	Brazil	-23.03	-45.575
Missouri, USA	USA	37.25	-93.299
Esikhaleni, ZAF	South Africa	-28.868	31.909
Bengaluru, IND	India	12.938	77.59

In order to facilitate a comprehensive comparison of sensitivity analysis results, we have employed the concept of relative change expressed as a percentage. This approach enables us to quantify and contrast the degree of variation across different factors under examination.

4.3.3 Health Implication Analysis

To examine the health consequences of altering $PM_{2.5}$ concentrations as a result of different reduction scenarios, the health exposure model was utilized. In this case, the Global Exposure Mortality Mode (GEMM) function was used to estimate the number or premature mortality related to $PM_{2.5}$, we considered five health outcomes: cerebrovascular disorders (stroke), ischemic heart disease (IHD), chronic obstructive pulmonary disease (COPD), lung cancer (LC), and acute respiratory lung infection (ALRI). Equation 3-3 was employed to determine the premature mortality due to $PM_{2.5}$ exposure.

4.4 Results

4.4.1 PM_{2.5} and O₃ sensitivity to NH₃ and NO_x emission reduction scenarios

NH₃ sensitivity simulations have provided valuable insights into the influence of NH₃ emissions on the annual average PM_{2.5} concentrations across global regions. The observed variations ranged from a neutral percentage to a substantial -64.9%, corresponding to a consequential reduction in concentrations from negligible levels to as much as -46.5 µg/m³, assuming the complete absence of anthropogenic ammonia emissions. This range was narrower under the 50% reduction scenario, spanning from neutral values to -24.0%, resulting in a corresponding concentration decline of up to -24.7 µg/m³. Particularly noteworthy were the prominent effects observed in geographical sectors such as Europe, China, and certain areas within North America. These findings underscore the pronounced impact of the prevailing anthropogenic ammonia emissions from these regions.

Subsequent investigations involved conducting simulations to assess the impact of ammonia emissions from agricultural sources on PM_{2.5} concentrations. The aim was to understand how reducing ammonia emissions by 50% and 100% would affect these concentrations. The results showed noticeable decreases in PM_{2.5} levels, specifically around 23.8 µg/m³ and 45.8 µg/m³ for the respective reductions (Figure 4-1a and 4-1b). Comparing the broader reduction of ammonia emissions with those limited to the agricultural sector highlighted a significant contribution of ammonia-related sources, particularly from cultivated lands, to PM_{2.5} levels. This finding was consistent across Europe, China, and specific areas of North America. The consistency in these observations can be attributed to the substantial amount of ammonia emissions generated by human activities in these regions, as visually represented in figure 4-1.

In Figures 4-1c and 4-1d, we observe significant reductions in NO_x emissions of 50% and 100%, resulting in a relatively slight decrease in PM_{2.5} concentrations compared to the considerable reductions achieved through adjustments in ammonia emissions. Our analysis underscores the need to appreciate the nuanced relationship between NO_x emissions and PM_{2.5} levels. Depending on specific geographical locations and prevailing meteorological conditions, we note a subtle potential increase in PM_{2.5} concentrations following the reduction of NO_x emissions.

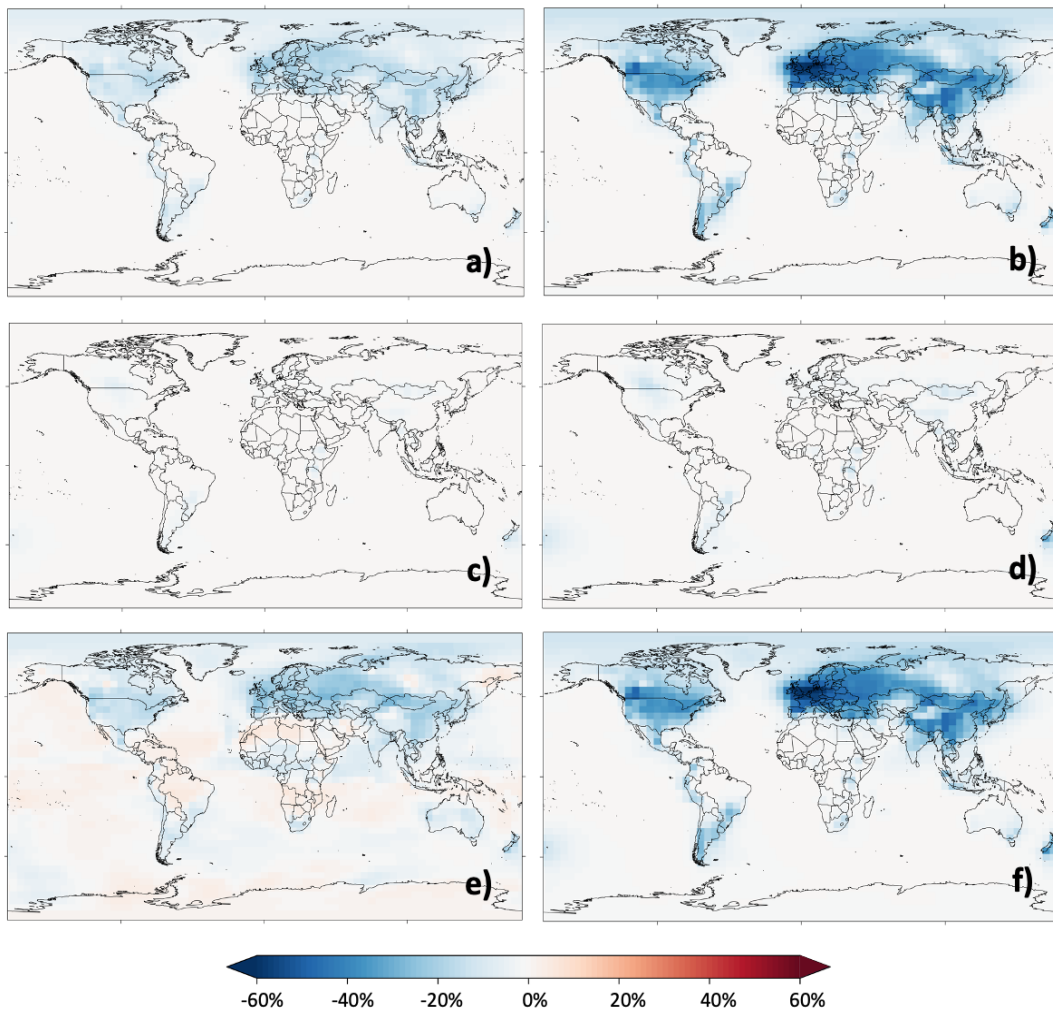


Figure 4-1 Spatial plot of PM_{2.5} concentration relative changing (%) between baseline and scenario 3 (a), scenario 4 (b), scenario 5 (c), scenario 6 (d), scenario 7 (e), and scenario 8 (f)

Furthermore, we conducted a thorough evaluation by comparing agricultural scenarios involving 50% and 100% reductions in both NO_x and NH₃ emissions. This investigation aims to clarify the combined impact of these pollutants on ambient PM_{2.5} levels. Notably, our findings presented in Figures 4-1e and 4-1f, and 4-2 reveal only a marginal difference in PM_{2.5} concentrations when contrasted with scenarios focusing solely on reducing NH₃ emissions at both levels. This outcome can be attributed to the limited influence of NO_x emissions from agricultural sources, underscoring their minimal effect within this specific context.

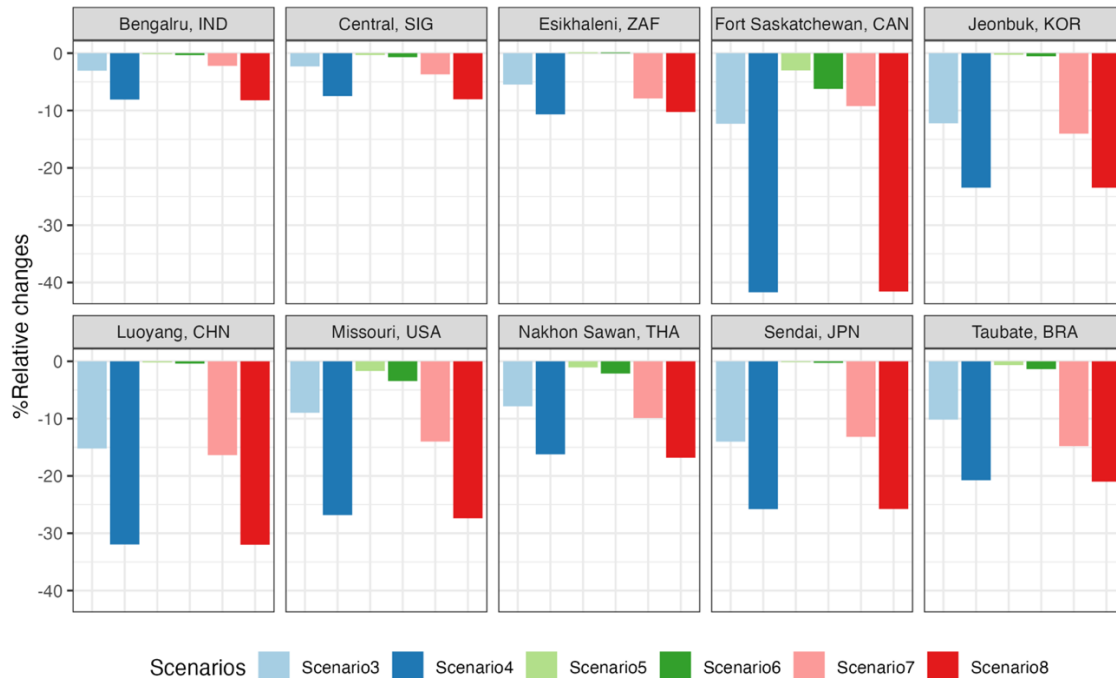


Figure 4-2 The relative annual PM_{2.5} concentrations changes between baseline scenario and sensitivity case (Scenario 3-8)

Figure 4-2 illustrates the percentage fluctuations in PM_{2.5} concentrations across multiple countries: Brazil, Canada, China, India, Japan, South Korea, Singapore, Thailand, the United States of America, and South Africa. When considering scenarios with no agricultural ammonia emissions, Canada experienced a notable reduction of around 41.69%, while China saw a relative decrease of 31.94%. Furthermore, we observed a distinct trend wherein the reduction of ammonia emissions to 100% resulted in a more pronounced decline in PM_{2.5} concentrations compared to scenarios with a 50% reduction. This trend was particularly evident in Canada and the United States.

Figure 4-3 presents the proportion of fine-particle mass that responds to changes in ammonia emissions, as indicated by the study conducted by Pozzer et al. in 2017. The outcomes reveal that Canada, and the United States exhibit a heightened sensitivity of PM_{2.5} concentrations to fluctuations in ammonia emissions, surpassing other countries. In Canada, this sensitivity percentage amounts to approximately 26%. Consequently, a substantial reduction in PM_{2.5} concentrations can be expected when ammonia emissions are decreased by 100%. On the other

hand, when reductions are set at 50% and 100%, the dissimilarity between these two scenarios is roughly halved in comparison to other countries.

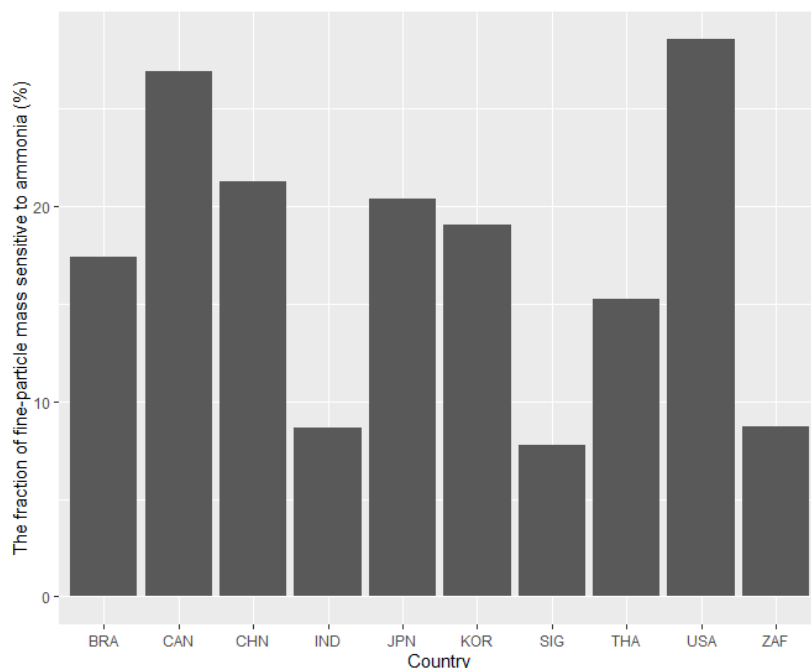


Figure 4-3 The fraction of fine-particle mass sensitive to ammonia (%)

Conversely, the reduction of agricultural ammonia emissions can lead to increased ground-level O₃ concentrations, particularly in Asia and Europe, where the primary contributors of ammonia emissions originate from the agricultural sector, as depicted in Figures 4-4a and 4-4b. In the fourth scenario examined, which involves the complete elimination of agricultural ammonia emissions, a noticeable uptick in O₃ concentration is observed. Specifically, in China, the O₃ concentration rises by up to 9.3%, while in the European Union, it experiences a 7.4% increase. Notably, when comparing the effectiveness of mitigating O₃ concentration, the reduction of NO_x emissions proves to be more impactful than that of NH₃ emissions. Our investigation further highlights a reduction in O₃ concentration across the southern hemisphere, particularly notable in regions like South Africa, when the complete elimination of NO_x emissions stemming from agricultural activities is considered. This reduction could reach approximately 31%, as demonstrated in Figure 4-4d.

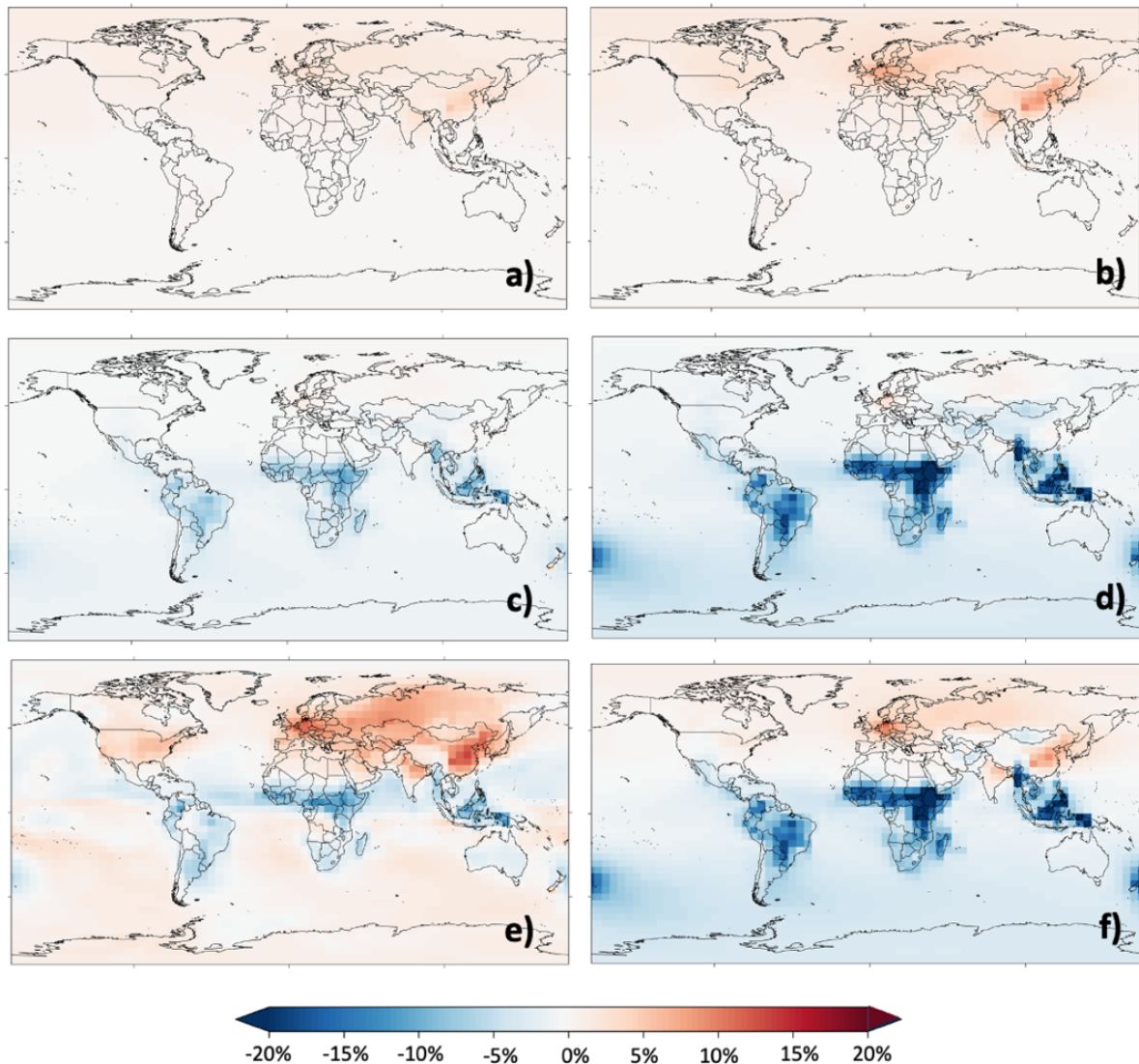


Figure 4-4 Spatial plot of O₃ concentration relative changing (%) between baseline and scenario 3 (a), scenario 4 (b), scenario 5 (c), scenario 6 (d), scenario 7 (e), and scenario 8 (f)

Figures 4-4e and 4-4f provide insight into the relative changes in O₃ concentration resulting from variations in NH₃ and NO_x emissions originating from the agricultural sector. We found that a concurrent reduction of both NH₃ and NO_x emissions by 50% (Scenario 7) triggers an elevation in O₃ levels across the northern hemisphere, notably in regions such as China and the European Union, with an increase of around 13.2%. Conversely, within the southern hemisphere, a decrease in O₃ concentration is observed, particularly in areas like South-east Asia and Central Africa.

Furthermore, when both NH₃ and NO_x emissions from agricultural sources are entirely eliminated (Scenario 8), the previously observed rise in O₃ concentration within the northern hemisphere following a 50% reduction reverses, leading to a decrease, as depicted in Figure 4-4f. Notably, in the southern hemisphere, a significant reduction in O₃ concentration becomes apparent, with a decline of approximately 30%. These findings highlight the intricate interplay between NH₃ and NO_x emissions and their effects on O₃ concentrations, emphasizing the importance of considering both emissions when formulating strategies to manage O₃ levels in different regions.

4.4.2 Seasonal effects of ammonia emission reductions on PM_{2.5}

As illustrated in Figure 4-5, the increase in wintertime PM_{2.5} concentration can be attributed to meteorological factors that influence chemical reactions and the dispersion of pollutants. While controlling pollution sources remains crucial in managing regional fine particulate matter, its effectiveness is more pronounced for primary PM rather than secondary PM. Therefore, the regulation of ammonia emissions emerges as a vital consideration in addressing levels of secondary PM. Ammonia plays a pivotal role by interacting with atmospheric sulfuric and nitric acids, leading to the formation of secondary particulate matter. Previous research highlights the utmost significance of reducing ammonia emissions as the primary strategy for mitigating secondary particulate matter, surpassing alternative approaches such as the reduction of NO_x and SO_x emissions.

Addressing the challenge of reducing total ammonia emissions and concentrating efforts solely within the agricultural sector has proven to be inadequate in effectively controlling PM_{2.5} levels across diverse regions. For instance, when the proposed ammonia reduction scenario was applied to mitigate PM_{2.5} levels, it became evident that the disparity in fine particle concentration between the baseline and reduction scenarios was less pronounced in Africa, in contrast to the more discernible differentiation observed in both Asia and Europe. This discrepancy could be attributed to varying emission sources and atmospheric processes unique to each region.

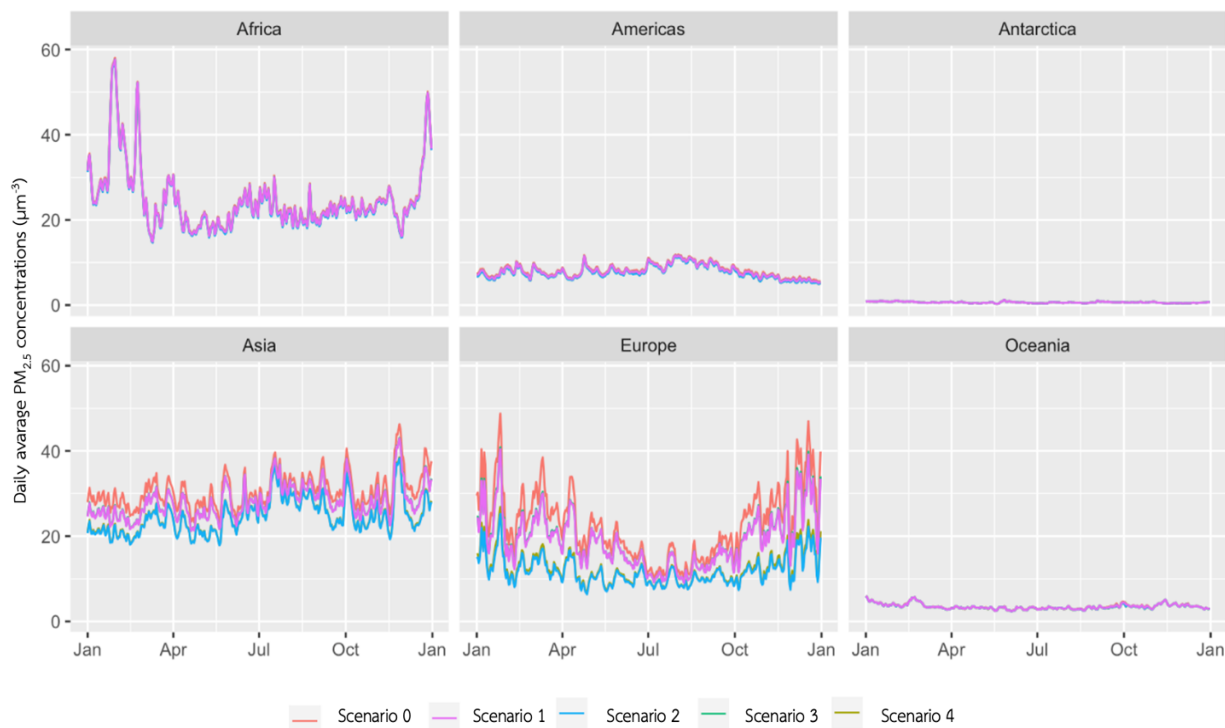


Figure 4-5 Daily average PM_{2.5} concentrations comparing between baseline (red), scenario 1 (pink), scenario 2 (blue), scenario 3 (green), and scenario 4 (dark yellow) in 2015.

A comprehensive analysis of a time series detailing the daily average PM_{2.5} concentration within the EU further sheds light on this matter. It becomes evident that the reduction of ammonia emissions, particularly in a zero-emission scenario, exhibits heightened efficacy in curtailing PM_{2.5} concentrations during the winter months (December to February, DJF) in comparison to the summer months (March to May, MAM). This observation could be attributed to meteorological factors, such as temperature inversions and stagnant air conditions during winter, which can exacerbate PM_{2.5} accumulation.

Analyzing the chemical interplay between NO_x and NH₃ offers valuable insights into the viability of emission reduction scenarios within mitigation policies. In this context, we employed the chemical regime calculation methodology outlined in Thunis et al. (2021) to present a spatial depiction of the contrasting impacts of two potential reductions: a 50% decrease in NH₃ emissions and a 50% decrease in NO_x emissions from agricultural sources.

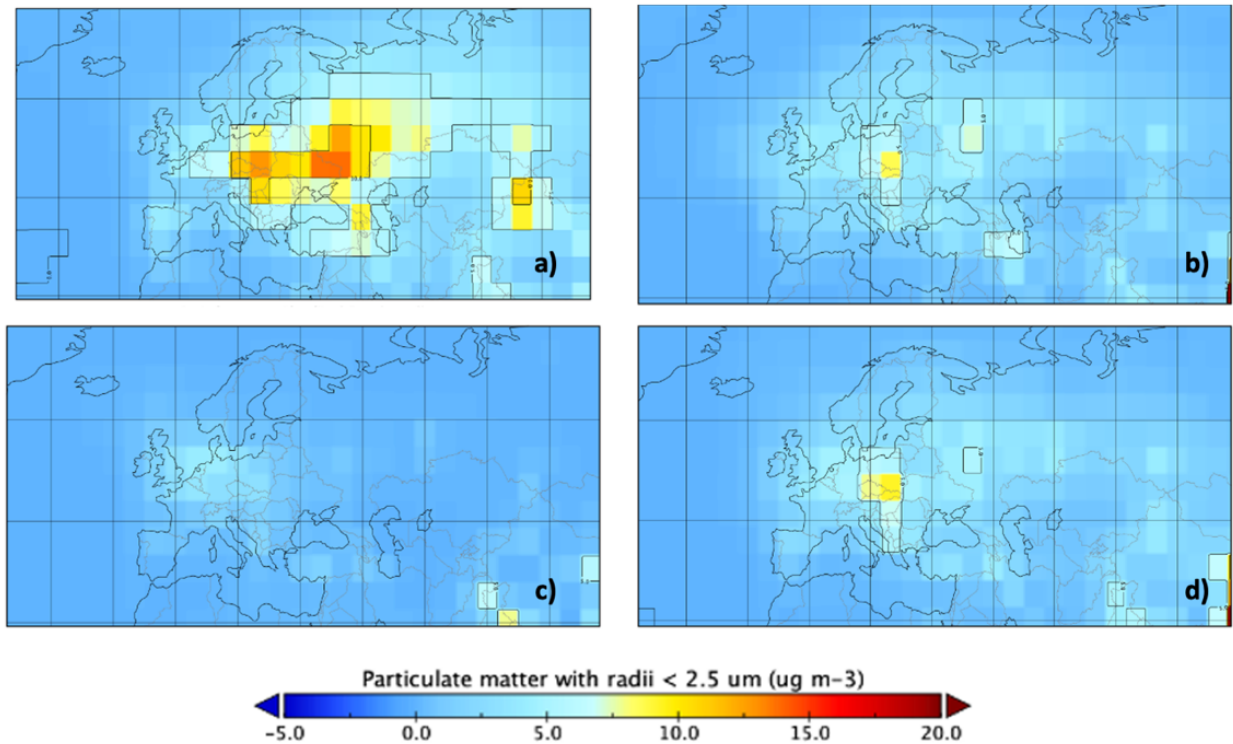


Figure 4-6 Winter (a), summer (b), spring (c), and fall (d) chemical regime from emission reduction at 50%. The spatial map shows the NO_x reduction 50% - NH₃ reduction 50%. Red/blue color represent the NO_x and NH₃ sensitivity area in EU.

The polarity of resulting values – whether positive or negative – serves as a key indicator of emission sensitivity concerning fluctuations in PM_{2.5} concentration across specific areas. A negative value indicates a predominance of NO_x control, suggesting that reduction efforts in NO_x emissions yield a more substantial influence on PM_{2.5} concentration changes. Conversely, a positive value signifies a prevalence of NH₃ control, highlighting the heightened efficacy of curbing NH₃ emissions in driving PM_{2.5} concentration alterations. In the winter season, the fine particulate matter was sensitive to the level NH₃ emission changing than NO_x emission. Thus, when cut half of NH₃ emission from agricultural sector, the concentration of PM_{2.5} in the central part of EU was significantly reduce. While in the fall and spring season, in Poland, Slovakia and Czech Republic are the most sensitivity area when the NH₃ emission control was applied as shown in Figure 4-6.

4.4.3 Health implication assessment of PM_{2.5} concentration change

To evaluate the health implications arising from variations in PM_{2.5} concentrations as influenced by reduction scenarios, we employ the GEMM function, as developed by Burnett et al. (2018). Figure 4-7 presents a comparative representation of premature mortality figures attributed to PM_{2.5} exposure, contrasting the baseline scenario with sensitivity cases. The quantification of premature deaths resulting from shifts in PM_{2.5} concentrations aligns with the outcomes obtained from the CTM.

In regions characterized by significant reductions in PM_{2.5} concentrations, a conspicuous decrease in mortality rates is observed across all geographic areas. The association between diminished PM_{2.5} concentrations and decreased premature mortality becomes evident. Under the purview of ammonia reduction scenarios, both at 50% and 100% levels, a noteworthy reduction in mortality, ranging from approximately 3.17% to 13.51%, is projected. Moreover, the conjoint application of NH₃ and NO_x reduction strategies yields a substantial decline in mortality, ranging from 5.95% to 15.85% for the cases of 50% emission reduction and complete emission eradication respectively. However, it is crucial to acknowledge that specific regions may encounter a marginal elevation in PM_{2.5} concentrations, leading to a commensurate upsurge in mortality rates within the ambit of emission reduction strategies.

Notably, in the context of exclusive NO_x reduction, a nuanced observation emerges. The reduction in NO_x emissions, while inducing a marginal increase in PM_{2.5} levels within NO_x-rich locales, results in a corollary increase in mortality rates. Hence, a discernible increase in mortality is anticipated under both the 50% and 100% emission reduction scenarios as indicate in Figure 4-7.

In the context of disease incidence distribution relative to PM_{2.5} exposure as shown in Table 4-4, a pronounced reduction in mortality rates is evident in cases of lung cancer. Precisely, the implementation of a 50% or 100% reduction in ammonia emissions originating from the agricultural sector is associated with noteworthy declines in mortality rates, amounting to -4.95% and -18.39% respectively. In a divergent pattern, the incidence of stroke demonstrates a mortality reduction of 15.81% when complete elimination of ammonia emissions is realized. Alternatively,

a discernible reduction of 4.15% is discerned when a 50% reduction in ammonia emissions is affected.

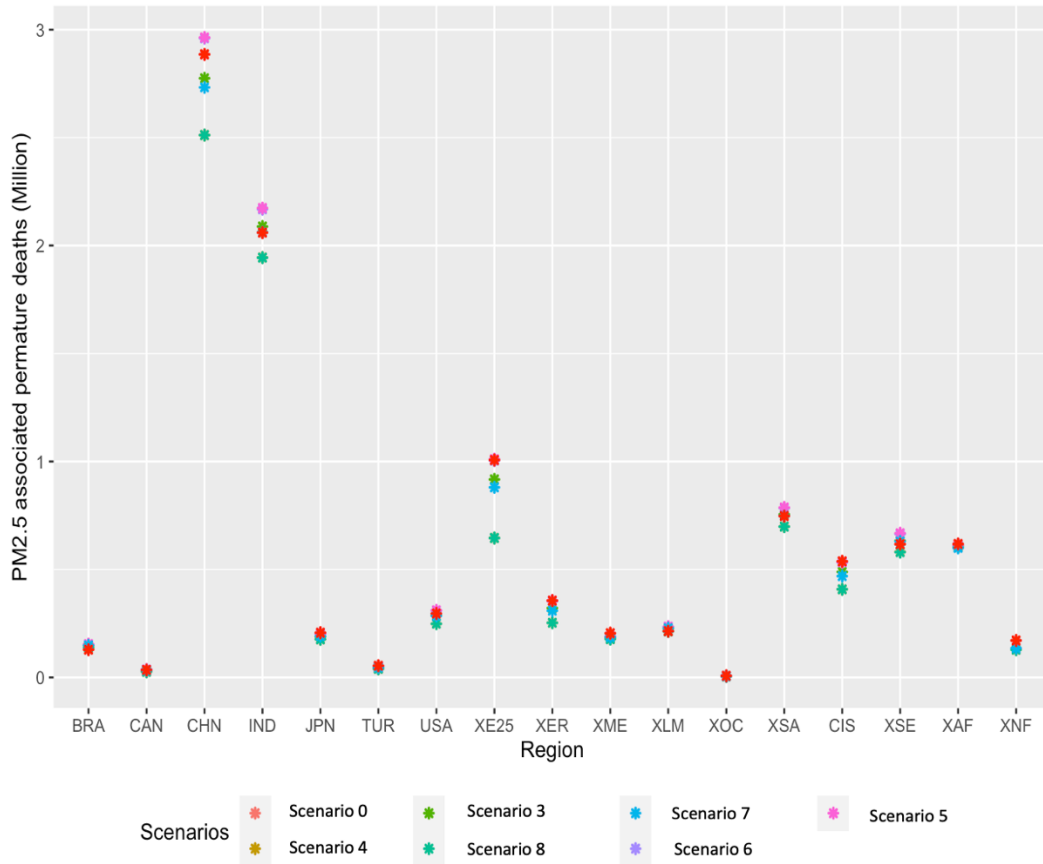


Figure 4-7 PM_{2.5} associated premature deaths (GEMM-5COD) change comparing between baseline (red), scenario 3 (green), scenario 4 (dark yellow), scenario 5 (pink), scenario (purple), scenario 7 (blue), and scenario 8 (ocean blue)

Conversely, an examination of mortality changes across different regions under varying reduction scenarios elucidates significant outcomes. In the scenario involving complete ammonia emission elimination, PM_{2.5} concentrations in Canada are projected to decrease by 41.69%, thereby resulting in a 35% reduction (-814 individuals) in mortality attributed to PM_{2.5} exposure. Similarly, in China, a reduction of approximately 31.94% in PM_{2.5} concentrations is estimated to mitigate PM_{2.5}-associated premature deaths by 373,893 individuals (-12.95%). Nonetheless, it is prudent to acknowledge that specific geographical areas may witness an elevation in mortality rates due to the induction of PM_{2.5} concentrations resulting from ammonia emission reduction.

Table 4-3 PM_{2.5} associated premature deaths change between baseline scenario and sensitivity cases separate by disease (%)

Scenarios/Disease	COPD	LC	LRI	IHD	STROKE	NCD+LRI	5-COD
Scenario 3	-1.77	-4.95	-1.73	-3.18	-4.15	-3.17	-3.20
Scenario 4	-11.50	-18.39	-9.88	-12.72	-15.81	-13.51	-13.38
Scenario 5	3.90	2.43	2.14	1.85	2.71	2.64	2.06
Scenario 6	3.60	2.08	1.81	1.55	2.34	2.31	2.38
Scenario 7	-3.26	-6.78	-2.86	-4.60	-5.95	-4.73	-4.71
Scenario 8	-11.53	-18.43	-9.97	-12.76	-15.86	-13.56	-13.43

*COPD= Chronic Obstructive Pulmonary Disease, LC=Lung Cancer, LRI=Low Respiratory Infection, IHD= Ischemic Heart Disease, NCD=Non-Communicated Disease, 5-COD=Fives Cohort Disease

4.5 Discussion

4.5.1 Effect of ammonia emission reduction on PM_{2.5} and O₃ level

Addressing PM_{2.5} concentration requires a focus on its primary sources as an effective strategy for mitigation. Our study highlights that while reducing agricultural ammonia emissions proves beneficial in mitigating the PM_{2.5} issue in the EU and Asia, its impact on fine particulate matter levels in the African region is less pronounced. This discrepancy is attributed to the dominant sources of particulate matter emissions in Africa, namely open burning, and the use of solid fuels in households. These activities play a pivotal role in driving elevated PM levels in the region (Tahri et al., 2022).

Furthermore, within the scope of this study, an additional scenario was developed wherein agricultural NO_x emissions were subjected to reduction measures. The outcomes of this scenario exhibited a subtle influence on PM_{2.5} concentrations, with discernible fluctuations being observed only in select areas and during specific temporal instances. This phenomenon can potentially be

attributed to the multifaceted role that NO_x plays in $\text{PM}_{2.5}$ dynamics, particularly in the context of ammonium nitrate formation (Thunis et al., 2021). Ammonium nitrate (NH_4NO_3), a notable contributor to $\text{PM}_{2.5}$, materializes through complex chemical interactions involving NH_3 and nitric acid (HNO_3), both of which are intricately influenced by NO_x emissions. The reduction of NO_x emissions engenders a decline in the availability of nitric acid. Consequently, residual ammonia may engage with sulfuric acid (H_2SO_4), causing the creation of ammonium sulfate, an alternate variant of $\text{PM}_{2.5}$. The residual ammonia, left unreacted, potentially serves as an excess substrate for the generation of ammonium nitrate. This intricate interplay can potentially lead to a discernible elevation in aggregate $\text{PM}_{2.5}$ levels.

On the contrary, the reduction of $\text{PM}_{2.5}$ through NH_3 emission mitigation may inadvertently lead to an elevation in O_3 levels across numerous regions. This phenomenon becomes particularly evident in countries situated near the equator. In contexts where NO_x emissions are curtailed in proximity to the equator, a diminished availability of NO_x for ozone-generating reactions becomes apparent. This deficiency in NO_x can counteract the reactions responsible for ozone formation, resulting in a discernible decline in ozone concentrations. These findings align with the observations presented in the study by Li et al. (2013), wherein the reduction of NO_x was observed to effectively lower peak ozone concentrations both spatially and temporally.

Conversely, in countries located within temperate zones, a notable increase in ozone concentration is observed when NH_3 emissions are reduced. Notably, China experienced the most significant surge in ozone concentrations following NH_3 reduction. This upsurge in ozone is attributed to the oxidation of NH_3 , which subsequently reacts with nitric acid to form NH_4NO_3 . The kinetics of these reactions are closely tied to the initial stoichiometric ratio of NH_3 to O_3 . Therefore, in instances where the reduction of oxidizing pollutants, such as NH_3 , is implemented, there is a discernible escalation in ozone concentration levels corresponding with Jian et al. (2023).

4.5.2 Limitation

Furthermore, it is important to acknowledge a noteworthy limitation of this study. The current scenario utilized in the analysis may not entirely encapsulate the dynamic and evolving conditions

that will characterize the future. As such, the need for the development of a novel and more representative scenario becomes evident. In this context, the establishment of a new scenario holds the potential to enhance the accuracy and applicability of the study's findings. Such a scenario should account for evolving agricultural practices, technological advancements, and potential shifts in emission sources over time. By incorporating a more realistic projection of future conditions, the study's outcomes could yield insights that are better aligned with the actual trajectory of ammonia emissions and their consequent impact on air quality and human health.

Addressing this limitation would undoubtedly strengthen the study's overall credibility and ensure that its conclusions remain robust in the face of changing environmental and societal dynamics. Thus, the pursuit of an updated and more comprehensive scenario is an essential step toward refining our understanding of the intricate relationships between ammonia emissions, PM_{2.5} concentrations, and their implications for the well-being of both ecosystems and populations.

4.6 Summary and conclusions

In this comprehensive study, the effects of reducing agricultural ammonia emissions on both air quality and human health were thoroughly investigated using a combination of the GEOS-chem chemical transport model and the GEMM function. The pivotal role of ammonia as a primary component of secondary particle matter (SNA), including sulfate, nitrate, and ammonium, emerged clearly. The study's focal point was the influence of such emissions on PM_{2.5} concentrations, a critical indicator of air quality.

Upon comparing the outcomes of emission inventory adjustments, a significant decline in PM_{2.5} concentrations was observed in regions with high agricultural emission rates, particularly in Asia, Europe, and North America. On the other hand, NH₃ emission reduction could escalate the O₃ concentration especially in the north hemisphere resulting from the oxidative of NH₃ phenomena. Interestingly, the study revealed an intricate relationship between NO_x emissions and PM_{2.5} levels, emphasizing that controlling NO_x might inadvertently lead to increased PM_{2.5} concentrations. This finding aligned with the findings of Thunis et al.'s 2021 study, which highlighted the role of atmospheric oxidative capacity in this phenomenon.

An intriguing aspect of the study was the consistent evidence supporting the greater potential of reducing ammonia emissions from agricultural activities, compared to tackling NO_x emissions from other sectors. This approach holds promise for effectively addressing PM_{2.5} concentrations and, consequently, averting premature mortality, a critical concern in highly polluted regions like China and India.

In conclusion, this study provides a comprehensive understanding of the complex interplay between agricultural ammonia emissions, PM_{2.5} and O₃ concentrations, and their implications for air quality and human health. The integration of the GEOS-chem model and GEMM function yielded insights that underscore the need for targeted interventions to mitigate ammonia emissions, thereby contributing to improved air quality and public health. The findings further highlight the importance of a nuanced strategy that accounts for the intricate interactions between various emission sources and their subsequent effects on air quality.

4.7 Reference

- Bey, I., Jacob, D. J., Yantosca, R. M., Logan, J. A., Field, B. D., Fiore, A. M., Li, Q., Liu, H. Y., Mickley, L. J., & Schultz, M. G. (2001). Global modeling of tropospheric chemistry with assimilated meteorology: Model description and evaluation. *Journal of Geophysical Research: Atmospheres*, *106*(D19), 23073–23095.
- Burnett, R., Chen, H., Szyszkwicz, M., Fann, N., Hubbell, B., Pope III, C. A., Apte, J. S., Brauer, M., Cohen, A., & Weichenthal, S. (2018). Global estimates of mortality associated with long-term exposure to outdoor fine particulate matter. *Proceedings of the National Academy of Sciences*, *115*(38), 9592–9597.
- EEA. (2018). *Annual European Union greenhouse gas inventory 1990–2016 and inventory report 2018*. Publications Office of the European Union.
- Fujimori, S., Hasegawa, T., Ito, A., Takahashi, K., & Masui, T. (2018). Gridded emissions and land-use data for 2005–2100 under diverse socioeconomic and climate mitigation scenarios. *Scientific Data*, *5*(1), 1–13.
- Gelencsér, A., May, B., Simpson, D., Sánchez-Ochoa, A., Kasper-Giebl, A., Puxbaum, H., Caseiro, A., Pio, C., & Legrand, M. (2007). Source apportionment of PM_{2.5} organic aerosol over Europe: Primary/secondary, natural/anthropogenic, and fossil/biogenic origin. *Journal of Geophysical Research: Atmospheres*, *112*(D23).
- Heald, C. L., Collett Jr, J., Lee, T., Benedict, K., Schwandner, F., Li, Y., Clarisse, L., Hurtmans, D., Van Damme, M., & Clerbaux, C. (2012). Atmospheric ammonia and particulate inorganic nitrogen over the United States. *Atmospheric Chemistry and Physics*, *12*(21), 10295–10312.
- Jian, J., Hashemi, H., Wu, H., & Glarborg, P. (2023). Study of ammonia oxidation with ozone addition. *Applications in Energy and Combustion Science*, *14*, 100137.
- Kampa, M., & Castanas, E. (2008). Human health effects of air pollution. *Environmental Pollution*, *151*(2), 362–367.
- Koziel, J. A., Aneja, V. P., & Baek, B.-H. (2006). *Gas-to-particle conversion process between ammonia, acid gases, and fine particles in the atmosphere*.
- Li, Y., Lau, A. K., Fung, J. C., Zheng, J., & Liu, S. (2013). Importance of NO_x control for peak ozone reduction in the Pearl River Delta region. *Journal of Geophysical Research: Atmospheres*, *118*(16), 9428–9443.

- Long, S., Zeng, J., Li, Y., Bao, L., Cao, L., Liu, K., Xu, L., Lin, J., Liu, W., & Wang, G. (2014). Characteristics of secondary inorganic aerosol and sulfate species in size-fractionated aerosol particles in Shanghai. *Journal of Environmental Sciences*, *26*(5), 1040–1051.
- Mabahwi, N. A. B., Leh, O. L. H., & Omar, D. (2014). Human health and wellbeing: Human health effect of air pollution. *Procedia-Social and Behavioral Sciences*, *153*, 221–229.
- Manisalidis, I., Stavropoulou, E., Stavropoulos, A., & Bezirtzoglou, E. (2020). Environmental and health impacts of air pollution: A review. *Frontiers in Public Health*, *8*, 14.
- Pozzer, A., Tsimpidi, A. P., Karydis, V. A., De Meij, A., & Lelieveld, J. (2017). Impact of agricultural emission reductions on fine-particulate matter and public health. *Atmospheric Chemistry and Physics*, *17*(20), 12813–12826.
- Querol, X., Alastuey, A., Rodriguez, S., Plana, F., Mantilla, E., & Ruiz, C. R. (2001). Monitoring of PM₁₀ and PM_{2.5} around primary particulate anthropogenic emission sources. *Atmospheric Environment*, *35*(5), 845–858.
- Tahri, M., Benchrif, A., & Zahry, F. (2022). Review of Particulate Matter Levels and Sources in North Africa over the Period 1990–2019. *Environmental Sciences Proceedings*, *19*(1), 3.
- Thunis, P., Clappier, A., Beekmann, M., Putaud, J. P., Cuvelier, C., Madrazo, J., & de Meij, A. (2021). Non-linear response of PM_{2.5} to changes in NO_x and NH₃ emissions in the Po basin (Italy): Consequences for air quality plans. *Atmospheric Chemistry and Physics*, *21*(12), 9309–9327.
- Von Schneidmesser, E., Monks, P. S., Allan, J. D., Bruhwiler, L., Forster, P., Fowler, D., Lauer, A., Morgan, W. T., Paasonen, P., & Righi, M. (2015). Chemistry and the linkages between air quality and climate change. *Chemical Reviews*, *115*(10), 3856–3897.
- Wang, X., Jacob, D. J., Fu, X., Wang, T., Breton, M. L., Hallquist, M., Liu, Z., McDuffie, E. E., & Liao, H. (2020). Effects of anthropogenic chlorine on PM_{2.5} and ozone air quality in China. *Environmental Science & Technology*, *54*(16), 9908–9916.
- Wang, Y., Wen, Y., Zhang, S., Zheng, G., Zheng, H., Chang, X., Huang, C., Wang, S., Wu, Y., & Hao, J. (2023). Vehicular ammonia emissions significantly contribute to urban PM_{2.5} pollution in two Chinese megacities. *Environmental Science & Technology*, *57*(7), 2698–2705.
- Zhang, T., Shen, Z., Su, H., Liu, S., Zhou, J., Zhao, Z., Wang, Q., Prévôt, A., & Cao, J. (2021). Effects of Aerosol Water Content on the formation of secondary inorganic aerosol during a Winter Heavy PM_{2.5} Pollution Episode in Xi'an, China. *Atmospheric Environment*, *252*, 118304.

Chapter 5

Co-benefits of air quality for human health from climate change mitigation through dietary change and food loss prevention policy

5.1 Abstract

Food production, particularly cattle husbandry, significantly contributes to air pollution and poses associated health hazards. However, making changes to dietary habits, such as reducing red meat intake and minimizing food waste, can lead to noteworthy improvements in both air quality and human health. Therefore, the primary objective of this study is to explore the impact of dietary changes on future air quality and human well-being. Additionally, the research aims to assess the influence of dietary transformation policies in the context of climate change mitigation, aiming to understand how policies can effectively complement each other. The Chemical Transport Model (CTM) and Integrated Assessment Model (IAM) were used to determine PM_{2.5} and ozone concentrations, while the exposure model would be applied to estimate the premature deaths. Our research findings reveal that dietary changes can play a crucial role in mitigating air pollution, particularly in regions where agricultural activities are significant sources of ammonia emissions. For instance, in the EU, it could lead to a notable reduction of approximately 5.34% in PM_{2.5} by the year 2050. Similarly, in Asia, a substantial reduction of 6.23% in PM_{2.5} is projected by 2100. Ground-surface ozone levels in Southeast Asia remarked reduction of up to 12.93% by 2100. A combined approach integrating dietary changes with climate change mitigation measures could offer more comprehensive air quality improvements in specific regions. However, it is essential to exercise caution and carefully consider potential adverse effects on ozone concentrations in certain areas. Furthermore, our results revealed that the dietary change led to a significant reduction in global mortality associated with PM_{2.5} and O₃, with reductions approximately 187.5, and 131.11 thousand avoided deaths per year expected by 2100, respectively. This reduction in premature mortality translates into a substantial decrease in the economic cost of mortality, estimated at approximately 391.37 billion USD/year (2010, PPP adjusted).

Keywords: Dietary changing, Human health, Climate change, Air pollution, GEOS-Chem, PM_{2.5}, Ozone

5.2 Introduction

Food production significantly impacts the environment, serving as a major driver of greenhouse gas (GHG) emissions and air pollution. The food sector alone contributes to 10–12% of total global emissions (Bauer et al., 2016; Smith et al., 2014; Tai et al., 2014). Recent studies highlight ammonia emissions, especially from the agricultural sector, notably livestock production, as a significant contributor to PM_{2.5} in ambient air (Bist et al., 2023; Choi & Sunwoo, 2022; Z. Liu et al., 2021; Mazzeo et al., 2022; Ti et al., 2022; Wang et al., 2023). However, policies targeting NH₃ emissions from agricultural sources are yet to be implemented in numerous countries, particularly in developing nations where agricultural activities play a pivotal role in the economy (Ma et al., 2021). Urgent action and global cooperation are imperative to develop comprehensive strategies addressing these emissions and mitigating their environmental impact.

The global population is projected to reach 9.7 billion by 2050. A 70% increase in global food production is forecasted to meet the demands of this growing population (High-Level Expert Forum, 2009). However, the anticipated rise in food production may exacerbate air pollution, placing additional strain on the environment and human health. Therefore, proactive and comprehensive measures are essential to ensure sustainable and environmentally responsible approaches to meet the increasing food demands while minimizing adverse impacts on air quality and overall environmental health. The health consequences of unfavorable air quality are deeply intertwined with agricultural activities. A study conducted by Domingo et al. (2021) investigated the impact of air pollution on agricultural production in the USA. Their research revealed that a significant portion of the 15,900 annual deaths caused by fine particulate matter (PM_{2.5}) pollution related to food is attributed to animal-based foods, accounting for 80% of these fatalities.

Climate change and air pollution are closely related because both are caused by the release of GHGs and other pollutants into the atmosphere. Thus, climate change mitigation efforts may contribute to reducing air pollution, and clean air policies may have a mitigation effect on climate change (Jiang et al., 2013; Nemet et al., 2010; Thurston & Bell, 2021; Vandyck et al., 2018; West et al., 2013). Dietary transformation has the potential to moderate GHG and pollutant emissions from the agricultural food chain (Pörtner et al., 2022). In 2019, the EAT-Lancet Commission

published a summary report that provided guidelines for transforming the food system toward greater sustainability and healthiness. One of its recommendations was to reduce the consumption of red meat by 50% by 2050 and to explore new protein sources including plants (Willett et al., 2019). This adjustment in eating habits has the potential to lessen the severity of future climate change and pollution. Moreover, EAT-Lancet also aspires to cut food losses and waste in half by 2030, in line with Sustainable Development Goal (SDG) 12.3 (United Nations, 2023). Although a number of investigations have attempted to establish a connection between dietary changes and GHG emissions, relatively few studies have investigated air pollution.

The connection between dietary changes and GHG emissions has been extensively researched. Currently studies have investigated the consequences of dietary choices and food production methods for GHG emissions. However, considerably fewer studies have examined the impact of dietary changes on air quality on a global scale. For example, in the EU, a 33% reduction in ammonia emissions was observed after the implementation of a flexitarian diet, leading to a decrease in the levels of PM_{2.5} and the number of mortalities (Himics et al., 2022). Furthermore, the integration of policies that effectively address both GHG emissions and air quality, together with the health consequences of dietary choices, remains underexplored. While the Intergovernmental Panel on Climate Change (IPCC) report has delved into the role of food production in escalating greenhouse gas (GHG) emissions and proposed mitigation policies for agricultural GHGs, a clear dietary framework for these policies remains ambiguous. For instance, the report recommends a shift towards more sustainable food choices, advocating a reduction in red meat consumption (Mbow et al., 2020). However, it does not specify the proportion of food that should be altered.

The primary objective of this study was to resolve deficits in our understanding of the connection between dietary changes and changes in air quality. Therefore, we have implemented a comprehensive and detailed framework for sustainable diets, taking from the EAT-Lancet Commission. Furthermore, we investigated the role of dietary change policies within the context of climate change mitigation scenarios to better understand their potential impact and contribute valuable insights to sustainable practices. By exploring the consequences of dietary choice and food production methods for GHG emissions and air pollution, we sought to shed light on the

environmental consequences of our food consumption patterns, as well as their potential impacts on public health and wellbeing.

We also explored the potential health benefits associated with air quality improvements that could result from GHG mitigation policies proposed by the IPCC and dietary changes proposed by the EAT-Lancet Commission. Overall, we hope to improve our understanding of the complex interactions among dietary choice, climate change mitigation measures, air quality improvements, and public health. Our findings on the potential health benefits of adopting sustainable diets will support the development of integrated policies to simultaneously address environmental improvements and health concerns, thereby contributing to a more resilient and sustainable future.

5.3 Methodology

5.3.1 Overview

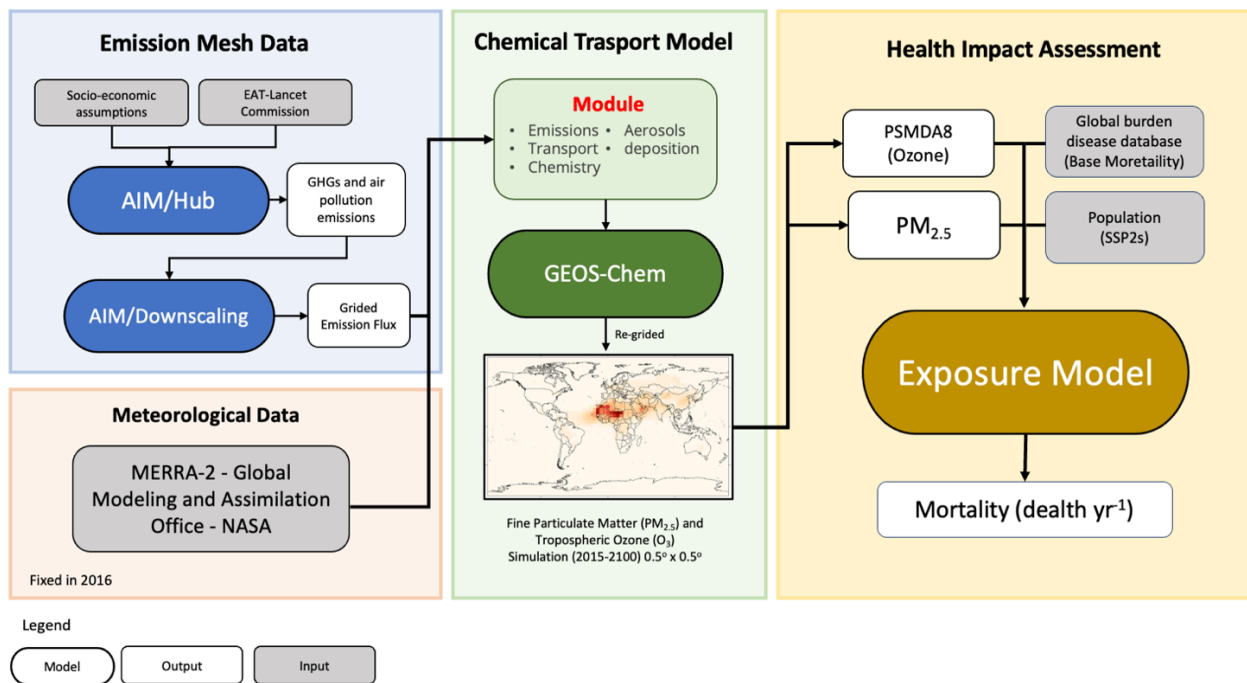


Figure 5-1 Research framework visualization

The Goddard Earth Observing System – Chemistry (GEOS-Chem) model was employed to estimate the surface-level concentrations of ambient PM_{2.5} and O₃ by utilizing a comprehensive

inventory of anthropogenic emissions and meteorological data as simulated inputs. To evaluate the prospective trajectory of air quality based on the simulation, we integrated future emissions scenarios derived from the Asia-Pacific Integrated Model (AIM/Hub). Subsequently, the health exposure model was employed to estimate premature mortality attributed to exposure to PM_{2.5} and O₃ as illustrated in Figure 5-1.

5.3.2 Scenario and experiment design

To examine the influence of dietary changes and climate change mitigation policies, we considered four scenarios for the study areas (Table 5-1). These included a baseline scenario with high GHG emissions (SC1), a dietary change and food loss prevention scenario (SC2), a climate change mitigation scenario (SC3), and a scenario based on the integration of climate change mitigation measures with dietary change and food loss prevention (SC4). By inputting these scenarios into the AIM/Hub Model, the potential air quality consequences based on specific assumptions about emissions, which may be influenced in part by dietary choices.

Baseline socioeconomic assumptions for all scenarios were derived from the Shared Socioeconomic Pathways 2 (SSPs) scenario, also known as the “middle of the road” scenario (Riahi et al., 2017). In the SC2 scenario, we assumed that people would switch to a healthier diet by consuming more plant-based protein from beans, lentils, and pulses from a diet including red meat and dairy products. The EAT-Lancet Commission recommends reducing red meat and sugar consumption by 50% by 2050. Additionally, the total daily food demand should not exceed 2,503 kcal per capita (Willett et al., 2019). We also considered food loss reduction under SDG 12.3, which aims to cut global per capita food waste by 50% by 2030 (Ardra & Barua, 2022). These targets, stretching to 2100, emphasize sustained efforts for dietary change and food waste reduction, forming a critical part of our long-term sustainability strategy.

To assess climate change mitigation scenarios, we aligned our analysis with the objective of maintaining cumulative CO₂ emissions below 500 Gt-CO₂ after 2020, which is consistent with a 50% chance of restraining warming to 1.5°C under SSP2 (Fujimori et al., 2016). In our SC4 scenario, we examined the potential influence of future dietary patterns under climate change

mitigation policy condition, which allowed us to explore the interconnected dynamics of climate change mitigation policies, dietary choices, and food loss reduction strategies on future air quality.

Table 5-1 Summarizes the scenario set

Identifier	Descriptor	Reference pathway
SC1	Baseline	National GDP and Population Projection
SC2	Dietary change and food losses prevention	- Red meat and sugar consumption would be cut by 50% by 2050 - by halving global per capita food waste in 2030 (EAT-Lancet)
SC3	Climate Change Mitigation	to keep cumulative CO ₂ emissions below 500 Gt after 2020 for a 50% chance of staying within 1.5°C warming (IPCC)
SC4	Integrated Policy (SC2+SC3)	Combination of strategies including climate change mitigation scenario and healthy dietary change.

5.3.3 Integrated Assessment Model (AIM/Hub)

In this study, we used AIM/Hub model framework coupled with other modelling tools for scenario quantification presented by Fujimori et al. (2018) which enabled the assessment of critical elements such as the energy system, land use, agriculture, greenhouse gas (GHG) and air pollutant emissions. In projecting future assumptions regarding population and income trends, we have employed the Shared Socioeconomic Pathways (SSPs), originally designed for primary application in climate change research, as outlined by O'Neill et al. (2017). In this study, we focused on the “middle of the road” SSP2 scenario. Details of the model structure and mathematical formulae are described by Fujimori et al. (2012). The assumption is that production sectors seek to maximize profits using multi-nested constant elasticity substitution functions, taking into account the price of each input. Emissions resulting from changes in land use are calculated by multiplying the alteration in forest area compared to the previous year by the carbon stock density. This density is specific to global agroecological zones, providing a differentiated

measure based on geographical and ecological considerations. Emissions not related to energy, excluding those associated with changes in land use, are presumed to be directly proportional to the magnitude of each respective activity, such as output (Fujimori et al., 2022).

The simulation in AIM was initiated from the year 2005 and extended until 2100, encompassing historical, present, and future periods. The choice of this timeframe is crucial for calibration purposes across various sectors. Specifically, the period from 2005 to 2015 serves as a calibration phase for all sectors, leveraging data from the Global Trade Analysis Project (GTAP) database (Dimaranan et al., 2006). In the energy sector calibration, the simulation utilizes data from the period 2007 to 2015, drawing from the International Energy Agency (IEA) [IEA, 2019]. This focused calibration ensures that the AIM/Hub model aligns with the empirical data available during these specific time intervals, enhancing the accuracy and reliability of the simulation across sectors and time periods.

Utilizing the AIM/Hub model, we derived GHG and air pollutants emissions across various scenarios. This encompassed an array of pollutants, including carbon dioxide (CO₂), methane (CH₄), nitrous oxide (N₂O), fluorine (F), black carbon (BC), carbon monoxide (CO), ammonia (NH₃), non-methane volatile organic compounds (NMVOC), nitrogen oxides (NO_x), organic carbon (OC), and sulfur oxides (SO_x). These emissions play a pivotal role in atmospheric processes, contributing to the formation of PM_{2.5} and O₃. These derived emissions are linked to factors such as food demand, supply, and trade dynamics based on population growth, GDP evolution, food prices, consumer preferences, and technological developments.

To generate gridded emissions at a 0.5° × 0.5° resolution, we applied the AIM downscaling tool (AIM/DS) to the regionally aggregated 17-region emission inventory. The method for downscaling would depend on sector and sources of emission which would be segregated into three groups as shown in Table 2-3. Different downscaling mechanisms were applied to each sector. Gross Domestic Product (GDP) and Population emerge as the principal catalysts behind emissions within the ambit of group 1 focusing on emissions from energy, industry, inland transport, building, solvent, and waste sectors. Within this framework, it is conjectured that the energy facet intertwined with emission dynamics could plausibly demonstrate an interconnection with either

GDP or Population. The second group was established in proportion to the base year (2015) including emission from agriculture, forestry, and land use. The third group was downscaled in proportion to the total global emissions from the base year's geographic distribution and was applied to aviation emissions. These approaches are described in greater methodological detail in Fujimori et al. (2017; 2018).

In this study, the influence of climate change on the climate system, particularly temperature changes, was not factored into the analysis. Consequently, meteorological conditions were assumed to be consistent across all scenarios and years based on 2016. Subsequently, the emission data was inputted into the GEOS-Chem model for further analysis. The years 2015, 2030, 2050, and 2100 were specifically selected for chemical transport model (CTM) simulations to evaluate the immediate, medium-term, and long-term implications of dietary change on air quality.

5.3.4 GEOS-Chem simulation

We used a chemical transport model to estimate the gridded concentrations of PM_{2.5} and O₃. The GEOS-Chem global three-dimensional model of atmospheric transport v13-04 (Bey et al., 2001; <http://www.geos-chem.org>) was used to simulate surface concentrations. To drive the GEOS-Chem model, we employed the NASA Global Modeling Assimilation Office MERRA2 reanalysis meteorological data product, which aggregates data at a coarse resolution. The list of meteorological parameters used in our analysis can be accessed at https://wiki.seas.harvard.edu/geos-chem/index.php/List_of_MERRA-2_met_fields.

The simulated surface concentrations of PM_{2.5} and O₃ were generated at a horizontal resolution of 4.0° × 5.0° with 72 vertical layers. The chemical mechanism used in the GEOS-Chem model included a detailed O_x–NO_x–hydrocarbon–aerosol–bromine mechanism (Mao et al., 2013; Parrella et al., 2012). The PM_{2.5} components were natural mineral dust, sea salt, primary black carbon aerosols, primary organic aerosols, secondary inorganic aerosols (sulfate, nitrate, and ammonium), and secondary organic aerosols. To simulate the thermodynamics of secondary inorganic aerosols, we used ISORROPIA II (Fountoukis & Nenes, 2007; Pye et al., 2010).

Data on GHG emissions and air pollution from the AIM/Hub model were fed into the GEOS-Chem model. To simulate natural emissions, we used the GEOS-Chem archived inventories from the Harmonized Emissions Component (HEMCO), which included NO_x emissions from lightning, dust, and sea salt emissions, biogenic emissions, and emissions from volcanic eruptions (Fritz et al., 2022; Lin et al., 2020).

In this study, we did not account for the influence of climate change on the climate system itself, particularly temperature changes. Consequently, meteorological conditions were assumed to be consistent across all scenarios and years, based on a 2016 baseline. Subsequently, emissions data were fed into the GEOS-Chem model for further analysis. The years 2015, 2030, 2050, and 2100 were selected for chemical transport model simulations to evaluate immediate, medium-term, and long-term implications of dietary change on air quality.

The quantification of the dietary change effect was done by percentage relative change (RC) for each PM_{2.5} and O₃ between reference and target scenario using the following equation:

$$RC_j(\%) = \frac{X_j - X_i}{X_i} \times 100 \quad (5 - 1)$$

where RC_j is percentage relative change of target scenario comparing with reference scenario (%); X_i is reference scenario in this study we have two reference scenarios including SC1: baseline scenario and SC3: climate change mitigation scenario; X_j is target scenario (SC2 and SC4)

5.3.5 Premature mortality attributable to long-term exposure to ambient PM_{2.5} and O₃

To estimate the premature mortality attributed to PM_{2.5} and O₃ exposure, Equation (3-3) developed by Apte et al. (2015) was applied. In this study, the Integrated Exposure–Response (IER) function, shown in equation (2-4), developed by Burnett et al. (2014) was used to estimate the burden of disease related to ambient PM_{2.5}. To estimate premature mortality attributable long term ozone exposure, the Peak Seasonal (six-month) Maximum of Daily 8-hour Average (PSMDA8) ozone concentrations of ozone in ambient air were used to calculate the RR in Equation (2-6).

5.3.6 Economic value of mortality reduction

In economic evaluations of policies and projects that aim to reduce mortality and morbidity risks, it is essential to estimate the social benefits. To estimate these benefits, we utilized the Value of a Statistical Life (VSL) in this study. VSL (Eq. 5-2) represents the monetary value that individuals place on reducing their risk of premature death and is derived from individuals' willingness-to-pay assessments of how much they are willing to pay to avoid a certain level of risk over a specified time frame (National Research Council, 2008; Roman et al., 2012).

$$VSL_{c,y} = WTP_{OECD} \times \left(\frac{GDP_{c,y}}{GDP_{OECD,y}} \right)^e \quad (5 - 2)$$

where WTP: Willingness To Pay (US\$3.54 million), $GDP_{c,y}$ is a gross domestic product in country c for year y, e is income elasticity, OECD is the Organisation for Economic Co-operation and Development

Another related measure is the Value of a Statistical Life Year (VSLY), which takes into account not only the probability of death but also the number of years of life that are saved. The VSLY is calculated by dividing the VSL by the expected life remaining (Robinson, 2018). Finally, we calculated the economic cost of health effects using the following equation:

$$VSLY_EC_{c,y} = \Delta Mortality_{c,y} \times \sum_{t=0}^{LE_{c,y,l}-1} \frac{VSLY_{c,y,l+t}}{(1+r)^t} \quad (5 - 3)$$

where $EC_{c,y}$ is economic costs in country c for year y, $\Delta Mortality_{c,y}$ is the premature death caused by long-term $PM_{2.5}$ and O_3 exposure in country c for year y, $LE_{c,y,l}$ is the remaining life expectancy in country c for year y for age l, r: discount rate; we set the discount rate at 6 percent for low- and middle-income countries, and 4 percent for high-income countries.

5.4 Results

5.4.1 Implication of dietary change policy on future food demand and supply

To assess the influence of dietary changes and food loss prevention policies, we refer to the EAT-Lancet suggestion for food demand as an input parameter in the AIM/Hub model. The EAT-Lancet Commission aims to shift current dietary patterns towards healthier and environmentally friendly options by reducing red meat consumption by 50% by 2050, alongside implementing food loss prevention measures. According to their recommendations, by 2050, adults should consume a healthy diet amounting to 2,503 kcal per capita per day, primarily sourced from whole grains, plant-based protein sources, fruits, and vegetables, while limiting the intake of red meat. More details about the EAT-Lancet are provided by Hirvonen et al. (2020).

By incorporating these recommendations into the AIM/Hub model, we could analyze the potential impacts of such dietary changes and policies on various aspects such as food availability, agricultural production, greenhouse gas emissions, and economic outcomes. Figure 5-2 illustrated the food demand (kilocalories/capita/day) compared to four scenarios. In the baseline scenario without the EAT-Lancet guidelines, the food demand per capita per day is projected to reach nearly 3,300 kcal/cap/day. However, when considering both the baseline and mitigation scenarios with the implementation of the EAT-Lancet recommendations, the total food demand per capita per day experiences a significant decline from 2015 to 2050. This decline is primarily attributed to the adoption of the EAT-Lancet policy, which aims to shift eating behaviors by reducing red meat and sugar consumption by more than 50%.

According to the recommendations put forth by the EAT-Lancet Commission, transforming the current food system to promote healthier and more environmentally friendly practices can have significant implications for agricultural production. Figure 5-3, In the dietary change scenario (SC2), where there is a reduction in red meat consumption and efforts to minimize food waste, the total agricultural production is projected to decrease by approximately 22.92%, 24.04%, and 25.56% for the years 2030, 2050, and 2100, respectively. These reductions are reflective of the shift in consumer preferences and the corresponding changes in farming practices required to meet the new dietary patterns

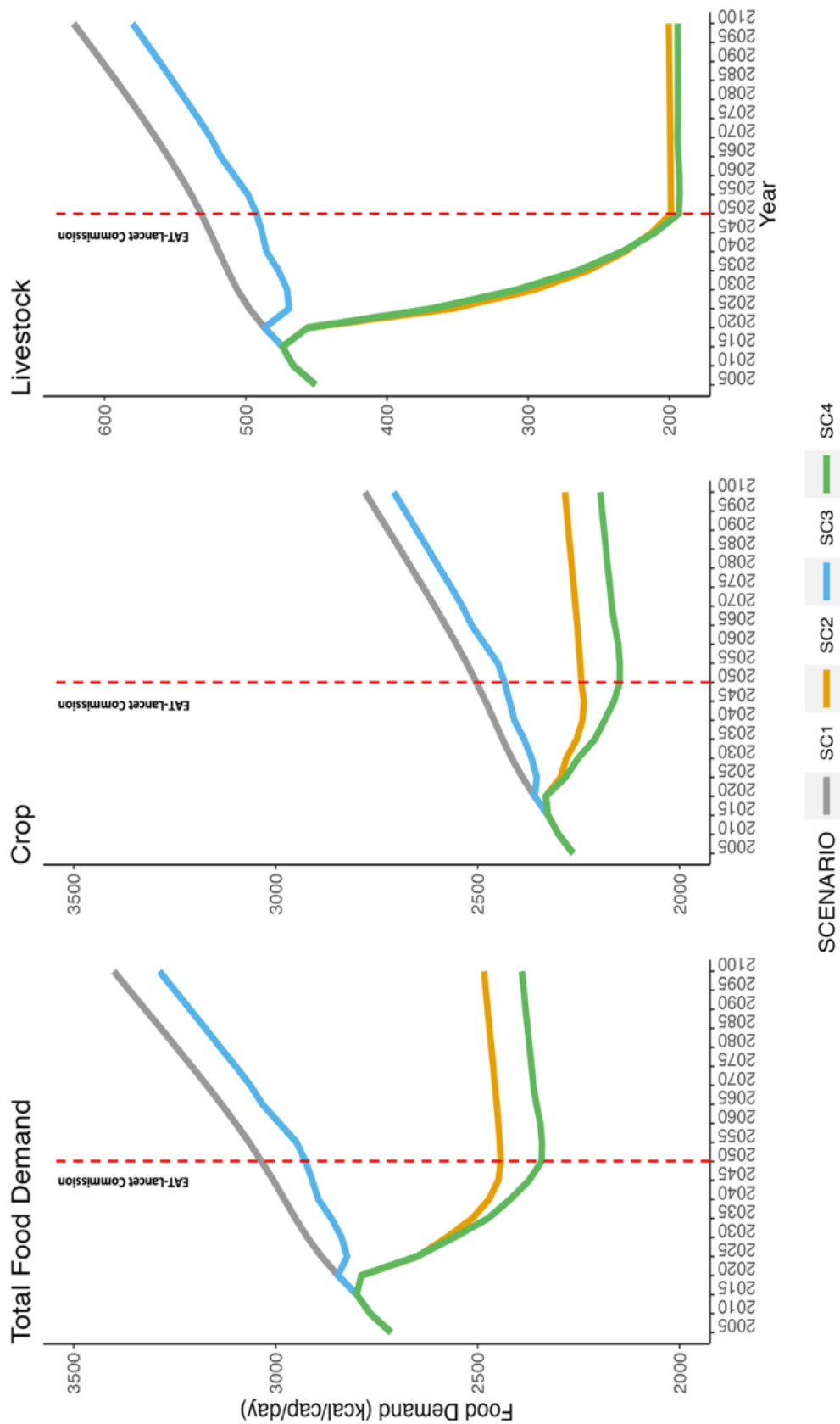


Figure 5-2 Total (left), crop (middle), and livestock (right) food demand (kcal/capita/day) for baseline scenario (gray), dietary change and food losses prevention (yellow), climate change mitigation (blue), and integrate policy (green) projection for 2005-2100

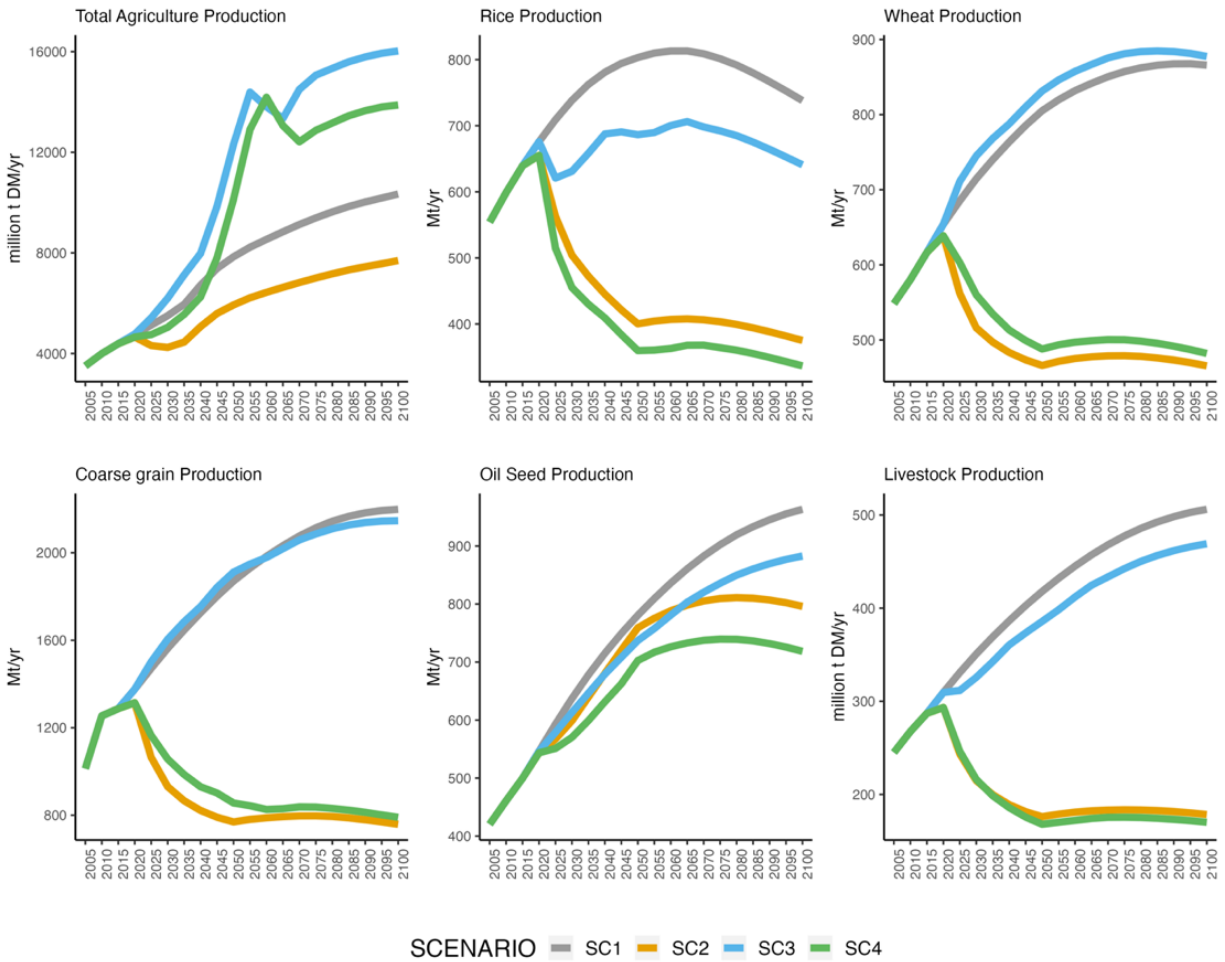


Figure 5-3 Crop production for baseline scenario (gray), dietary change and food losses prevention (yellow), climate change mitigation (blue), and integrate policy (green) projection for 2005-2100

Conversely, the climate change mitigation policy can lead to an increase in the demand for energy crops in the future. This increased demand may have the opposite effect on agricultural production, resulting in rising total agricultural production levels for the climate change mitigation scenario (SC3) and the integrated policy scenario (SC4).

When the dietary change scenario is combined with the climate change mitigation scenario (SC4), the results indicate that the impact on agricultural production aligns with that of the dietary change scenario alone. This suggests that the dietary change component has a dominant influence on agricultural production in this integrated scenario. As a result, both crop and livestock production

may be reduced, reflecting the changes in dietary preferences and the corresponding adjustments in farming practices required to support the dietary change goals.

5.4.2 Impact of dietary changes on future global GHGs and air pollutant precursor gases

Dietary changes can exert a profound influence on food demand, thereby potentially affecting future GHG emissions and air pollution. The EAT-Lancet report indicates that the implementation of these dietary changes may lead to a notable reduction of approximately 300 kcal/capita/day in livestock demand, accompanied by a decline in food crop demand. These alterations in consumption patterns hold substantial promise in significant reductions in GHGs and air pollutant precursor gases such as PM_{2.5} and O₃. These reductions have the potential to mitigate the adverse effects of air pollution on public health, including a decrease in premature mortality in both direct and indirect effect rates as shown in Figure 5-4.

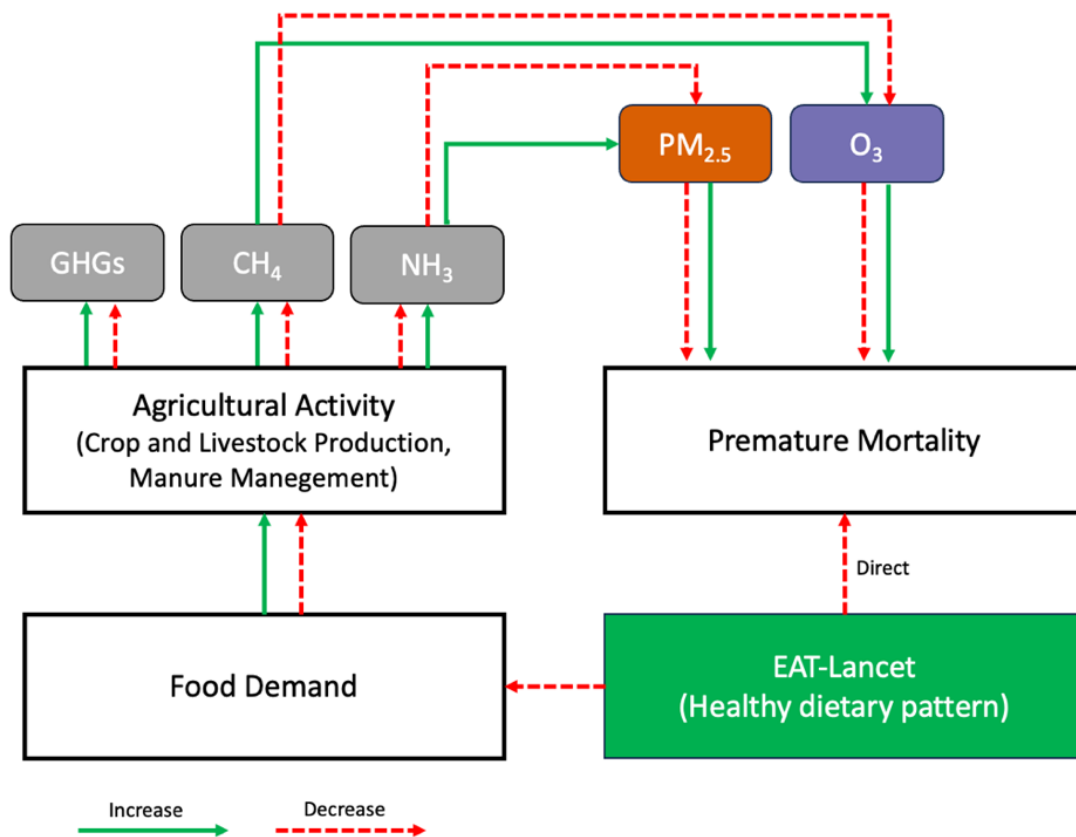


Figure 5-4 Mechanisms of dietary changes on GHG emissions, air pollutant precursors, and human health

According to the baseline scenario, greenhouse gas (GHG) emissions are projected to increase steadily, reaching nearly 90 Gt CO₂-equivalent by 2100. However, the implementation of Sustainable Development Goal 12.3 in 2030, which focuses on reducing food loss and waste, has led to a noticeable reduction in GHG emissions. It is important to note that despite this intervention, emissions continue to rise. By 2050, the adoption of dietary changes can potentially result in a reduction of approximately 5.89 Gt CO₂-equivalent in GHG emissions, which accounts for around 8% of the emissions compared to the baseline scenario. The transformation in dietary patterns (SC2) primarily affects the emissions of nitrous oxide (N₂O) and methane (CH₄), which are two significant GHGs from livestock sector. However, the impact on other GHG species is relatively small in comparison, although still important to consider. While total GHG emissions will continue to be dramatically reduced and reach zero by 2100 with the implementation of climate change mitigation measures (SC3), it is worth noting that the integration of dietary changes with these policies does not significantly reduce GHG emissions, except for CH₄ and N₂O as shown in Figure 5-5.

The implementation of the food transformation strategy, as evidenced by simulation models, has yielded substantial reductions in ammonia emissions. By the year 2050, the strategy has demonstrated an impressive decrease of approximately 17% (-13.03 Mt/yr) in ammonia emissions. Importantly, this downward trend is projected to persist, with continuous declines anticipated to reach -33% (-29.04 Mt/yr) by the year 2100, when compared to the baseline scenario. In addition to ammonia emissions, the food transformation strategy has also shown promising results in reducing CH₄ emissions. In particular, an approximately 23 percent (-138 Mt/yr) reduction in total emissions by 2050 has been found. This loss is primarily attributable to the cattle producing industry. As depicted in Figure 5-3, dietary modifications could result in a significant reduction in animal productivity over the time. In the climate change mitigation scenario, ammonia emissions are projected to decrease from 2015 to 2050 compared to the baseline scenario. The reduction in ammonia emissions amounts to approximately 23.33 Mt/yr, representing a 17% decrease. It is important to note that a significant portion of these emissions originates from crop production activities.

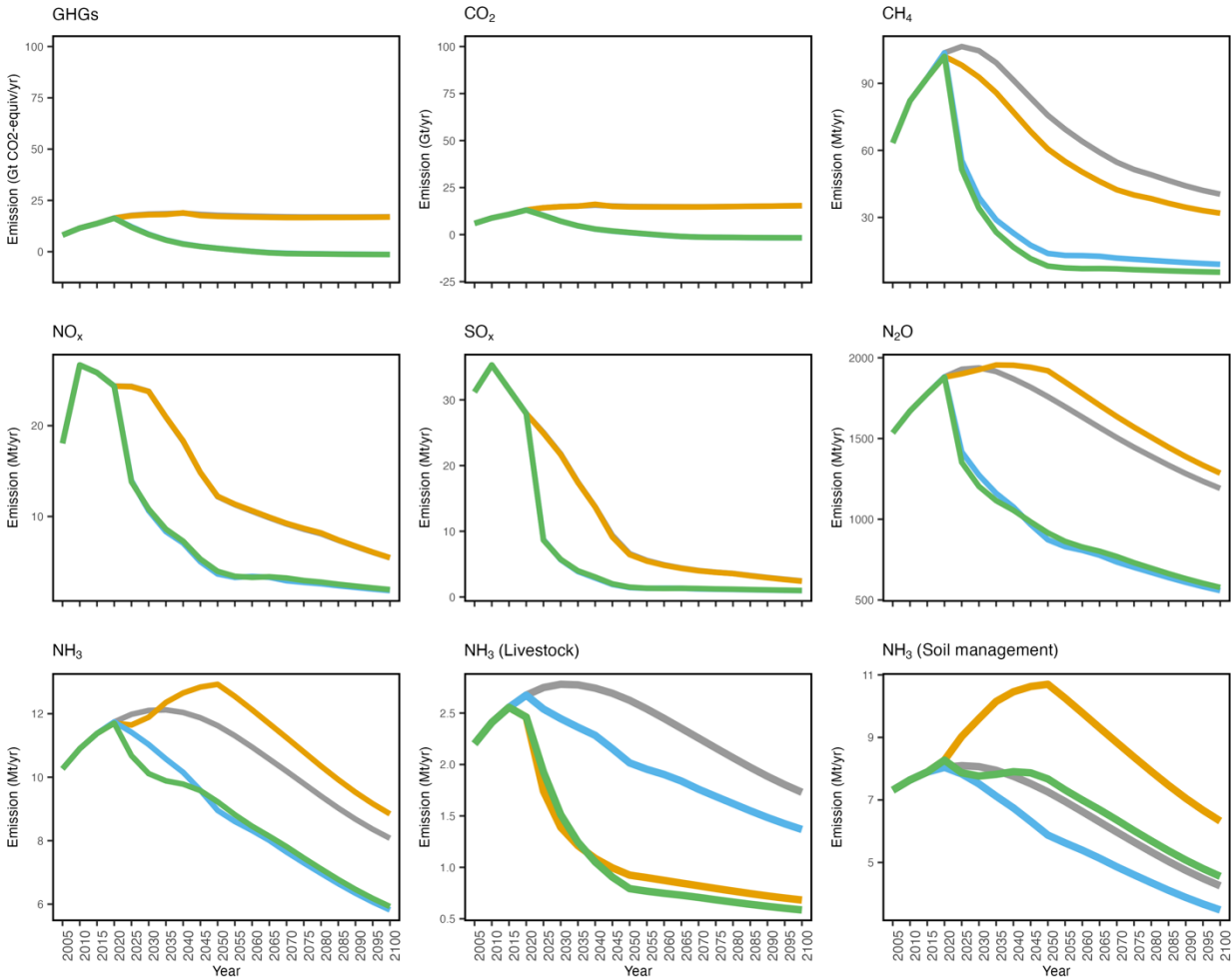


Figure 5-5 Comparison of global GHGs and air pollutants emission for baseline scenario (gray), dietary change and food losses prevention (yellow), climate change mitigation (blue), and integrate policy (green) projection for 2005-2100

However, when considering an integrated policy approach that combines climate change mitigation measures with dietary changes, the reduction in ammonia emissions is expected to be even greater. The integrated policy could potentially achieve a reduction of approximately 29.23 Mt/yr, with an additional decrease of 11.4 Mt/yr compared to the climate change mitigation scenario alone. This represents a 19% reduction in ammonia emissions especially from livestock activity as shown in Figure 5-5. On the other hand, the NH₃ emission in soil management sector increased in 2050 due to the food system transformation from livestock to plant-based protein.

5.4.3 Effect of dietary change on future air quality

The impact of dietary changes on PM_{2.5} (upper) and O₃ (lower), as compared to the Baseline (SC1) scenario, is illustrated in Figure 5-6. Scenario SC2 demonstrated significant potential for mitigating PM_{2.5} pollution, particularly in regions where agricultural activities are a significant source of NH₃, including the EU, Brazil, and Southeast Asia. Reductions in PM_{2.5} induced by dietary changes were particularly prominent in Europe. Compared to their baseline concentrations, average PM_{2.5} concentrations in the EU were forecast to decline by 1.79% (maximum: 3%, minimum: -8%) by 2030, 5.34% (maximum: 0.98%, minimum: -10.38%) by 2050, and 9.88% (maximum: -0.39%, minimum: -17%) by 2100. In Asia, the projected reductions in PM_{2.5} were 1.08% (maximum: 2.49%, minimum: -4.61%) by 2030, 2.36% (maximum: 1.73%, minimum: -7.77%) by 2050, and 6.23% (maximum: 0.08%, minimum: -16.72%) by 2100.

The initial adoption of dietary changes appeared to lead to a slight increase in average PM_{2.5} levels in China. By 2030, PM_{2.5} concentrations in China were projected to increase by approximately 2%. This temporary increase could be attributed to alterations in food production and consumption practices, which directly influence agricultural emissions especially from the soil management sector as detailed in Table 5-2. However, a long-term positive shift was observed, with PM_{2.5} concentrations projected to decline by approximately 5% by 2100.

Dietary policies under the baseline scenario were able to achieve reductions in O₃ in Southeast Asia and South America between 2030 and 2100. In Southeast Asia, dietary modifications were forecast to play a part in mitigating surface-level O₃ concentrations, with declines of 3.21% by 2050 (maximum: -2.06%, minimum: -4.75%) and 9.29% by 2100 (maximum: -4.56%, minimum: -12.98%). However, in 2030, only minimal changes in O₃ concentrations were forecast, with an average decline of 1.75% (maximum: -0.72%, minimum: -2.73%). By contrast, dietary transformation was projected to lead to an initial upsurge in tropospheric O₃ concentrations in China, primarily in eastern China. However, as dietary changes become established, increases in O₃ are expected to be mitigated by 3–9% by 2100 as show in Figure 5-6.

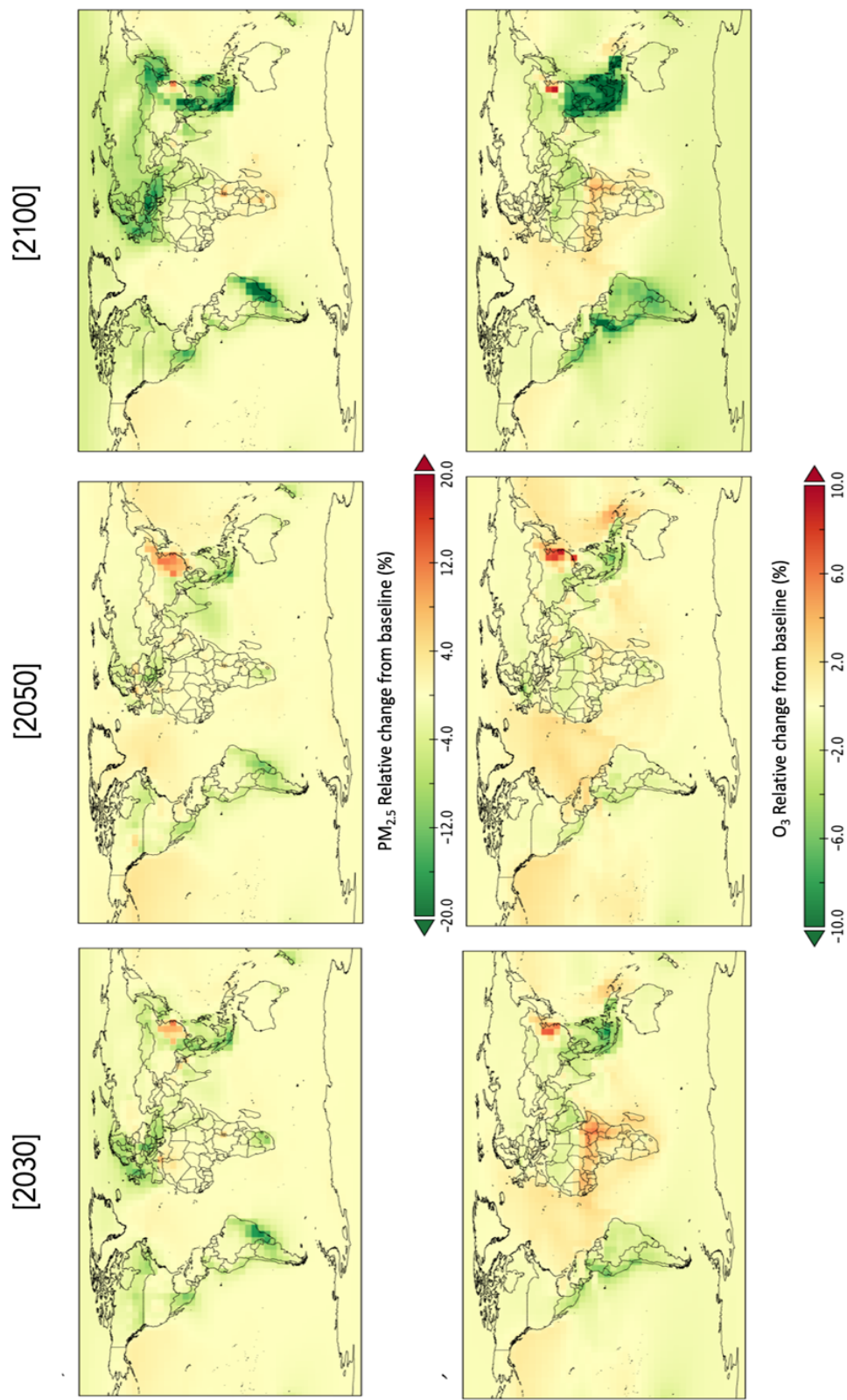


Figure 5-6 the percent relative change (%) of PM_{2.5} (upper) and O₃ (lower) concentrations due to dietary change and food loss prevention policy comparing with baseline scenario in 2030, 2050, and 2100

The implementation of SC3 demonstrates significant potential for reducing PM_{2.5} levels, particularly with notable impacts anticipated in the Asia and Europe regions (Figure 5-7a). Concurrently, the climate change mitigation scenario in the Americas and Asia is expected to contribute to a decline in O₃ concentration (Figure 5-7b). Notably, despite the implementation of climate mitigation measures, Africa is not forecasted to experience substantial reductions in PM_{2.5} and O₃ concentrations.

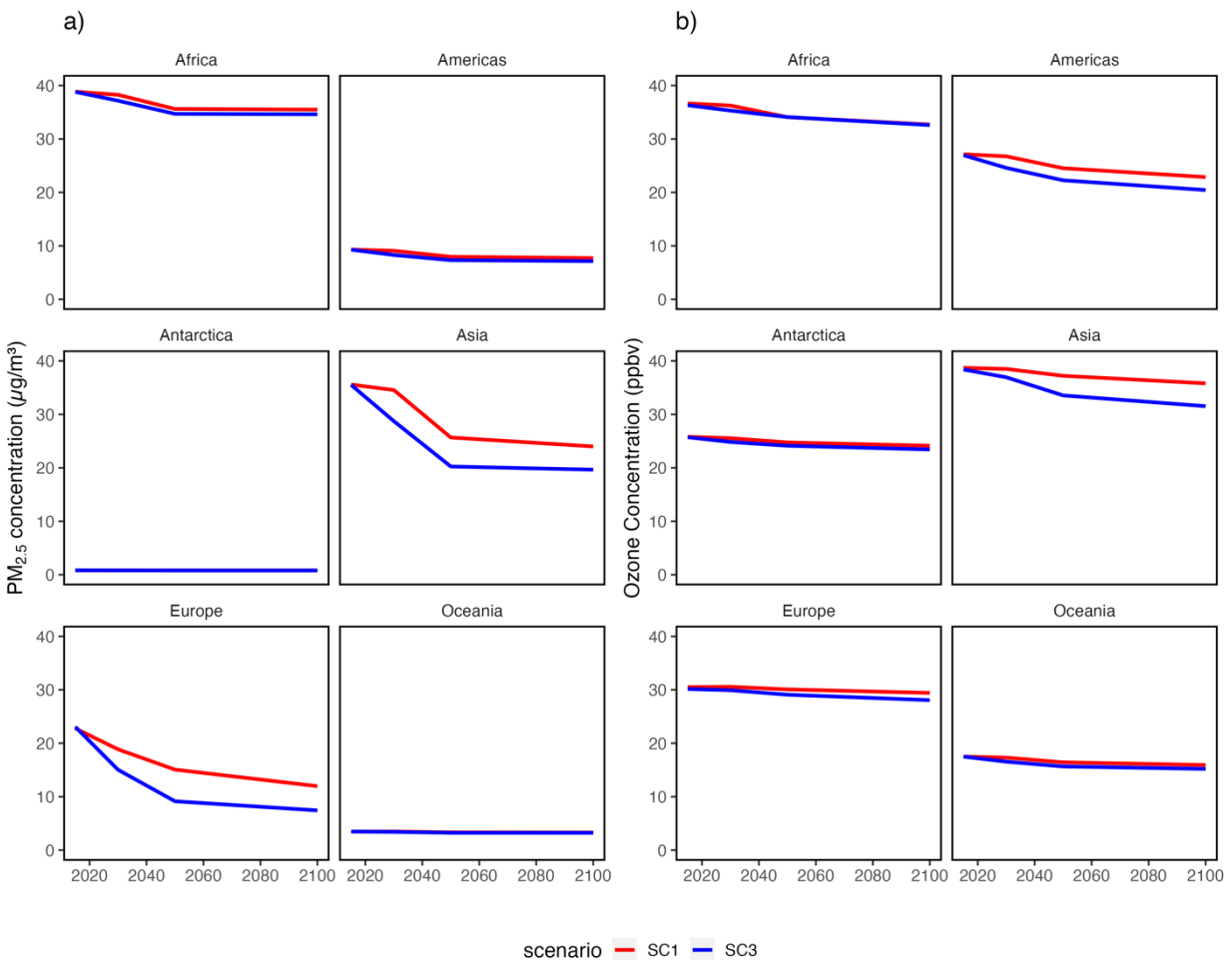


Figure 5-7 temporal resolution PM_{2.5} (a) and O₃ (b) concentrations comparing between baseline scenario: SC1 (red) and climate change mitigation policy: SC3 (blue) between 2015 to 2100

Table 5-2 Regional Ammonia (NH₃) emissions (Mt/yr) comparing across sector, scenario and simulation year (2015, 2030, 2050, 2100)

Region	Scenario	NH ₃ Emission (Total)				NH ₃ Emission (Livestock)				NH ₃ Emission (Soil Management)				
		2015	2030	2050	2100	2015	2030	2050	2100	2015	2030	2050	2100	
Brazil	SC1		3.922	4.399	4.525		0.688	0.817	0.915		1.163	1.380	1.493	
	SC2	3.460	2.673	2.391	2.235		0.301	0.186	0.190		0.941	1.061	1.175	
	SC3		3.168	3.065	2.914	0.506		0.536	0.525	0.546		1.054	1.068	1.038
	SC4		2.242	1.859	1.702		0.257	0.136	0.135		0.884	0.907	0.942	
China	SC1		12.104	11.626	8.076		2.780	2.624	1.730		8.064	7.257	4.251	
	SC2		11.890	12.928	8.844		1.390	0.925	0.682		9.601	10.699	6.325	
	SC3	11.377	11.031	8.954	5.817	2.556		2.446	2.015	1.368		7.513	5.874	3.480
	SC4		10.112	9.226	5.926		1.513	0.793	0.586		7.763	7.671	4.554	
USA	SC1		4.659	5.226	6.103		1.437	1.626	1.900		2.155	2.481	2.974	
	SC2		3.791	4.209	4.817		0.668	0.370	0.425		2.296	3.119	3.636	
	SC3	4.100	4.256	4.212	4.878	1.256		1.319	1.283	1.515	1.894	2.007	2.071	2.448
	SC4		3.300	3.060	3.398		0.646	0.315	0.363		1.939	2.198	2.492	
Europe (EU25)	SC1		5.498	5.678	5.597		2.475	2.597	2.609		2.516	2.574	2.469	
	SC2		4.164	3.500	3.374		1.449	0.647	0.622		2.324	2.569	2.460	
	SC3	5.255	5.159	4.621	4.604	2.356		2.337	2.131	2.195	2.434	2.356	2.091	2.019
	SC4		3.950	2.775	2.645		1.478	0.586	0.570		2.103	1.966	1.869	

Table 5-2 Regional Ammonia (NH₃) emissions (Mt/yr) comparing across sector, scenario and simulation year (2015, 2030, 2050, 2100), Continued.

Region	Scenario	NH ₃ Emission (Total)					NH ₃ Emission (Livestock)					NH ₃ Emission (Soil Management)				
		2015	2030	2050	2100	2150	2015	2030	2050	2100	2150	2015	2030	2050	2100	2150
North	SC1		1.105	1.576	1.499		0.137	0.187	0.244		0.541	0.654	0.698			
	SC2	0.742	0.940	1.328	1.049		0.090	0.078	0.078		0.496	0.683	0.680		0.423	
	SC3		0.919	0.915	1.082	0.094	0.120	0.144	0.195		0.494	0.498	0.539			
	SC4		0.776	0.736	0.713		0.084	0.063	0.063		0.450	0.534	0.526			
Southeast	SC1		8.438	8.210	5.986		1.403	1.685	1.727		2.716	2.896	2.395			
	SC2		7.667	6.664	3.954		0.789	0.531	0.456		2.340	2.438	1.855			
	SC3	8.062	7.318	6.199	4.445	1.067	1.229	1.252	1.325		2.360	1.923	1.700			
	SC4		6.636	5.069	2.879		0.749	0.435	0.378		2.039	1.613	1.272			
World	SC1		67.273	76.445	86.571		13.918	15.864	17.738		29.349	32.233	31.902			
	SC2		58.618	63.144	57.526		8.018	5.810	5.633		29.749	36.864	32.493			
	SC3	58.514	59.773	58.605	64.055	11.813	12.235	11.944	13.474		25.597	26.846	25.141			
	SC4		51.267	47.208	41.308		7.703	4.516	4.411		25.288	26.557	23.465			

When considering the role of dietary change under climate mitigation policies (SC4), it appears that its impact on PM_{2.5} levels may be lower compared to the implementation of climate mitigation measures alone (Figure 5-8). The influence of dietary change within the climate change scenario is particularly evident in the Europe region, where it has the potential to further reduce annual average PM_{2.5} concentrations by approximately 3.86% (maximum: -2.11%, minimum: -7.21%), 2.58% (maximum: -0.17%, minimum: -5.92%), and 2.68% (maximum: -0.39%, minimum: -5.73%) by 2030, 2050, and 2100, respectively, in addition to the reductions achieved through the climate change mitigation scenario (SC3). However, our findings show that the reduction rate in PM_{2.5} in 2050 begins to decelerate, persisting through 2100 because of a slight increase in NH₃ emissions from soil management observed in Europe, Brazil, and Latin America.

Furthermore, an integrated policy approach could mitigate the expected increase in PM_{2.5} concentrations in eastern China relative to the implementation of dietary changes alone. Specifically, the combined policy approach resulted in a smaller increase in PM_{2.5} levels of approximately 4%. By contrast, dietary change as a standalone policy (SC2) was associated with an increase in PM_{2.5} levels up to 12% by 2050 (Figure 5-8). In Southeast Asia, the impact of dietary change under the climate change mitigation scenario on PM_{2.5} is not as conspicuous as when SC3 mitigates alone.

The role of dietary changes on O₃ concentrations would be inconsequential when implemented together with climate mitigation measures. The implementation of SC4 may result in a marginal increase in O₃ levels across all regions comparing with SC3. The relative reductions in global average O₃ concentrations were -0.50% by 2030, -0.80% by 2050, and -0.13% by 2100. These findings indicate that the implementation of dietary changes in conjunction with climate change mitigation measures would have minimal additional impact on O₃ concentrations compared to climate mitigation alone. However, in South Africa, scenario SC4 was projected to increase tropospheric O₃ by only 1–3% by 2050.

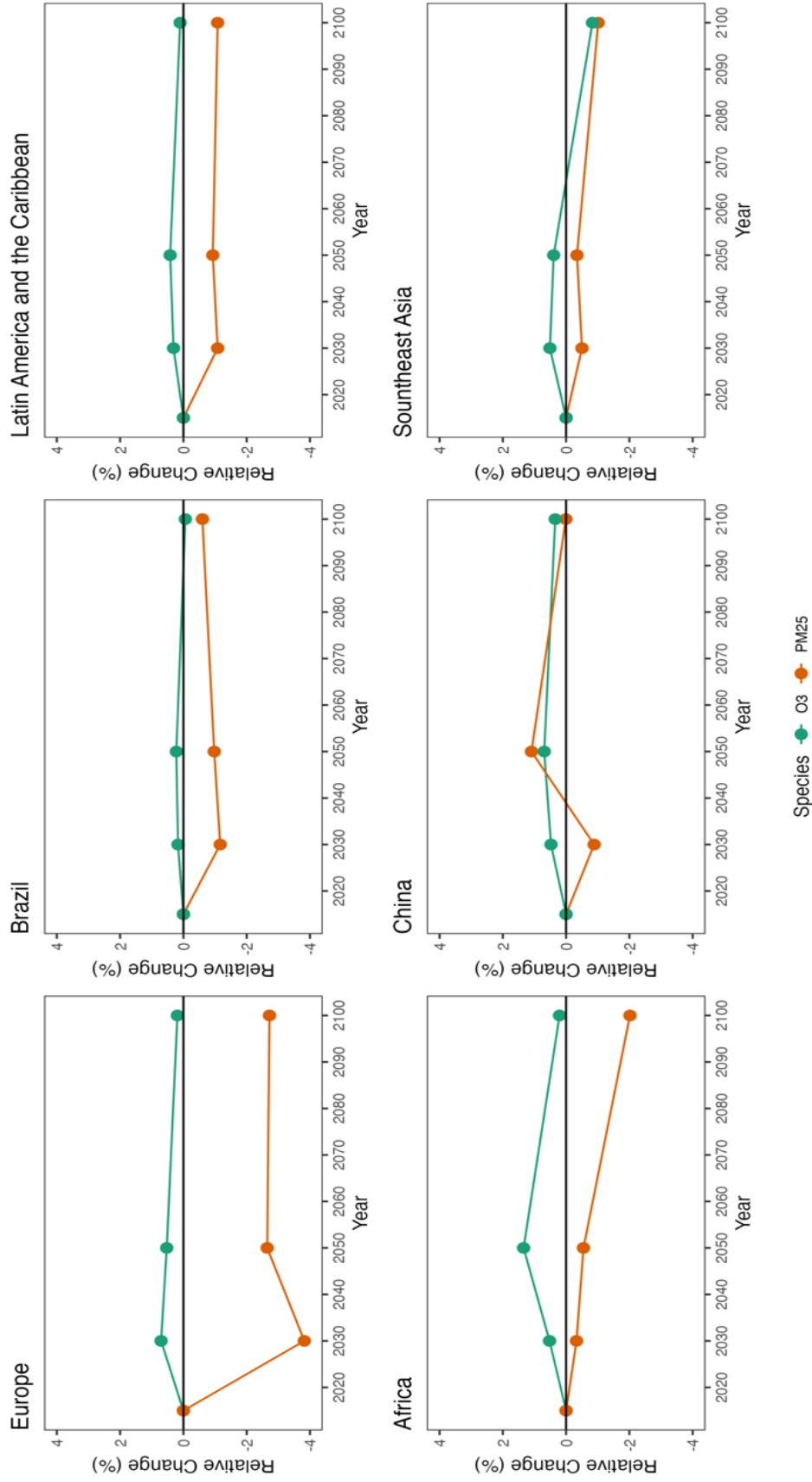


Figure 5-8 Regional comparison relative change (%) of PM_{2.5} (orange) and O₃ (green) due to Integrated Policy (SC2+SC3) comparing with climate change mitigation scenario (SC3)

5.4.4 Reductions in premature mortality.

The baseline scenario (SC1) predicts a gradual increase in global mortality associated with PM_{2.5} exposure from 2015 to 2030. However, this trend is expected to be followed by a rapid decrease in mortality due to a reduction in PM_{2.5} concentration. Conversely, mortality from ozone exposure is projected to continue rising over time due to an increase in ozone concentration. Moreover, even with the implementation of climate change mitigation policies (SC3) or food transformation scenarios, the levels of tropospheric ozone are expected to continue rising, leading to a further increase in ozone-related mortality in the future. Nevertheless, the implementation of climate change mitigation policies (SC3) has the potential to bring about significant reductions in mortality from the baseline scenario. These policies offer the opportunity to save a considerable number of lives in various timeframes.

To evaluate the additional benefits of dietary changes on air quality and mortality, we compared scenario SC2 with SC1 (Figure 5-9: green line). The results indicated that dietary changes have the potential to contribute to significant improvements in air quality and mortality outcomes. Compared to the baseline scenario, SC2 could reduce PM_{2.5}-related mortality by 120 induced deaths per year in 2030, 40,300 deaths per year in 2050, and 187,500 deaths per year in 2100. Dietary changes were also projected to prevent 10,850, 25,560, and 131,110 O₃-related deaths per year in 2030, 2050, and 2100, respectively.

Scenario SC4 resulted in additional avoidance of premature deaths due to PM_{2.5} compared to SC3 (Figure 8: orange line). Additional avoided mortality of 51,260, 3,920, and 44,010 deaths per year was forecast for 2030, 2050, and 2100, respectively. However, O₃-related mortality increased by 6,090, 11,570, and 240 deaths per year compared to SC3.

Regional analysis revealed that the Southeast Asian and European regions experienced substantial benefits from dietary modifications in mitigating PM_{2.5}-related mortality (Figure 5-9). In Southeast Asia, the implementation of dietary changes resulted in a significant decline in mortality rates by 35% compared to the baseline scenario. Furthermore, the adoption of dietary reform policies in 2100 has the potential to save approximately 15.97 thousand deaths per year from ozone exposure

in Southeast Asia. In the European Union and the United States, the impact of dietary changes under climate change mitigation policies was even more significant compared to the baseline scenario, indicating the amplified positive effects on reducing PM_{2.5}-related mortality. In China, the adoption of an integrated policy has demonstrated positive outcomes in reducing PM_{2.5}-related mortality following the implementation of dietary changes.

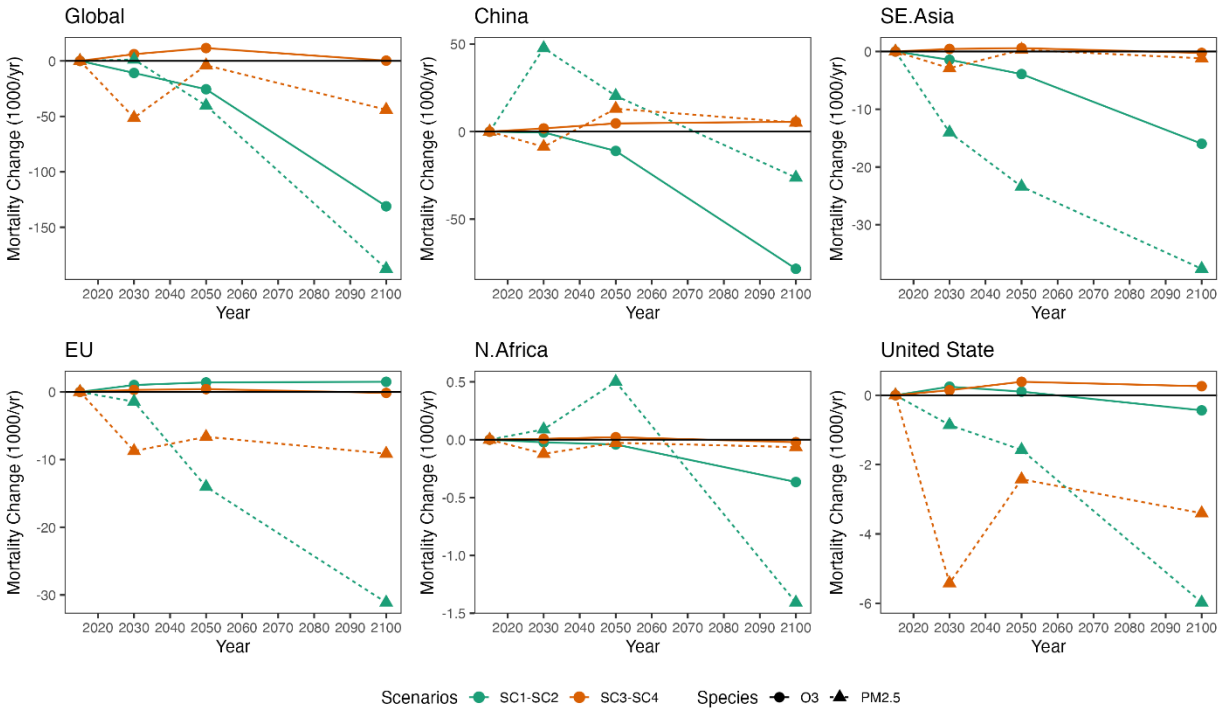


Figure 5-9 Regional comparison mortality change (1000 yr⁻¹) of PM_{2.5} (triangle) and O₃ (circle) between dietary change and food loss prevention policy and baseline and (SC1-SC2: green) and climate change mitigation scenario and integrated policy (SC3-SC4: orange)

5.4.5 Economic impact

Figure 5-10, the implementation of dietary changes (SC2) is projected to increase the Value of Statistical Life Years (VSLY) cost by 23.99 billion USD/year (2010, PPP adjusted) in 2030. In contrast, in 2050 and 2100, the cost is expected to decrease by 66.24 billion USD/year (2010, PPP adjusted) and 391.37 billion USD/year (2010, PPP adjusted), respectively, representing reductions of approximately 1.27% and 6.43%. Notably, our research findings indicate that in China, the

increase in PM_{2.5} concentrations is associated with an induced VSLY cost of approximately 58.15 billion USD/year (2010, PPP adjusted) in 2030 and 17.48 billion USD/year (2010, PPP adjusted) in 2050. However, by 2100, this cost is expected to decrease significantly compared to the baseline scenario, by approximately 135 billion USD/year (2010, PPP adjusted) or 8%. In both Southeast Asia and Europe, the implementation of dietary changes has shown potential effectiveness in reducing the number of mortalities associated with ambient air exposure. Our analysis reveals that by adopting these dietary changes, the VSLY cost could decline by up to 35% or 69.95 billion USD/year (2010, PPP adjusted) in 2100. Furthermore, in Southeast Asia, the cost is projected to experience slight reductions of approximately 27.75 billion USD (13.31%) and 10.57 billion USD (4.41%) in 2030 and 2050, respectively.

In terms of the climate change mitigation scenario (SC3), there is a significant reduction in the VSLY cost compared to the baseline. By 2030, the estimated VSLY cost is 4,646.91 billion USD/year (2010, PPP adjusted), representing a reduction of approximately 817 billion USD/year (2010, PPP adjusted) or 17% compared to the baseline. However, in 2050 and 2100, the cost of VSLY is higher than the 2030 level, nearly doubling and reducing from the baseline by approximately 2,198.96 billion USD/year (39.54%) and 1,863.77 billion USD/year (36.25%) (2010, PPP adjusted), respectively.

Under the integrated policy scenario (SC4), the impact of dietary changes on the economic value of the climate change mitigation scenario is not significant. Only three regions, namely Canada, Europe, and the United States, experience a reduction in VSLY cost due to dietary changes in addition to the climate change mitigation scenario. For example, in Canada, there is an additional reduction in VSLY cost under SC4, with approximately 1.74 billion USD/year (2010, PPP adjusted) (29.96%), 2.06 billion USD/year (2010, PPP adjusted) (24.95%), and 3.01 billion USD/year (2010, PPP adjusted) (31.67%) further reduced for 2030, 2050, and 2100, respectively.

These findings demonstrate the trade-off between the number of lives saved and the economic costs associated with dietary changes and climate change mitigation policies. While the implementation of dietary changes may initially increase costs, their long-term benefits in terms of reducing premature mortality are substantial. Furthermore, the reductions achieved in the VSLY

cost under the climate change mitigation scenario highlight the potential value of these strategies in mitigating the economic burden associated with air pollution-related mortality.

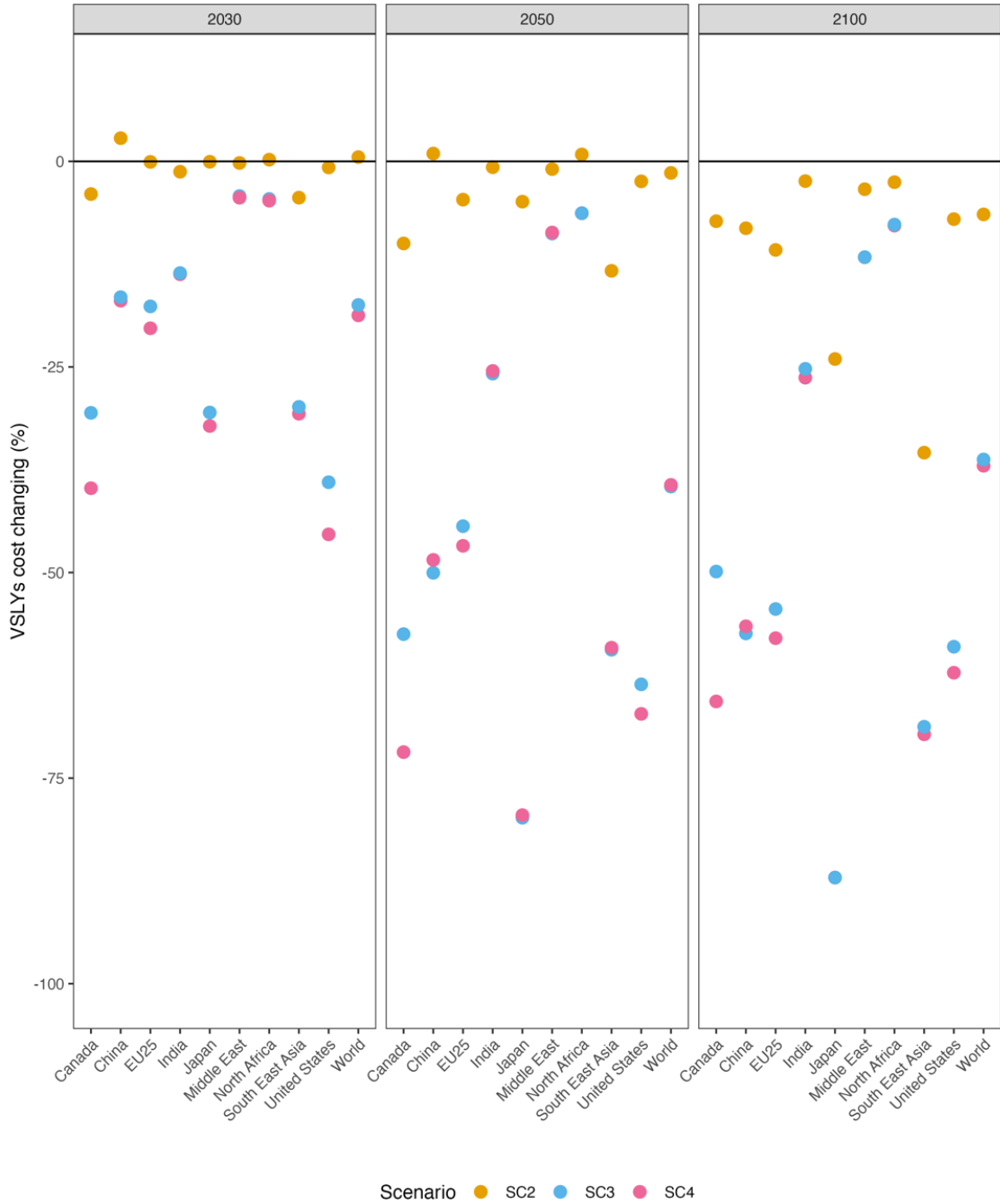


Figure 5-10 VSLY cost changing (%) comparing of dietary and food loss prevention policy (orange), climate change mitigation (blue), and integrated policy (pink) with the baseline scenario.

5.5 Discussion

5.5.1 The Potential for emission reduction through dietary change and food losses prevention policy

In accordance with the findings of the comprehensive study conducted by Poore & Nemecek (2018), it was revealed that livestock and fisheries collectively contribute to 31% of global greenhouse gas emissions, accompanied by co-pollutants such as NH_3 and CH_4 . In contrast, emissions from food processing constitute a modest 4% of the total GHGs. Moreover, 81% of global ammonia emissions are a result of agriculture, especially from livestock (Wyer et al., 2022). Thus, our discussion will strategically narrow its focus to NH_3 emissions from the agriculture sector. This deliberate choice stems from the recognition of NH_3 distinct significance as a pollutant, impacting not only global warming but also air quality, ecological integrity, and human health.

In this study, we found that a combination of reducing red meat consumption and implementing effective food loss and waste control policies could be highly effective in mitigating NH_3 and CH_4 emissions from the agricultural sector. These findings are consistent with numerous studies conducted over the past few decades (e.g., Domingo et al., 2021; Liu et al., 2021; Ma et al., 2021; Malherbe et al., 2022). However, at the regional scale, particularly in China, our results forecast an increase in NH_3 emissions from the agricultural sector in 2030 due to a combination of high demand for plant-based foods and unsustainable agricultural practices. These emissions are expected to decline rapidly from 2030 to 2100. In the European Union, upon comparing our current study with the research conducted by Himic et al. (2022), we observed that implementing a 50% reduction in red meat consumption, as suggested in our study, could lead to an approximate 35.79% reduction in NH_3 emissions. This contrasts with the findings of Himic et al., where a flexitarian approach resulted in a reduction of 30%. The variations in the percentage reductions between our current study (AIM/Hub) and the research conducted by Himic et al. (GLOBIOM) may be attributed to the differences in the uncertainty associated with IAMs as Fujimori et al., (2022) study.

To achieve substantial reductions in NH_3 emissions, an integrated policy that combines various strategies will yield better results than standalone dietary change policies. Although dietary changes play a role in reducing NH_3 emissions, their impact was projected to be relatively small

under a 1.5°C climate change mitigation scenario compared to the baseline scenario. Improvements in agricultural practices, including better manure management, optimized feeding regimes, and the use of efficient nitrogen-based fertilizer, have already led to considerable reductions in NH₃ emissions.

While the combined impact on NH₃ emissions from our integrated policies (SC4) may not exhibit a significant reduction compared to climate change measures scenario (SC3), it is crucial to underscore the substantial positive effect on mitigating climate change through the significant reduction in CH₄ and N₂O emissions which are key contributors to global warming (Jones et al., 2023) and our comprehensive approach has proven notably effective in curbing their release. This underscores the importance of addressing multiple greenhouse gases simultaneously for a more comprehensive and impactful climate strategy.

5.5.2 The impact of agricultural emissions on ambient PM_{2.5} and O₃ concentration

In this study, we have investigated the impact of ammonia emissions resulting from the reaction between ammonia and oxidizers, such as sulfuric and nitric acids. These emissions contribute significantly to the composition of ambient PM_{2.5}, which is a form of fine particulate matter that can have adverse effects on human health and the environment. Our findings suggest that altering dietary behaviors could be a potential strategy to reduce ammonia emissions in regions where agriculture plays a key role as a significant anthropogenic activity.

By addressing the sources of NH₃, we can effectively mitigate the formation of ammonium, sulfate, and nitrate pollutants, which contribute to PM_{2.5} formation. Our findings highlighted Europe and Asia as the regions with the highest levels of sulfate–nitrate–ammonium (SNA) aerosols, aligning with the conclusions drawn in the study conducted by Pai et al. (2022) and Himics et al., (2022). In Europe, SNA compounds account for 46.3% of the PM_{2.5} composition. Thus, when NH₃ emissions are reduced through dietary changes and sustainable agricultural practices, there will be a significant decline in PM_{2.5} levels, as also suggested in a previous study (Jonson et al., 2022).

On the other hand, in the African region, it appears that dietary changes and climate change mitigation policies may not be as effective in controlling PM_{2.5} levels. Our study suggests that the proportion of SNA aerosol components in PM_{2.5} is relatively low in this region, indicating that other sources of PM_{2.5} pollution, such as dust and biomass burning, may have a more significant impact in Africa. This finding aligns with the findings of Tahri et al. (2022), who reviewed that the primary sources of particulate matter in the region are related to industrial emissions, transportation, and solid fuel burning in buildings.

Furthermore, our findings in China differ from previous studies (Guo et al., 2022; X. Liu et al., 2021) regarding the effect of dietary change on PM_{2.5} and O₃ concentrations. In our study, we discovered that dietary change could increase both NH₃ and NO_x emissions from the agriculture sector, particularly from soil management activities. As a result, this increase in emissions can lead to elevated levels of both PM_{2.5} and O₃ in the atmosphere. It is important to note that our study focused on a scenario (SC1) where the dietary change occurred without incorporating sustainable agricultural practices. Consequently, when livestock production was reduced, there was a rapid increase in demand for plant-based foods, which in turn intensified soil management activities.

5.5.3 The societal benefits of reducing mortality through improved air quality from dietary change and climate change mitigation policy.

Sustainable eating habits combined with climate change mitigation efforts could have significant positive effects on public health, including a lower probability of illness from air pollution. These methods could help to reduce the production of PM_{2.5} and O₃, which are important contributors to air pollution and poor health. According to a WHO report, climate change is expected to cause approximately 250,000 additional deaths per year between 2030 and 2050 (WHO, 2023). Dietary change and climate change mitigation policies could help to reduce this burden of mortality. In our study, we estimated that 171,410 deaths per year could be avoided by 2050 due to air quality improvements brought about by dietary change. There would be an associated reduction in the costs of healthcare. Because healthier people typically have higher work productivity and lower healthcare expenses, this reduction in health spending costs may have economic benefits. However, implementing dietary change as a standalone policy will have little effect on most drivers of

climate change. Combining dietary changes with climate change mitigation policies is a viable solution to simultaneously mitigate climate change, low-nutrition and reduce the health impacts of ambient air pollution.

The IPCC Special Report on Global Warming of 1.5°C emphasizes that addressing climate change may involve economic costs, especially when moving toward a low-carbon economy and implementing climate change mitigation initiatives. These efforts could lead to GDP losses of 2.6–4.2% per year by 2050. The integration of policies that combine dietary changes and climate change mitigation could help to offset some of these economic costs. One significant advantage of such integrated policies is the potential for improved health outcomes. By reducing harmful emissions and air pollution, we can promote better public health, resulting in healthier populations. For example, implementing such integrated policies could prevent 55,580 pollution-related deaths per year by 2050 due to reduced exposure to pollutants such as PM_{2.5} and O₃.

In addition, The EAT-Lancet study reveals a substantial potential for averting 10.8–11.6 million deaths annually by adopting recommended dietary changes, resulting in a significant reduction of 19.0–23.6% in mortality attributed to low nutrition. This emphasizes the profound impact that dietary shifts can have on public health. While this section does not directly compare these mortality results with those from other sectors, it underscores the multifaceted benefits of combining policies targeting both dietary habits and environmental factors. By doing so, not only can mortality from air quality-related issues be mitigated, but also mortality stemming from nutritional deficiencies, particularly in developing areas, can be addressed. This dual approach to policy formulation holds the potential to yield comprehensive benefits for both public health and the economic sector.

Further research and comparative studies across various sectors are warranted to provide a more nuanced understanding of the relative impacts and trade-offs associated with different mitigation strategies. Nonetheless, the synergistic effects of combining policies, as highlighted by the EAT-Lancet study, advocate for a holistic approach to address diverse health and environmental challenges.

5.5.4 Policy recommendation

In light of the interconnected challenges posed by climate change, air pollution, and public health, a comprehensive policy approach is warranted. To address these issues effectively, we propose the implementation of a synergistic policy framework that integrates sustainable dietary changes with climate change mitigation efforts. This holistic approach aims to achieve multiple benefits, including improved public health outcomes and economic advantages.

Developing a robust and comprehensive policy framework necessitates the explicit integration of climate change mitigation strategies with dietary guidelines. This entails seamlessly incorporating sustainable and low-carbon dietary recommendations into national climate action plans, fostering a unified approach to concurrently address environmental and health concerns. Currently, various regions worldwide are actively formulating dietary policies to tackle pressing health and nutrition challenges. Simultaneously, ambitious National Determined Contributions (NDCs) plans are being crafted with the goal of achieving net-zero emissions by 2050. It's noteworthy that these policies are independently implemented at the national scale. Through our research, we have empirically demonstrated that the integration of policies, combining dietary guidelines with climate change mitigation strategies, holds significant potential to effectively address both health and environmental challenges concurrently.

To promote behavioral change, it is imperative to create educational and awareness campaigns that highlight the interconnectedness of individual dietary choices with personal well-being and environmental impact. This educational initiative aims to empower citizens to make informed decisions, encouraging a shift towards diets that are not only health-conscious but also environmentally sustainable. In addition to addressing behavioral change among individuals, it is crucial to enhance agricultural practices. This research indicates that simply reducing red meat consumption, without concurrent adoption of sustainable agricultural practices, may result in elevated ammonia emissions from soil management activities, subsequently contributing to increased PM_{2.5} levels in specific regions. Therefore, the implementation of policies and financial incentives is imperative to encourage farmers to embrace sustainable and climate-friendly agricultural practices. These initiatives will not only mitigate environmental impacts but also

contribute to a holistic approach in achieving both dietary and agricultural sustainability. For example, in EU, The European Union is extending financial backing and inducements to farmers through various channels, encompassing funding under the Green Deal, as well as participation in rural development programs and agricultural subsidies. The Green Deal funding specifically targets farmers committed to enhancing the sustainability and environmental friendliness of their operations, offering resources to support their endeavors (European Commission, 2021).

Moreover, advocating for the integration of sustainable dietary recommendations and public health considerations within international climate agreements is vital, especially in light of the significant findings highlighted in the IPCC reports. While the IPCC recognizes the substantial impact of dietary choices on greenhouse gas emissions and land use, it is crucial to note that the dietary framework in the IPCC report may not be entirely clear. Positioning these issues as integral components of global efforts to combat climate change underscores the interconnected nature of environmental and health challenges.

Given the potential ambiguity in the dietary framework outlined by the IPCC, there is an opportunity to further clarify and strengthen the role of dietary guidelines in climate mitigation strategies. By enhancing the clarity of the dietary recommendations within the IPCC framework, we can better emphasize their importance in promoting planetary health and aligning with the IPCC's overarching goals. This concerted effort ensures a more comprehensive approach to addressing the complex interplay between human activities, the environment, and public well-being while ensuring the efficacy of dietary interventions in the fight against climate change.

5.5.5 Uncertainty and limitation

To develop grid emission, AIM/DS would be applied. The approach of downscaling emissions from the AIM/CGE model in proportion to total regional emissions in the agricultural section can introduce uncertainties, especially when considering long-term impacts on land cover and land use change. Downscaling emissions based on total regional emissions, for instance, assumes a proportional connection, which may not capture the spatial distribution of agricultural activity and

emissions effectively. This technique may overlook changes in agricultural practices and land use patterns within the region, so introducing uncertainty into estimates of greenhouse gas emissions. In addition, there are physical and chemical process can contribute to the model biases in air pollutants simulation via GEOS-Chem model. For example, it is difficult to capture the actual surface wind fields. According to Carvalho (2019) study, all reanalyzes, including MERRA-2, shown an inclination to underestimate ocean surface winds (especially in the tropics) and overestimate inland surface winds. Thus, it could be led to underestimate of PM_{2.5} in inland area. Moreover, the GEOS-Chem simulation of surface nitrate aerosol in USA is biases high following Heald et al. (2012) study. In eastern China, Wang et al. (2014) discovered that model nitrate concentrations are likewise too high, whereas nitrate concentrations in western and central China are lower and have less bias compared to observation data. In term of O₃ simulation, due to in the full chemistry mechanism, CH₄ is a constant by using data from NOAA GMD flask observations. Thus, although the emission is changing according to the dietary change and climate change mitigation scenario, it could be not having an impact on the ground surface concentration.

5.6 Summary and conclusions

This study investigates the impact of dietary changes on future air quality and assesses the associated health implications. Four scenarios are developed, including baseline, dietary change with food loss prevention, climate change mitigation, and integrated policy, all operating under the SSP2 scenario. Emissions are quantified using the AIM/Hub model, which is then used as input for the chemical transportation model (GEOS-Chem) to estimate PM_{2.5} and O₃ concentrations, indicators of air quality. The study also estimates premature mortality attributed to these concentrations. This analysis provides a comprehensive understanding of health consequences resulting from dietary modifications on air quality.

The study indicates that implementing dietary changes can have a positive impact on air quality and associated health outcomes. Europe, Southeast Asia, and China are regions that show significant potential for reducing PM_{2.5} levels and preventing premature deaths through dietary modifications. However, the study also highlights the limited impact of dietary changes on ozone concentrations, particularly when combined with climate change mitigation efforts. Overall, the

findings suggest that dietary changes, in conjunction with climate change mitigation policies, can contribute to improving air quality and reducing health risks related to PM_{2.5} exposure. Moreover, an integrated approach combining dietary changes and climate change mitigation measures could provide more comprehensive air quality improvements in specific regions, but careful consideration is needed to address any potential adverse effects on ozone concentrations in certain areas.

Implementing dietary modifications to improve future air quality can also result in a decrease in the expense of the health burden. The convergence of climate change mitigation and dietary modification based on the suggestions of the EAT-Lancet commission offers a viable path for achieving a sustainable and healthier future for both humans and the planet. It represents an opportunity to address environmental and health concerns in a complementary manner, resulting in enormous advantages for society.

5.7 Reference

- Apte, J. S., Marshall, J. D., Cohen, A. J., & Brauer, M. (2015). Addressing global mortality from ambient PM_{2.5}. *Environmental Science & Technology*, *49*(13), 8057–8066.
- Ardra, S., & Barua, M. K. (2022). Halving food waste generation by 2030: The challenges and strategies of monitoring UN sustainable development goal target 12.3. *Journal of Cleaner Production*, *380*, 135042.
- Bauer, S. E., Tsigaridis, K., & Miller, R. (2016). Significant atmospheric aerosol pollution caused by world food cultivation. *Geophysical Research Letters*, *43*(10), 5394–5400.
- Bey, I., Jacob, D. J., Yantosca, R. M., Logan, J. A., Field, B. D., Fiore, A. M., Li, Q., Liu, H. Y., Mickley, L. J., & Schultz, M. G. (2001). Global modeling of tropospheric chemistry with assimilated meteorology: Model description and evaluation. *Journal of Geophysical Research: Atmospheres*, *106*(D19), 23073–23095.
- Bist, R. B., Subedi, S., Chai, L., & Yang, X. (2023). Ammonia emissions, impacts, and mitigation strategies for poultry production: A critical review. *Journal of Environmental Management*, *328*, 116919.
- Burnett, R. T., Pope III, C. A., Ezzati, M., Olives, C., Lim, S. S., Mehta, S., Shin, H. H., Singh, G., Hubbell, B., & Brauer, M. (2014). An integrated risk function for estimating the global burden of disease attributable to ambient fine particulate matter exposure. *Environmental Health Perspectives*, *122*(4), 397–403.
- Carvalho, D. (2019). An assessment of NASA's GMAO MERRA-2 reanalysis surface winds. *Journal of Climate*, *32*(23), 8261–8281.
- Choi, H., & Sunwoo, Y. (2022). Environmental benefits of ammonia reduction in an agriculture-dominated area in South Korea. *Atmosphere*, *13*(3), 384.
- Dimaranan, Betina V., Editor (2006). Global Trade, Assistance, and Production: The GTAP 6 Data Base, Center for Global Trade Analysis, Purdue University. https://www.gtap.agecon.purdue.edu/databases/v6/v6_doco.asp
- Domingo, N. G. G., Balasubramanian, S., Thakrar, S. K., Clark, M. A., Adams, P. J., Marshall, J. D., Muller, N. Z., Pandis, S. N., Polasky, S., Robinson, A. L., Tessim, C. W., Tilman, D., Tschofen, P., & Hill, J. D. (2021). Air quality-related health damages of food. *Proceedings*

- of the National Academy of Sciences*, 118(20), e2013637118.
<https://doi.org/10.1073/pnas.2013637118>
- Fountoukis, C., & Nenes, A. (2007). ISORROPIA II: a computationally efficient thermodynamic equilibrium model for K⁺-Ca²⁺-Mg²⁺-NH₄⁺-Na⁺-SO₄²⁻-NO₃⁻-Cl⁻-H₂O aerosols. *Atmospheric Chemistry and Physics*, 7(17), 4639–4659.
- Fritz, T. M., Eastham, S. D., Emmons, L. K., Lin, H., Lundgren, E. W., Goldhaber, S., Barrett, S. R., & Jacob, D. J. (2022). Implementation and evaluation of the GEOS-Chem chemistry module version 13.1.2 within the Community Earth System Model v2.1. *EGUsphere*, 1–54.
- Fujimori, S., Hasegawa, T., Ito, A., Takahashi, K., & Masui, T. (2018). Gridded emissions and land-use data for 2005–2100 under diverse socioeconomic and climate mitigation scenarios. *Scientific Data*, 5(1), 1–13.
- Fujimori, S., Masui, T., & Matsuoka, Y. (2012). AIM/CGE [basic] manual. Center for Social and Environmental Systems Research, NIES: Tsukuba, Japan.
- Fujimori, S., Su, X., Liu, J.-Y., Hasegawa, T., Takahashi, K., Masui, T., & Takimi, M. (2016). Implication of Paris Agreement in the context of long-term climate mitigation goals. *SpringerPlus*, 5, 1–11.
- Fujimori, S., Wu, W., Doelman, J., Frank, S., Hristov, J., Kyle, P., ... & Takahashi, K. (2022). Land-based climate change mitigation measures can affect agricultural markets and food security. *Nature Food*, 3(2), 110-121.
- Gaita, S. M., Boman, J., Gatari, M. J., Pettersson, J. B., & Janhäll, S. (2014). Source apportionment and seasonal variation of PM_{2.5} in a Sub-Saharan African city: Nairobi, Kenya. *Atmospheric Chemistry and Physics*, 14(18), 9977-9991.
- Guo, Y., He, P., Searchinger, T. D., Chen, Y., Springmann, M., Zhou, M., Zhang, X., Zhang, L., & Mauzerall, D. L. (2022). Environmental and human health trade-offs in potential Chinese dietary shifts. *One Earth*, 5(3), 268–282.
- High-Level Expert Forum. (2009). *FAO How to Feed the World in 2050*.
- Himics, M., Giannakis, E., Kushta, J., Hristov, J., Sahoo, A., & Perez-Dominguez, I. (2022). Co-benefits of a flexitarian diet for air quality and human health in Europe. *Ecological Economics*, 191, 107232.

- IEA. World Energy Balances 2019. In IEA webstore., 2019. <https://webstore.iea.org/world-energy-balances-2019>.
- Jiang, P., Chen, Y., Geng, Y., Dong, W., Xue, B., Xu, B., & Li, W. (2013). Analysis of the co-benefits of climate change mitigation and air pollution reduction in China. *Journal of Cleaner Production*, 58, 130–137.
- Jonson, J. E., Fagerli, H., Scheuschner, T., & Tsyro, S. (2022). Modelling changes in secondary inorganic aerosol formation and nitrogen deposition in Europe from 2005 to 2030. *Atmospheric Chemistry and Physics*, 22(2), 1311–1331.
- Li, Y., Martin, R. V., Li, C., Boys, B. L., van Donkelaar, A., Meng, J., & Pierce, J. R. (2023). Development and evaluation of processes affecting simulation of diel fine particulate matter variation in the GEOS-Chem model. *EGUsphere*, 2023, 1-27.
- Lin, H., Jacob, D., Lundgren, E. W., Payer Sulprizio, M., Keller, C., Fritz, T., Eastham, S. D., Goldhaber, S., & Emmons, L. K. (2020). *Development of the Harmonized Emissions Component (HEMCO) 3.0 as a general emissions component for atmospheric models. 2020*, A022-04.
- Liu, X., Tai, A. P., Chen, Y., Zhang, L., Shaddick, G., Yan, X., & Lam, H.-M. (2021). Dietary shifts can reduce premature deaths related to particulate matter pollution in China. *Nature Food*, 2(12), 997–1004.
- Liu, Z., Zhou, M., Chen, Y., Chen, D., Pan, Y., Song, T., Ji, D., Chen, Q., & Zhang, L. (2021). The nonlinear response of fine particulate matter pollution to ammonia emission reductions in North China. *Environmental Research Letters*, 16(3), 034014.
- Long, S., Zeng, J., Li, Y., Bao, L., Cao, L., Liu, K., Xu, L., Lin, J., Liu, W., & Wang, G. (2014). Characteristics of secondary inorganic aerosol and sulfate species in size-fractionated aerosol particles in Shanghai. *Journal of Environmental Sciences*, 26(5), 1040–1051.
- Ma, R., Li, K., Guo, Y., Zhang, B., Zhao, X., Linder, S., Guan, C., Chen, G., Gan, Y., & Meng, J. (2021). Mitigation potential of global ammonia emissions and related health impacts in the trade network. *Nature Communications*, 12(1), 6308.
- Malashock, D. A., Delang, M. N., Becker, J. S., Serre, M. L., West, J. J., Chang, K.-L., Cooper, O. R., & Anenberg, S. C. (2022). Global trends in ozone concentration and attributable mortality for urban, peri-urban, and rural areas between 2000 and 2019: A modelling study. *The Lancet Planetary Health*, 6(12), e958–e967.

- Malherbe, L., German, R., Couvidat, F., Zanatta, L., Blannin, L., James, A., Létinois, L., Schucht, S., Berthelot, B., & Raoult, J. (2022). *Emissions of ammonia and methane from the agricultural sector. Emissions from livestock farming (Eionet Report—ETC HE 2022/21)*. European Topic Centre on Human Health and the Environment.
- Mao, J., Paulot, F., Jacob, D. J., Cohen, R. C., Crouse, J. D., Wennberg, P. O., Keller, C. A., Hudman, R. C., Barkley, M. P., & Horowitz, L. W. (2013). Ozone and organic nitrates over the eastern United States: Sensitivity to isoprene chemistry. *Journal of Geophysical Research: Atmospheres*, *118*(19), 11–256.
- Mazzeo, A., Zhong, J., Hood, C., Smith, S., Stocker, J., Cai, X., & Bloss, W. J. (2022). Modelling the impact of national vs. Local emission reduction on PM_{2.5} in the West Midlands, UK using WRF-CMAQ. *Atmosphere*, *13*(3), 377.
- Mbow, C., Rosenzweig, C. E., Barioni, L. G., Benton, T. G., Herrero, M., Krishnapillai, M., ... & Diouf, A. A. (2020). Food security (No. GSFC-E-DAA-TN78913). IPCC.
- Miao, R., Chen, Q., Zheng, Y., Cheng, X., Sun, Y., Palmer, P. I., ... & Zhang, Y. (2020). Model bias in simulating major chemical components of PM_{2.5} in China. *Atmospheric Chemistry and Physics*, *20*(20), 12265–12284.
- Nemet, G. F., Holloway, T., & Meier, P. (2010). Implications of incorporating air-quality co-benefits into climate change policymaking. *Environmental Research Letters*, *5*(1), 014007.
- Parrella, J., Jacob, D. J., Liang, Q., Zhang, Y., Mickley, L. J., Miller, B., Evans, M., Yang, X., Pyle, J., & Theys, N. (2012). Tropospheric bromine chemistry: Implications for present and pre-industrial ozone and mercury. *Atmospheric Chemistry and Physics*, *12*(15), 6723–6740.
- Poore, J., & Nemecek, T. (2018). Reducing food's environmental impacts through producers and consumers. *Science*, *360*(6392), 987–992.
- Pörtner, H.-O., Roberts, D. C., Adams, H., Adler, C., Aldunce, P., Ali, E., Begum, R. A., Betts, R., Kerr, R. B., & Biesbroek, R. (2022). *Climate change 2022: Impacts, adaptation and vulnerability*. IPCC Geneva, Switzerland:
- Pye, H., Chan, A., Barkley, M., & Seinfeld, J. (2010). Global modeling of organic aerosol: The importance of reactive nitrogen (NO_x and NO₃). *Atmospheric Chemistry and Physics*, *10*(22), 11261–11276.
- Riahi, K., Van Vuuren, D. P., Kriegler, E., Edmonds, J., O'Neill, B. C., Fujimori, S., Bauer, N., Calvin, K., Dellink, R., & Fricko, O. (2017). The Shared Socioeconomic Pathways and

- their energy, land use, and greenhouse gas emissions implications: An overview. *Global Environmental Change*, 42, 153–168.
- Pai, S. J., Carter, T. S., Heald, C. L., & Kroll, J. H. (2022). Updated World Health Organization air quality guidelines highlight the importance of non-anthropogenic PM_{2.5}. *Environmental science & technology letters*, 9(6), 501-506.
- Smith, P., Bustamante, M., Ahammad, H., Clark, H., Dong, H., Elsiddig, E. A., Haberl, H., Harper, R., House, J., & Jafari, M. (2014). Agriculture, forestry and other land use (AFOLU). In *Climate change 2014: Mitigation of climate change. Contribution of Working Group III to the Fifth Assessment Report of the Intergovernmental Panel on Climate Change* (pp. 811–922). Cambridge University Press.
- Tahri, M., Benchrif, A., & Zahry, F. (2022). Review of Particulate Matter Levels and Sources in North Africa over the Period 1990–2019. *Environmental Sciences Proceedings*, 19(1), 3.
- Tai, A. P., Martin, M. V., & Heald, C. L. (2014). Threat to future global food security from climate change and ozone air pollution. *Nature Climate Change*, 4(9), 817–821.
- Thurston, G. D., & Bell, M. L. (2021). The human health co-benefits of air quality improvements associated with climate change mitigation. In *Climate Change and Global Public Health* (pp. 181–202). Springer.
- Ti, C., Han, X., Chang, S. X., Peng, L., Xia, L., & Yan, X. (2022). Mitigation of agricultural NH₃ emissions reduces PM_{2.5} pollutions in China: A finer scale analysis. *Journal of Cleaner Production*, 350, 131507.
- Travis, K. R., Crawford, J. H., Chen, G., Jordan, C. E., Nault, B. A., Kim, H., ... & Kim, M. J. (2022). Limitations in representation of physical processes prevent successful simulation of PM_{2.5} during KORUS-AQ. *Atmospheric Chemistry and Physics*, 22(12), 7933-7958.
- Turner, M. C., Jerrett, M., Pope III, C. A., Krewski, D., Gapstur, S. M., Diver, W. R., Beckerman, B. S., Marshall, J. D., Su, J., & Crouse, D. L. (2016). Long-term ozone exposure and mortality in a large prospective study. *American Journal of Respiratory and Critical Care Medicine*, 193(10), 1134–1142.
- United Nations. (2023). The Sustainable Development Goals Report 2023: Special Edition. <https://unstats.un.org/sdgs/report/2023/The-Sustainable-Development-Goals-Report-2023.pdf>

- Vandyck, T., Keramidas, K., Kitous, A., Spadaro, J. V., Van Dingenen, R., Holland, M., & Saveyn, B. (2018). Air quality co-benefits for human health and agriculture counterbalance costs to meet Paris Agreement pledges. *Nature Communications*, 9(1), 1–11.
- Wang, Y., Wen, Y., Zhang, S., Zheng, G., Zheng, H., Chang, X., Huang, C., Wang, S., Wu, Y., & Hao, J. (2023). Vehicular ammonia emissions significantly contribute to urban PM_{2.5} pollution in two Chinese megacities. *Environmental Science & Technology*, 57(7), 2698–2705.
- West, J. J., Smith, S. J., Silva, R. A., Naik, V., Zhang, Y., Adelman, Z., Fry, M. M., Anenberg, S., Horowitz, L. W., & Lamarque, J.-F. (2013). Co-benefits of mitigating global greenhouse gas emissions for future air quality and human health. *Nature Climate Change*, 3(10), 885–889.
- World Health Organization. (2023, October 12). Climate change and health. <https://www.who.int/news-room/fact-sheets/detail/climate-change-and-health#:~:text=Research%20shows%20that%203.6%20billion,diarrhoea%20and%20heat%20stress%20alone>.
- Willett, W., Rockström, J., Loken, B., Springmann, M., Lang, T., Vermeulen, S., Garnett, T., Tilman, D., DeClerck, F., & Wood, A. (2019). Food in the Anthropocene: The EAT–Lancet Commission on healthy diets from sustainable food systems. *The Lancet*, 393(10170), 447–492.
- Wyer, K. E., Kelleghan, D. B., Blanes-Vidal, V., Schauburger, G., & Curran, T. P. (2022). Ammonia emissions from agriculture and their contribution to fine particulate matter: A review of implications for human health. *Journal of Environmental Management*, 323, 116285.
- Zhai, S., Jacob, D. J., Brewer, J. F., Li, K., Moch, J. M., Kim, J., ... & Liao, H. (2021). Relating geostationary satellite measurements of aerosol optical depth (AOD) over East Asia to fine particulate matter (PM_{2.5}): insights from the KORUS-AQ aircraft campaign and GEOS-Chem model simulations. *Atmospheric Chemistry and Physics*, 21(22), 16775-16791.

Chapter 6

Summary and Conclusion

6.1 Summary

Our investigation into the intricate relationship between climate change mitigation policies, agricultural practices, air quality, and human health has yielded compelling insights with profound implications for global well-being. Utilizing the GEOS-Chem model, our research challenged conventional assumptions about the efficacy of high-resolution nested-grid simulations in air quality modeling. We found that, whether at high or coarse spatial resolution, the model's performance tends to overestimate compared to observation data. While high-resolution simulations consume significant computational resources and time, the model's performance does not show significant improvement when compared to low-resolution simulations. To understand the implications of climate change mitigation on air quality and human health, the results from the model should be provided as soon as possible after the policy is already being planned. This will help policymakers easily decide or suggest to communities the pros and cons of the policy in all dimensions, not only considering the impact on climate change.

In this study, we focus on shedding light on the role of agriculture under a climate change mitigation scenario on air quality and human health. Thus, we conducted a sensitivity study to understand the influence of agricultural emissions, especially NH_3 and NO_x , which are the main contributors to the formation of secondary pollutants such as $\text{PM}_{2.5}$ and O_3 . We assumed several scenarios to predict the levels of pollutants under different reduction scenarios. For example, NH_3 from agricultural emissions was reduced by 50% and 100%, respectively. Our results illustrate that reducing NH_3 emissions positively impacts $\text{PM}_{2.5}$ concentration mitigation but poses the paradoxical risk of elevating O_3 levels, particularly in the Northern Hemisphere. However, in the real world, we cannot set the same conditions for all regions like the model due to differences in the capacity for competition, economy, and society. Thus, we applied the current policy which suggested by international panel such as climate change mitigation policy from IPCC and sustainable dietary frame suggested by EAT-Lancet commission in this research.

Delving into the impact of dietary changes recommended by the EAT-Lancet Commission under the baseline and climate change mitigation scenarios, the role of dietary change under the baseline scenario on GHG emissions and air quality was quite clearly observed, mainly in agricultural regions, especially in Europe and Southeast Asia. However, reducing red meat consumption led to an increase in food-crop production demand and supply, which can result in an increase in NH₃ emissions from the soil management sector. This phenomenon could lead to elevated levels of PM_{2.5} concentration in China. However, we also recognized the limited impact on O₃ reduction.

Under the climate change mitigation scenario, the role of dietary change is not pronounced in reducing the level of PM_{2.5}, except in Europe and Asia, where dietary changes can significantly improve air quality. To couple both dietary and climate change mitigation policies, it leads to solving the problem of NH₃ from soil management increasing because, in climate change mitigation, sustainable agricultural techniques were already applied. On the other hand, O₃ concentrations seem to slightly rise when this combined policy is implemented because the reduction of emission from agricultural sector especially NH₃ and NO_x which are main O₃ oxidation. To reduce PM_{2.5} and O₃ through dietary changes can significantly improve public health and yield social benefits. Our model shows that dietary changes can help prevent approximately 40.3 thousand deaths per year in 2050, resulting in cost savings for the public health sector of about 66.24 billion USD/year (2010, PPP adjusted), with continued reductions anticipated through 2100. As mentioned earlier, under the climate change mitigation scenario, dietary changes have the potential to improve air quality in specific regions. This slight improvement could also lead to additional avoidance of premature deaths resulting from the climate change mitigation scenario. Simultaneously, shifting food choices to be healthier and more sustainable can also contribute to preventing deaths associated with nutritional deficiencies. Pointed out that, combining policy can promote human health impact from both clear air and healthier diet.

We also proposed policy framework advocates a holistic approach, integrating sustainable dietary changes with climate change mitigation efforts. We emphasize the multifaceted benefits, including improved public health and economic advantages, and propose incorporating low-carbon dietary recommendations into national climate action plans. The framework further highlights the need for simultaneous enhancements in agricultural practices, with proposed policies and incentives for

climate-friendly approaches. International collaboration is urged, emphasizing the integration of sustainable dietary recommendations and public health considerations within global climate agreements. The framework also underscores the importance of clarity in the IPCC's dietary guidelines, concluding by emphasizing the opportunity to strengthen the role of dietary adjustments in comprehensive climate mitigation strategies.

Our research underscores the promising potential of integrating dietary adjustments into global climate change mitigation strategies. This integrated approach not only aids in reducing greenhouse gas emissions and mitigating air pollution but also holds the promise of advancing human health. As we embrace this comprehensive strategy, we pave the way for a more sustainable and healthier future for our planet and its inhabitants.

6.2 Limitation and recommendation

The application of the AIM/DS methodology in developing grid emissions presents various challenges and introduces uncertainties, especially when downscaling emissions from the AIM/Hub model in proportion to total regional emissions in the agricultural sector. Assuming a proportional link between total regional emissions and the spatial distribution of agricultural activity may not adequately capture changes in agricultural practices and land use patterns. This limitation could compromise the accuracy of greenhouse gas emission estimates. Regarding the chemical transport model, our study utilized GEOS-Chem to simulate air quality. However, to gain a comprehensive understanding of future air quality behavior, the meteorological data should align with emission data. Although we fixed the meteorological year in 2016 to disregard the impact of climate change, this approach may hinder our ability to fully grasp the dynamics of future air quality. Moreover, the model tends to produce overestimated data, exemplified by biases in surface nitrate aerosol concentrations. Additionally, using a constant CH₄ value in the full chemistry mechanism for O₃ simulation, based on NOAA GMD flask observations, raises concerns about the model's capability to reflect changes in ground surface concentration in response to variations in emissions resulting from dietary changes and climate change mitigation scenarios. These aspects highlight potential limitations in accurately representing real-world scenarios and emphasize the need for further refinement in model parameters and assumptions.

List of publications

Chapter 3

Jansakoo, T.; Watanabe, R.; Uetani, A.; Sekizawa, S.; Fujimori, S.; Hasegawa, T.; Oshiro K.:
Comparison of global air pollution impacts across horizontal resolutions,
(Under review in “*Atmospheric Environment*”)

Chapter 4

Jansakoo, T.; Fujimori, S.:

The influence of agricultural ammonia emissions reduction on air pollution and human health,
環境衛生工学研究= Environmental & sanitary engineering research: 京都大学環境衛生工学
研究会機関誌, 36(3). 2022, 44-47.

Chapter 5

Jansakoo, T., Fujimori, S., & Hasegawa, T.:

Dietary shifting and their implications for future air quality,
環境衛生工学研究= Environmental & sanitary engineering research: 京都大学環境衛生工学.
37(3). 2023, 60-64.

Jansakoo, T.; Sekizawa, S.; Fujimori, S.; Hasegawa, T.; Oshiro K.:

Benefits of air quality for human health resulting from climate change mitigation through dietary
change and food loss prevention policy,
(Under review in “*Sustainability Science*”)

Other publication

Internship

Jansakoo, T.; Surapipith, V.; Macatangay, R.:

2019 Emission Inventory Development in the Northern Part of Thailand,
EnvironmentAsia 15. 2022. [DOI 10.14456/ea.2022.19]

Acknowledgement

The author would like to express my heartfelt gratitude to Prof. Shinichiro FUJIMORI, Atmospheric and Thermal Environmental Engineering at the Department of Environmental Engineering, Graduate School of Engineering, Kyoto University. His unwavering support and guidance have been invaluable to the successful completion of this research dissertation.

Prof. Fujimori's expertise, wisdom, and dedication to the field of environmental engineering have provided me with a solid foundation for this thesis. His willingness to take me under his mentorship has not only been an honor but a significant opportunity for personal and academic growth.

The author also would like to extend my sincere gratitude to Assistant Professor Ken OSHIRO for his invaluable contributions to this research. His technical expertise and insightful advice have been instrumental in shaping the direction of this thesis.

The author would like to thank Associate Professor Tomoko Hasegawa (College of Science and Engineering Department of Civil and Environmental Engineering, Ritsumeikan University) and Dr. Saritha Sudharmma VISHWANATHAN (Graduate school of Engineering, Kyoto University) for their valuable instructions and comments in this study.

The author feels thankful to Ms. Kayo OTANI (Secretariat of Atmospheric and Thermal Environmental Engineering at the Department of Environmental Engineering, Graduate School of Engineering, Kyoto University) and the other members of the Fujimori's Laboratory for supporting both related to thesis work and daily life in Japan.

The author wishes to express their gratitude for the financial support provided by the Ministry of Education, Culture, Sports, Science and Technology, Japan (MEXT) and the Fujimori Laboratory. The author is especially thankful for the MEXT scholarship, which made it possible for the author to pursue their Ph.D. studies in Japan.

I would like to extend my heartfelt appreciation to my dear friend in Thailand and Japan, whose unwavering support, encouragement, and friendship have been a source of strength and inspiration throughout this

journey. Your enduring belief in me and your constant presence in my life have made all the difference. I would also like to express my deepest gratitude to my family, who have been the pillars of my life, supporting me in every decision I've made. Your love, guidance, and understanding have been my foundation, and I am endlessly thankful for your unwavering support. My achievements are, in large part, a reflection of your love and belief in me, and for that, I am eternally grateful. Thank you for being a vital part of my life and my journey.

January 2024
JANSAKOO Thanapat